MECHANISTIC EVALUATION OF *N*-DEALKYLATION BY CYTOCHROME P450 USING *N*,*N*-DIMETHYLANILINE *N*-OXIDES AND KINETIC ISOTOPE EFFECTS

By

KENNETH M. ROBERTS

A dissertation submitted in partial fulfillment of
the requirements for the degree of

DOCTOR OF PHILOSOPHY

WASHINGTON STATE UNIVERSITY
School of Molecular Biosciences

DECEMBER 2009

To the Faculty of Washington State University:

The members of the Committee appointed to examine the dissertation of KENNETH M. ROBERTS find it satisfactory and recommend that it be accepted.

_____

Jeffrey P. Jones, Ph.D., Chair

_____

William B. Davis, Ph.D.

_____

Lisa M. Gloss, Ph.D.

_____

ChulHee Kang, Ph.D.

MECHANISTIC EVALUATION OF *N*-DEALKYLATION BY CYTOCHROME P450 USING *N*,*N*-DIMETHYLANILINE *N*-OXIDES AND KINETIC ISOTOPE EFFECTS

Abstract

by Kenneth M. Roberts, Ph.D.
Washington State University
December 2009

Chair: Jeffrey P. Jones

Cytochrome P450 enzymes (P450) are a large family of heme-containing monooxygenases found throughout nature. Five isoforms in humans have gained the attention of the pharmaceutical industry due to their responsibility for the oxidation of the majority of pharmaceutical compounds. Due to unconstrained active sites which permit multiple orientations of a given substrate and an arsenal of oxidations attributed to the enzyme, the drug-metabolizing P450s are promiscuous enzymes. Development of predictive models for the oxidation of a given compound by P450 is a major goal for drug development. Since a drug may be oxidized in several ways, prediction of P450-mediated metabolism requires understanding the mechanisms of the possible oxidations that can be performed. This work is focused on evaluating the mechanism of *N*-dealkylation by P450s using *N*-oxides as competent models of the native P450 oxidant.

N-dealkylation is a common form of metabolism of drug compounds. P450s frequently opt for *N*-dealkylation over other potential oxidations due to its apparent ease. Recent work has argued a hydrogen atom abstraction mechanism contingent upon a heme-centered iron-oxene, termed Cmpd I. In this work, we used anilinic *N*-oxides as surrogate oxygen donors in attempts to directly form Cmpd I. The ability to donate only a single oxygen atom and *N*-dealkylation rate measurements permitted us to exclude formation of other oxidants in favor of Cmpd I. Further, products formed from the mechanistic probe *N*-cyclopropyl-*N*-methylaniline excluded a single electron transfer method. When considered together with previous observations of similar KIEs for the native and *N*-oxide-supported systems, we have concluded that both systems follow a hydrogen atom transfer mechanism originating from a Cmpd I species. We have also determined KIE profiles in an active site mutant implicated in switching P450 from Cmpd I to a "second oxidant". These profiles support contributions of this second oxidant to *N*-dealkylation in these mutants, suggesting a role in oxidations performed by P450.

TABLE OF CONTENTS

LIST OF TABLES

LIST OF FIGURES

Dedication

This dissertation is dedicated to my wife
for her love, friendship and patience
through the culmination of this work

CHAPTER ONE

Introduction

A. Overview of Cytochrome P450s

Cytochromes P450 (P450s) are a superfamily of heme-containing monoxygenases. As of August 2009, over 11,000 P450 genes have been identified throughout the natural world including animals, plants, fungi, prokaryotes and even two in viruses.[1] Currently, 57 P450 genes and 58 pseudogenes have been sequenced in the human genome. Many of the human P450s are responsible for oxidations of lipophilic compounds including sterols, fatty acids and eicosanoids and can be found expressed in different tissues throughout the body. A specific group of isoforms are expressed in the liver with the role of metabolizing xenobiotic compounds. Specifically, five of these isoforms are important in drug metabolism as they comprise approximately 70% of the metabolism of pharmaceutical drugs.[2] These isoforms are 1A2, 2C9, 2C19, 2D6 and 3A4 (Figure 1.1). With such a significant role in drug metabolism, P450s and their oxidation of drug compounds have been given much attention over the past several decades.

P450s show very broad substrate specificity ranging from small molecules such as vinyl chloride and ethanol in 2E1 to the very large 1.2 kDa cyclosporine A in 3A4. Further, individual isoforms can show broad specificity. Unlike the vast majority of enzymes, the drug-metabolizing P450s can act on a wide variety of substrates. For example, P450 3A4 oxidizes large substrates varying from the multicyclic steroids, such as testosterone, to the rod-like azole antifungals, e.g. itraconazole, to the above mentioned cyclosporine A. It is this capacity to act on varied substrates that contributes to the participation of P450s in such a large percentage of drug metabolism.

As monoxygenases, P450s catalyze the insertion of a single oxygen atom into a substrate. The uniqueness of P450s lies in the fact that substrate oxidation can take many forms including aliphatic and aromatic hydroxylations, dealkylations, heteroatom oxidations and epoxidation

(Figure 1.2). The study of P450s and their ability to promote this large diversity of oxidations is decades old. The consensus mechanism is centered upon activation of molecular oxygen with one oxygen atom incorporated into water and one into the substrate. Because the primary role of the enzyme is the reduction of oxygen, the culmination of the P450 mechanism is the generation of a reactive oxygen species (ROS) capable of directly acting on a given substrate through a variety of possible oxidations.

Hepatic P450s are responsible for the metabolism of lipophilic endogenous and exogenous compounds for excretion from the body. Insertion of one or more oxygens into a substrate increases the compound's polarity, decreasing its ability to harbor in the lipid membrane and increasing its water solubility, a critical factor in compound excretion. Thus, P450-mediated metabolism has a direct effect on the lifetime of a given pharmaceutical. Slow metabolism by P450s will promote the metabolic stability of a given compound while fast metabolism will decrease its metabolic stability. In the philosophy of drug design, five topics, together termed ADMET, are the critical areas of importance for any given candidate. These five are **A**bsorption of the drug into the body, **D**istribution throughout the body (or to target tissues), **M**etabolism of the drug, **E**xcretion of the drug and its metabolites and the **T**oxicity of the drug and/or its metabolites. With their significant role in drug metabolism, the effect of P450s on a potential drug's metabolic stability is an important part of the drug design process. If a potential drug is metabolized quickly, an increased size or number of doses will be required to maintain enough compound in the system to be beneficial. If metabolized too quickly, the drug may not last long enough to elicit any effect. In contrast, if a drug is metabolized too slowly, it may elicit its effect for longer than intended or may accumulate in the system, especially if received in multiple doses. A drug that is metabolized too slowly can be particularly dangerous if it attains toxic

levels, as it will take a long time to return to therapeutic concentrations. Additionally, slowly metabolized drugs also take a long time to reach steady state concentrations. With these considerations, the importance of understanding how P450s will act on a given potential drug compound is apparent.

In addition to affecting the metabolic stability of compounds, oxidation of compounds by P450s can lead to bioactivation, with metabolites having behaviors unique from the substrate including toxicity or carcinogenicity. Perhaps the most well studied example of P450-mediated formation of a toxic metabolite is the oxidation of acetaminophen. Acetaminophen is oxidized by several liver P450s into the toxic metabolite *N*-acetyl-*p*-benzoquinone imine (NAPQI).[3] Toxicity resulting from the metabolism of acetaminophen is the #1 cause of acute liver failure in the United States.[4] Further, P450s have an active role in drug-drug interactions. Drug-drug interactions arise from one drug compound eliciting an effect on the metabolism of a second drug compound. Frequently, this is seen as a drug inhibiting the metabolism, and thus clearance, of another drug. The metabolism of the drug warfarin is an excellent example of P450-related drug-drug interactions. Warfarin is a potent anticoagulant given both acutely and chronically. However, the therapeutic window for warfarin is very narrow. (The therapeutic window is the difference in concentrations between a therapeutic and a toxic dose.) As such, warfarin overdosing is common, resulting in excessive and often lethal bleeding. Warfarin is metabolized almost solely by the drug-metabolizing P450 2C9. Since clearance of warfarin requires oxidation by 2C9, other drugs that are also metabolized by 2C9 would expectedly interfere with warfarin's metabolism. As one of the five major isoforms involved in drug metabolism, 2C9 is involved in the metabolism of a large number of pharmaceuticals. Drugs.com currently lists 670 drugs

known to interact with warfarin. For this reason, warfarin levels are regularly checked both in inpatient and outpatient settings.

With drug metabolism directed by P450s and the potential for adverse drug effects directly resulting from their function, understanding how P450s will interact on a potential drug is an important aspect for the future of drug design. The ultimate goal is the successful prediction of metabolism for any given potential drug. With their varieties of substrate preferences and the arsenal of oxidations they can perform, understanding P450s requires an underlying understanding of both how given substrates will bind and what types of oxidations might be performed. Oxidation by P450 can take many forms and a given drug compound can be a potential target for any one of several forms of oxidation. Since each oxidation follows a unique mechanism, the relative energetics of each possible oxidation contributes to their relative occurance. Easier oxidations would be expected to dominate metabolism over more difficult oxidations. However, substrate binding can alter the ratio of possible products. This can occur by protecting a highly reactive site from the ROS or by orienting a less reactive site towards the ROS. Thus, the ability to predict the metabolism of a given compound requires both understanding the energetics of the possible oxidations to predict major metabolites as well as understanding the active site dynamics to predict compound orientations in a given P450 and their contributions to regioselectivity.

B. Cytochrome P450 Structure and Redox Partners

As described above, thousands of P450s have been identified throughout nature. Until recently, crystal structures had been limited to bacterial and fungal enzymes. However, at the time of this writing, crystal structures of 11 unique human P450s have been published, including

the pharmaceutically-relevant 1A2, 2C9 and 3A4 isoforms. Comparison of these structures reveals that, though sequence homology between families is as low as 20%, P450s share a global fold specific for this class of enzymes.[5] The major contribution to the P450 fold is a four helix bundle made up of the D, E, I and L-helices (Figure 1.3). Unlike most other four-helix bundles where all four helix pairs are antiparallel, the D, I and L helices of P450s are parallel and the E-helix is anti-parallel (Figure 1.4).[6] The heme prosthetic group is set between the I and L helices and has a single axial cysteine-thiolate ligand, in contrast to the one or two histidine residues common in the majority of other heme enzymes.

The active center of the P450 enzyme is its prosthetic group. This heme group, consists of a protoporphyrin IX with an iron occupying the center, bound to the four nitrogens of the porphyrin ring (Figure 1.5). This group is covalently linked to the enzyme through the iron via a cysteine-thiolate ligand, located on the "proximal" face of the heme. The "distal" face of the heme borders the active site and includes the oxygen binding position of the heme iron. The heme group acts as both an electron sink, receiving electrons originating from NAD(P)H, as well as the binding site for molecular oxygen. It is these two roles that allow the P450 to direct the electrons into oxygen for its activation into a reactive species.

While the heme group is the center of activity for P450s, the enzyme requires a source of electrons from a partner reductase. P450 reductases are responsible for delivering electrons that originate from NAD(P)H to the P450 heme. P450s are commonly divided into two classes defined by the nature of the reductase partner. "Class I" enzymes accept electrons from iron-sulfur proteins. This class is primarily populated by bacterial isoforms and mitochondrial P450s. P450cam isolated from *Pseudomonas putida* is a common example of a Class I enzyme. Its reduction partner, putidaredoxin, is an Fe_2S_2-complex enzyme that receives its electrons from a

third enzyme, putidaredoxin reductase. Putidaredoxin reductase is an FAD-containing enzyme that catalyzes the two electron oxidation of NADH, transferring an electron to each of two putidaredoxins.[7] The putidaredoxins then each transfer their electron to P450 as part of the oxidative cycle as described below.

"Class II" P450s are reduced by FAD- and FMN-containing enzymes that oxidize NAD(P)H, transferring the two electrons, in a stepwise mechanism, directly to the P450. The drug-metabolizing isoforms found in the liver are important members of this class. These isoforms are membrane-tethered enzymes found along the endoplasmic reticulum. The hepatic isoforms are all reduced by a single enzyme, human P450 reductase, also a membrane-tethered enzyme.

P450BM3, from *Bacillus megaterium*, is a member of a third class of P450s, "Class III". These enzymes are similar to the Class II enzymes, with the distinction of being fusions of both the heme-containing domain and the FAD/FMN-containing reductase. Unlike the membrane-bound Class II enzymes, Class III enzymes are soluble.

C. Cytochrome P450 Catalytic Cycle

As monooxygenases, P450s catalyze the insertion of a single oxygen atom derived from molecular oxygen into a substrate. The reaction requires two electrons derived from NAD(P)H with the formation of water as a second product (Eq. 1.1). In fact, the role of the P450 is the

$$\mathbf{R + O_2 + 2\ e^- + 2\ H^+ \rightarrow RO + H_2O\ (Eq.\ 1.1)}$$

activation of molecular oxygen to generate an ROS capable of performing the many oxidations attributed to the enzyme. Generation of this ROS makes up the majority of the enzyme's catalytic cycle (Figure 1.6). The catalytic cycle is a multi-step mechanism comprised of electron

and proton transfers to reduce molecular oxygen to a water molecule and an oxene coordinated to the heme iron.

The catalytic cycle is initiated by the binding of a substrate. In its resting state, the heme iron is in a hexacoordinate, octahedral state with a formal charge of +3. The four heme nitrogens and a cysteine thiolate contribute five of the ligands to the iron. The sixth position is occupied by a coordinated water molecule on the active site face of the heme. This face is termed the distal face with the cysteine thiolate located on the proximal face. The hexacoordinate iron has a low reduction potential, approximately -400 mV and -330mV as measured in the bacterial isoforms BM3 [8, 9] and P450cam,[10] respectively. However, when a substrate is bound in the active site, the water molecule is displaced, forcing the heme iron to become pentacoordinate (Figure 1.6, Step I). Loss of the sixth ligand increases the reduction potential of the heme iron. In BM3, saturated with arachidonate, the reduction potential was measured at -249 mV [8] and -289 mV.[9] For P450cam, saturated with its native substrate camphor, the reduction potential was measured as -163 mV.[10] The large increase in reduction potential poises the heme iron to accept an electron from the partner reductase, progressing the catalytic cycle (Figure 1.6, Step II). The change in the reduction potential is important since the hexacoordinate iron has a potential too low to be reduced by the partner reductase. Requiring the displacement of water by a substrate prevents the reduction of the heme iron and, in turn, the initiation of the cycle in the absence of substrate.

Upon accepting an electron from the reductase, the heme iron is formally reduced to a +2 state and is now able to bind molecular oxygen (Figure 1.6, Step III), which begins oxygen activation. In a rate-determining step, the Fe^{II}-O_2 species accepts a second electron from the reductase to reduce the O_2 to an iron-peroxo species, Fe^{II}-$O_2^{\cdot -}$ (Figure 1.6, Step IV). The iron-

peroxo species then accepts the first of two proton transfers to become an iron-hydroperoxo species, termed Cmpd 0 (Figure 1.6, Step V). Both the iron-peroxo and Cmpd 0 species are hypothesized ROSs in P450-mediated oxidation and are a focus of discussion later in this work. The second proton transfer can occur at either of the two oxygen atoms. Protonation of the proximal oxygen (closest to the iron) results in the formation of hydrogen peroxide which is released to solution returning the enzyme to its resting state (Figure 1.6, Step S). This unproductive pathway is frequently observed in systems with loosely bound substrates and is characterized by partial decoupling of NAD(P)H consumption from substrate oxidation.

Protonation of Cmpd 0 at the distal oxygen results in the release of water to form a species equivalent to atomic oxygen (or oxene) coordinated to the heme iron (Figure 1.6, Step VI). This species has long been proposed as the major contributor to P450-mediated oxidations. The electrophilic nature of the iron-oxene (Cmpd I) is the driving force for its ability to perform the many oxidations that are attributed to P450s, including aliphatic hydroxylation. While substrate oxidation is represented as a single step in Figure 1.6 (Step VII), the actual mechanisms of oxidation are dependent on the type of oxidation and may involve multiple steps for product formation. The processes involved in Step VII for the mechanism of carbon hydroxylation are the focus of this work.

The final step in the P450 catalytic cycle is the release of the product in exchange for a water to return the enzyme to its resting state (Figure 1.6, Step VIII). As can be seen, the majority of the P450 enzyme's contribution to oxidation is the activation of molecular oxygen to the reactive Cmpd I and that this activation is dependent only on the presence of the substrate and not on the nature of the substrate. With an expectedly powerful oxidant in the iron-oxene and a substrate

preference dependent only on its ability to bind and displace water, P450s are unsurprisingly promiscuous enzymes capable of oxidizing almost any compound that initiates its cycle.

D. Surrogate Oxygen Donors

For decades, the Cmpd I species of Cytochrome P450s had only been hypothesized, remaining unobserved. However, since its proposal by Groves, *et al*,[11] it has been generally accepted as the major reactive species in P450-mediated oxidations. Recently, reports of spectroscopic verification of Cmpd I have been published.[12-14] To observe Cmpd I, Newcomb, *et al*, used laser flash photolysis (LFP) on a peroxynitrite-generated P450 Cmpd II species in P450 119.[12] Cmpd II is a one-electron reduced Cmpd I, essentially a seven-electron oxygen coordinated to the heme. Upon excitation of Cmpd II via LFP, a new species was observed with UV-visible absorption spectroscopy which they report as Cmpd I. Further work by Newcomb's group demonstrated temperature-dependent oxidation rates of benzyl alcohol in a low-temperature LFP system that they tie to Cmpd I, again, with UV-Visible absorption spectra.[14] Around the same time as the first work with LFP-generated Cmpd I was published, Raner, *et al*, published their work observing oxygen intermediates derived from surrogate oxygen donors. Using stopped-flow UV-visible absorption spectroscopy, they demonstrated the formation of a short-lived intermediate with *m*-chloroperbenzoic acid (mCPBA). They assigned this species as Cmpd I.

Interestingly, in the reported observations of Cmpd I, the species is generated through a method other than the native P450 catalytic cycle. This is because the putative Cmpd I is expected to be very reactive to the substrate and, in comparison to the prior, slower steps of electron, and even, proton transfer, much shorter lived than prior intermediates. It is for this

reason that surrogate oxygen donors have been developed as a means to directly form Cmpd I. With Cmpd I essentially a six-electron oxygen, or oxene, coordinated to the heme iron, the species could, in theory, be generated by direct donation of an oxene to the resting enzyme. Organic chemistry offers many possible oxene carriers including peroxides, peracids, iodosylbenzenes, periodates, and *N*-oxides, all of which have been used as oxygen donors for generation of a proposed Cmpd I species.

The first examples of oxygen surrogates came in the early 70's from the finding that hydrogen peroxide could support substrate oxidations in the absence of NADPH and molecular oxygen. This was quickly followed by the discovery that organic peroxides, such as cumene hydroperoxide (CHP), and oxidized halogens, such as periodate, perchlorate and iodosylbenzene (PhIO), were also capable of supporting substrate oxidation (Figure 1.7).[15, 16] Since then, CHP and PhIO have been used extensively as mechanistic probes in P450-mediated oxidations.[13, 17-20]

As models of the native P450-mediated oxidations, it is required that these oxygen surrogates demonstrate mechanisms similar to the native system. Yet, discrepancies have been seen between the native and surrogate-supported systems. Bichara, *et al* evaluated the oxidation of propranolol by P450 2D6 with the native and CPH-supported systems.[21] Where the CPH-supported system only demonstrated hydroxylation of propranolol, as had been seen in previous studies, the native NADPH/O_2 system generated the hydroxylated product and an *N*-desisopropylation product. They concluded that caution should be taken in the interpretation of CPH-generated results as CPH is not universal in its reflection of the native system. In work with *N*-methyl-4-phenyl-1,2,3,6-tetrahydropyridine (MPTP) oxidation also in P450 2D6, Modi, *et al* found differences in product formations between the native NADPH/O_2- and CHP-

supported systems.[22] Where the CHP-supported system only demonstrated *N*-demethylation of MPTP to 4-phenyl-1,2,3,6-tetrahydropyridine (PTP), the native system showed two products, PTP and *N*-methyl-4-(*p*-hydroxyphenyl)-1,2,3,6-tetrahydropyridine. They attributed the product branching to allosteric effects from the binding of the reductase. Hanna, *et al*, expanded upon the previous work observing the product formations from MPTP, metoprolol and bufurolol with P450 2D6 in native, CPH-supported and PhIO-supported systems.[23] CPH and PhIO both demonstrated different product formation ratios than the native system, however, these ratios were unaffected by the presence or absence of reductase. They concluded that CHP and PhIO must follow mechanisms of oxidation that differed from the native system. In the case of the PhIO-supported reactions, this conclusion was further supported by the incorporation of ^{18}O from labeled water into the products, a feature not seen in the native or CHP-supported systems. Support for the differences in mechanisms between the native, CPH-supported and PhIO-supported systems had been seen earlier by Guengerich, *et al*. In a study evaluating the mechanism of *N*-demethylation of substituted *N*,*N*-dimethylanilines (DMAs), they observed differing kinetic isotope effects between the three different systems.[18] The native system demonstrated small isotope effects of 1.7 and 2.3 for *N*,*N*-dimethylaniline (DMA) and 4-methoxy-*N*,*N*-dimethylaniline, respectively. In contrast, the surrogate-supported systems showed higher isotope effects of 3.7/3.4 and 6.7/7.3, for CPH and PhIO, respectively.

To explain the isotope effect differences seen with the native and PhIO-supported systems, Cho, *et al* performed theoretical calculations for the oxygen donation by PhIO and the subsequent *N*-demethylation of DMA. They demonstrated that differences in kinetic isotope effects may arise from different spin-states of the Cmpd I generated: Cmpd I generated in the

native system would be in a doublet state, but Cmpd I generated from PhIO might be in a quartet spin-state.

In contrast to the inconsistencies that are seen with CPH and PhIO, *N*,*N*-dimethyl aniline *N*-oxides (DMAOs) (Figure 1.7) have been shown to follow a mechanism of *N*-dealkylation similar to that of the native P450 system. Dowers, *et al* tested a series of *p*-substituted DMAOs with bacterial P450cam and human P450 2E1, with the expectation that the reactive species generated from oxygen donation would then react with the product aniline (Figure 1.8).[19] They measured isotope effects for the *N*-demethylation of the DMAOs and compared them to those generated by the native system. They observed an isotope effect profile identical to that seen in the native NAD(P)H/O_2 systems. They concluded that DMAOs generate an oxidant that performs *N*-dealkylation with the same mechanism as the native system, and that this oxidant was Cmpd I. This was supported by Cho, *et al* in their study with PhIO, where they concluded that DMAOs generate a low-spin (doublet) Cmpd I, similar to the native system.[20] However, where DMAOs show significant metabolism of their product anilines, they had not been shown to support oxidation of secondary compounds, including other DMAs. Further, while spectroscopic evidence has been recently published for the formation of Cmpd I in P450s, its formation and connection to known oxidations has not been demonstrated. Development of a new DMAO for the purpose of extending oxygen surrogacy to secondary compounds as well as a means to confirm the formation of a Cmpd I species is the focus of Chapter 2. Chapter 3 addresses the use of such a surrogate for elucidating the mechanism of *N*-dealkylation by Cytochrome P450.

E. P450-Mediated *N*-Dealkylation

Cytochrome P450s catalyze a variety of oxidations including *N*- and *S*-oxidation, *N*- and *O*-dealkylation, olefin epoxidation, and aromatic and aliphatic hydroxylations (Figure 1.2). The mechanisms of these oxidations have been a focus of P450 research for decades. Since Groves, *et al* proposed a mechanism of hydrogen atom abstraction by an iron-oxene species for aliphatic hydroxylation,[11] the iron-oxene, as Cmpd I, has been the consensus species for the majority of P450-mediated oxidations. However, even if Cmpd I is assigned as the oxygenating species in P450-mediated reactions, mechanisms of oxidation may still be unclear. P450-mediated *N*-dealkylation of amines is such an example. In the early 80's, Miwa, *et al* measured isotope effects for the *N*-demethylation of *N*-methyl-*N*-(trideuteriomethyl)aniline in various heme-containing enzymes measuring small values of 1.6-1.8 in P450s and chloroperoxidase and high values ranging from 5-10 in other enzymes.[24] They explained that the large isotope effect values seen with peroxidases and hemoglobin and myoglobin indicated a symmetrical breaking of the C-H bond, supporting a mechanism in these enzymes of abstraction of an α-hydrogen by Cmpd I, similar to the consensus mechanism for aliphatic hydroxylation (Figure 1.9). This reaction would generate a carbon-centered radical and a protonated Cmpd II, which then rebounds to form a carbinolamine. Hereafter, this mechanism will be referred to as the hydrogen atom abstraction (HAT) mechanism. In contrast, the small isotope effects seen with P450s were related directly to those seen in α-hydrogen deprotonations of aliphatic amine radical-cations. They concluded that P450-mediated *N*-dealkylation must occur through a mechanism that included an aminium radical-cation. In this mechanism, a single electron transfer occurs between the amine and Cmpd I, to form the aminium radical-cation and a one-electron reduced Cmpd I,

or Cmpd II (Figure 1.10). Formation of the aminium radical-cation greatly increases the acidity of the α-proton which is transferred in a second step to the Cmpd II. The result, as with HAT, is a carbon-centered radical and a protonated Cmpd II, followed by rebound to from the carbinolamine. This mechanism is referred to as the single electron transfer (SET) mechanism.

The arguments of Miwa, *et al* were the accepted views of the mechanism of P450s until work by Dinnocenzo and Banach demonstrated that deprotonation of aminium radical-cations need not be small. They found that the deprotonation of *p*-$An_2NCH_3^{\cdot+}$ demonstrated large isotope effects (6.0-9.0) when tested against several different bases.[25] To complement the work with radical-cation deprotonation, Dinnocenzo, *et al* measured the isotope effects for the *N*-dealkylation of *para*-substituted DMAs by phenobarbital-induced rat liver microsomes and by *t*-butoxyl radical, a known hydrogen atom abstractor.[26] They found the KIEs, and their dependence on substituent groups, to be identical between the two systems, and so concluded that P450-mediated *N*-dealkylation actually undergoes a HAT mechanism. This was further supported by the work of Guengerich, *et al* who found the similar isotope effects (1.56-3.9) and dependence on substituent groups in purified P450 2B1. In contrast, similar to the earlier studies, they found large isotope effects (2.9-13.3) in horseradish peroxidase (HRP), which showed a reversed, though less stringent, dependency on substituent groups. The current consensus on HRP is a SET mechanism for *N*-dealkylation. Strong evidence for this comes from the observation of aminium radical-cations formed from amines by HRP in EPR studies.[27, 28]

In recent years, work by Hanzlik's group has further supported HAT for *N*-dealkylation by P450.[29, 30] They found that the metabolism of *N*-cyclopropyl-*N*-methylaniline (CPMA) by HRP generated strictly cyclopropyl ring-opened products with *N*-methylquinolinium as the major product (Figure 1.11).[29] This was explained with a SET mechanism, where generation of the

nitrogen-centered radical results in a rapid ring-opening prior to any subsequent deprotonation. In contrast, the metabolism of CPMA by P450 results solely in the ring-closed products *N*-cyclopropylaniline and cyclopropanone hydrate (Figure 1.11).[30] This was rationalized by hydrogen abstraction at the α-carbon to form a carbon-centered radical, which would not induce opening of the cyclopropyl ring.

While these studies point strongly toward a HAT mechanism, the mechanism still requires the role of the putative P450 Cmpd I. However, with the common surrogates of CHP and PhIO demonstrating behavior dissimilar to P450s, a different probe for the modeling of P450-mediated reactions and the formation of Cmpd I is necessary. A potential probe may be found in the DMAOs. Dowers, *et al* have shown that DMAOs present a possible model for oxygen donation to form a Cmpd I species followed by an *N*-dealkylation similar to that seen by the native system. Demonstrating that DMAOs generate a Cmpd I species and that this species performs *N*-dealkylation similar to that seen in the native system would support DMAOs as important models for P450-mediated oxidations. Use of these probes to support a Cmpd I-directed HAT mechanism for *N*-dealkylation by P450 is the focus of Chapters 2 and 3.

F. Reactive Oxygen Species and the Active Site Threonine

Though sequence homology between P450 isoforms is low, there are a few residues that are highly conserved. In addition to the requisite cysteine for heme ligation, an active site "acid-alcohol" pair is found in a large variety of P450s.[5] This pair generally consists of an aspartate and a threonine. The highly conserved nature of the alcohol has led to studies involving the site-directed mutagenesis of this residue. These studies have implicated the hydroxyl group in the proton transfer mechanism for formation of Cmpd I (and perhaps Cmpd 0) (Figure 1.6, Steps V

and VI). Mutations of this threonine to aliphatic residues in P450cam (Thr-252) and P450BM3 (Thr-268) showed a marked reduction in the hydroxylations of camphor and laurate, respectively.[31-33] Further, uncoupling of NAD(P)H from product formation was observed in the formation of water and hydrogen peroxide. These studies concluded that loss of the hydroxyl group disrupted the productive protonation of Cmpd 0, prolonging its existence and permitting the unproductive protonation of Cmpd 0 to form hydrogen peroxide.

The proposed buildup of Cmpd 0 in the mutant enzymes has led to implications of the role of Cmpd 0 in P450-mediated reactions. In studies comparing epoxidation to allylic hydroxylation in small molecule olefins, Vaz, *et al* observed a shift in the ratio of products towards epoxidation in mutants compared to wild-type 2E1 and 2B4.[34] They concluded that Cmpd 0 was responsible for the observed epoxidation and that slow conversion to Cmpd I explained the reduced rates of allylic hydroxylation. Through the use of cyclopropyl-containing compounds as radical clocks, Newcomb and coworkers concluded that a carbocation intermediate derived from Cmpd 0 contributed to product formation.[35-37] In work with *N*,*N*-dimethyl-4-(methylthio)aniline, Volz, *et al* showed an increase in the ratio of sulfoxidation to *N*-demethylation with the T268A mutant of P450BM3 relative to the wild-type.[38] They also showed that deuterium labeling of the *N*-methyl groups did not demonstrate isotopically sensitive branching[39] to sulfoxidation. While offering the role of Cmpd 0 in sulfoxidation as only one of the possible explanations, they concluded the two oxidations must derive from two different oxidants.

Shaik and coworkers have proposed a different model to explain the “second oxidant”.[40, 41] Using density functional calculations, they have compared ethene epoxidation by Cmpd 0 and Cmpd I. Where low barriers (14-15 kcal/mol) were found for the epoxidation of ethene by Cmpd I,[40] large barriers (37-53 kcal/mol) were observed for epoxidation mediated by Cmpd

0.[41] Further, protonation of Cmpd 0 decomposed to Cmpd I formation and loss of water estimating the basicity of Cmpd 0 between water and hydroxide anion.[41] They concluded that the large barriers for epoxidation argued against Cmpd 0 as an effective oxidant, reinforcing its role as a base for conversion to Cmpd I. Interestingly, the calculations described different pathways for epoxidation by Cmpd I depending on its spin-state. Where the quartet-state Cmpd I demonstrated a stepwise mechanism for epoxidation of ethene, the doublet-state showed an essentially barrierless conversion from the intermediate to epoxide, resulting in a concerted mechanism. These studies led to the proposal that Cmpd I behaves as two unique oxidants through unique spin-states. This model has been termed the "two-state reactivity" model (TSR). Theoretical calculations of sulfoxidation[42] and *N*-dealkylation[20] by Shaik and coworkers have further demonstrated unique mechanisms dependent on spin-states and that each chemistry has an energetic preference for a specific spin-state.

Coon and coworkers have offered the iron-peroxo species prior to Cmpd 0 as a nucleophilic oxidant in the deformylation of aldehydes by P450.[43, 44] They showed that deformylation of cyclohexanecarboxaldehyde occurred both by the T302A mutant of P450 2B4[44] and by wild-type supported by the oxygen surrogate hydrogen peroxide.[43] As both systems were expected to result in the accumulation of Cmpd 0 and the iron-peroxo species, they concluded that the nucleophilic iron-peroxo species was responsible for the deformylation.

With a variety of oxidations appearing to derive from disparate oxidants, a clear picture of the involvement of the proposed oxidants has been elusive. However, all the examples have been comparisons of product formation rates and ratios with the assumption that observations are the result of a buildup of Cmpd 0. Largely unrecognized is that changes in the active site may elicit regioselectivity changes, directly affecting product formations. Clear mechanistic evaluations of

single oxidations comparing wild-types and mutants have not been performed. To begin to address this, we evaluated the mechanism of *N*-demethylation by P450 BM3 F87A, containing the wild-type threonine-268, and its T268V mutant. This work is discussed in Chapter 4.

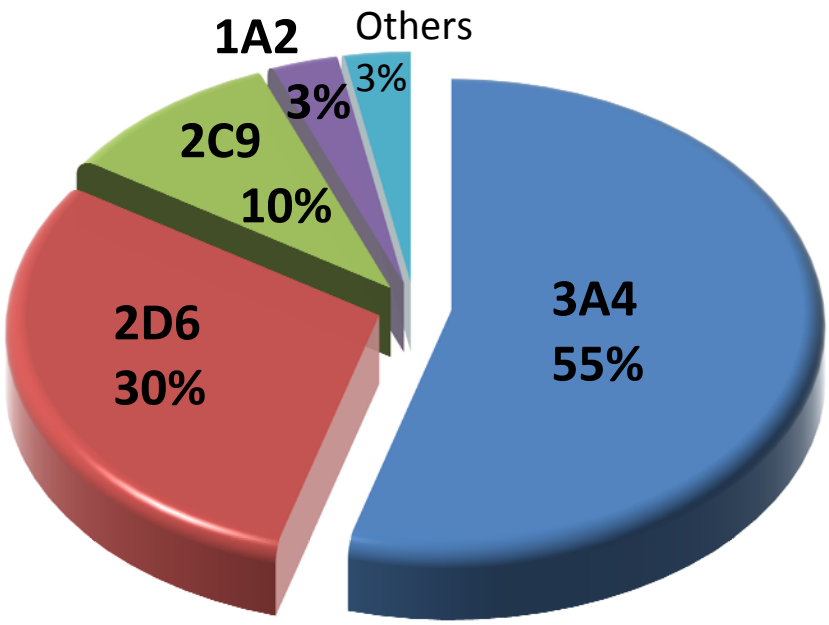

Figure 1.1. Contributions of P450 isoforms to the total metabolism of marketed drugs by Cytochromes P450.

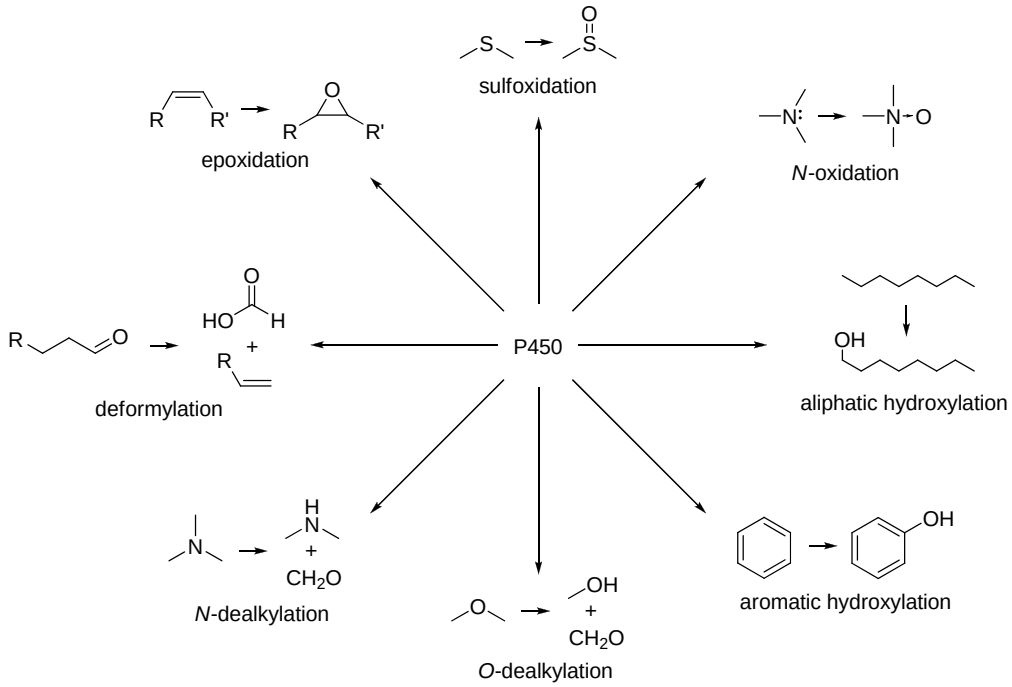

Figure 1.2. Oxidations catalyzed by Cytochromes P450.

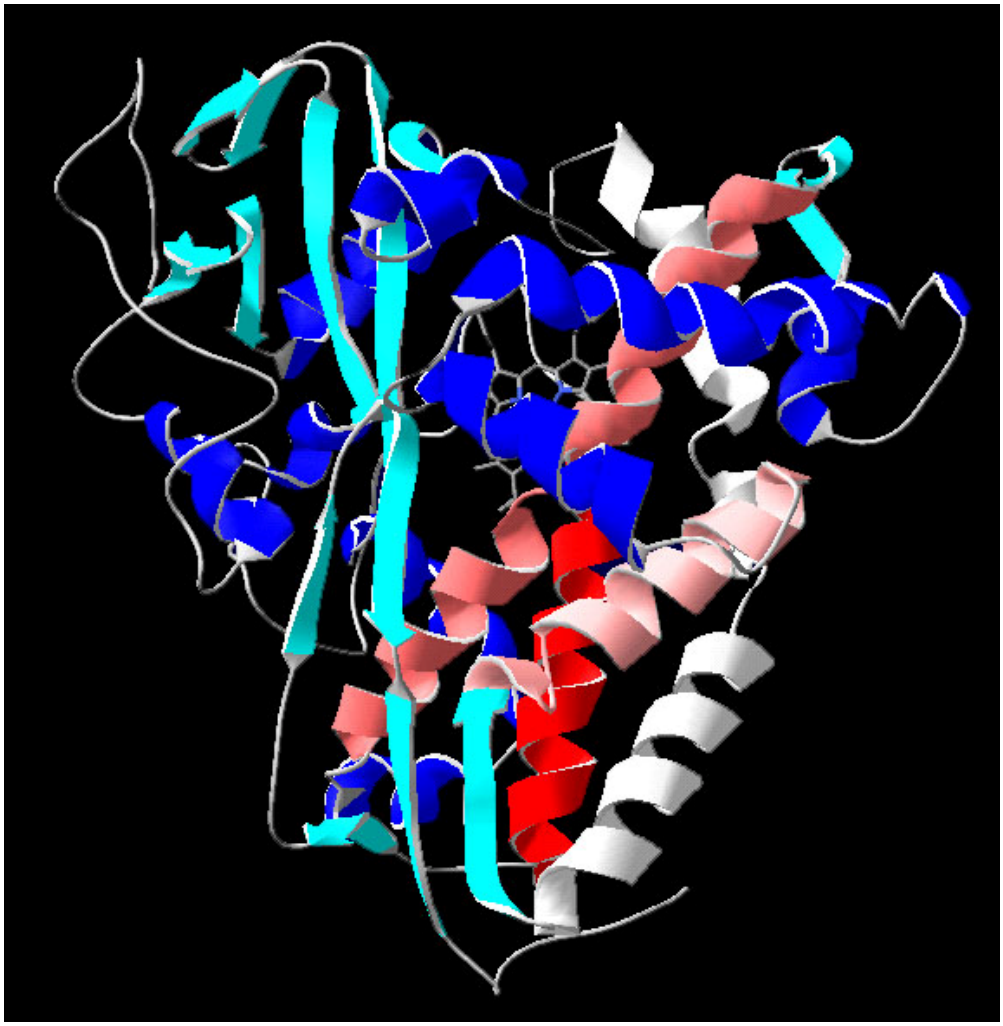

Figure 1.3. P450cam crystal structure (2CPP).[45] White: D-helix; Pink: E-helix; Rose: I-helix; Red: L-helix; Blue: other helices; Cyan: β-strands; Heme is in center of picture in stick model.

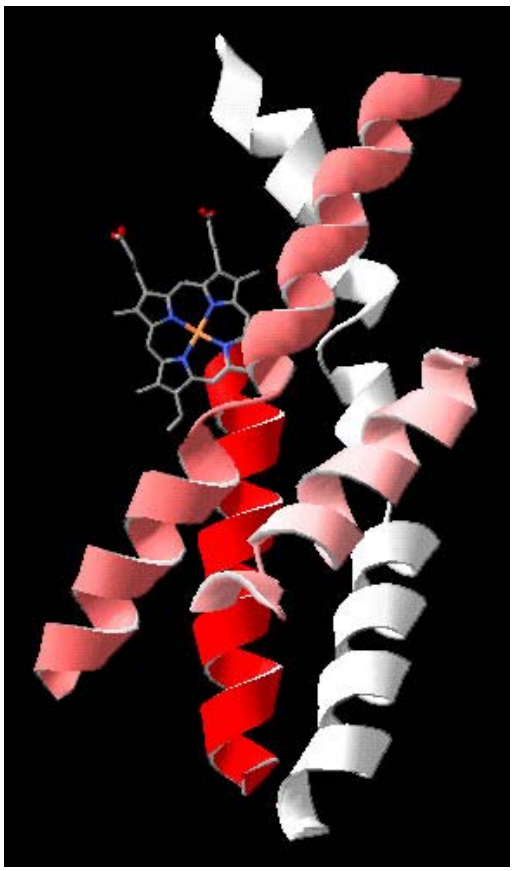

Figure 1.4. Crystal structure of P450cam showing only the heme and four-helix bundle. White: D-helix; Pink: E-helix; Rose: I-helix; Red: L-helix; Heme is represented in stick model.

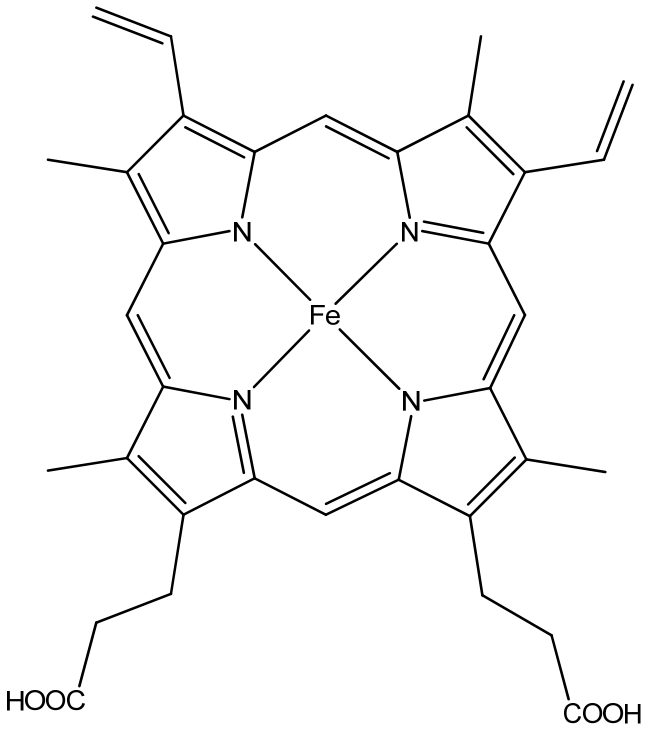

Figure 1.5. Heme prosthetic group of Cytochromes P450. The view is of the proximal (thiolate-binding) face.

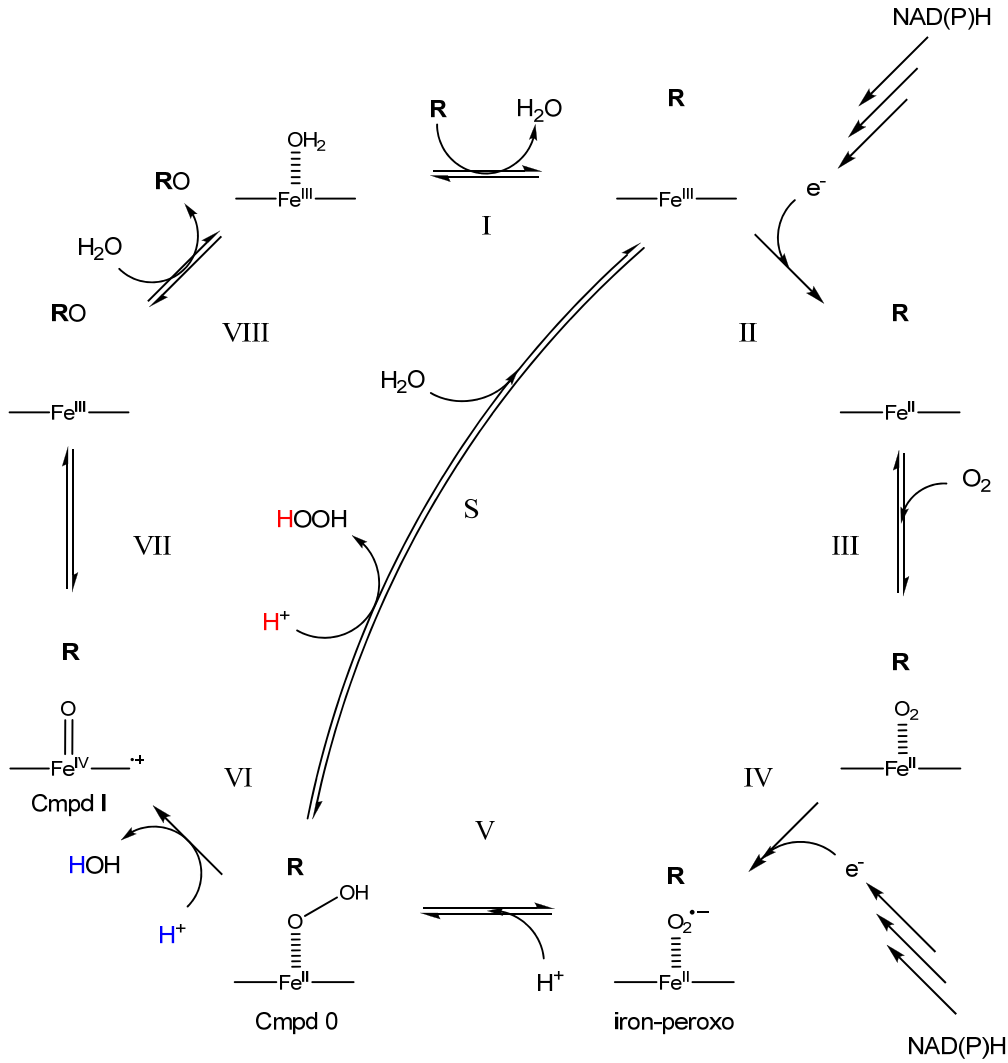

Figure 1.6. The P450 catalytic cycle. R, substrate; S, peroxide shunt

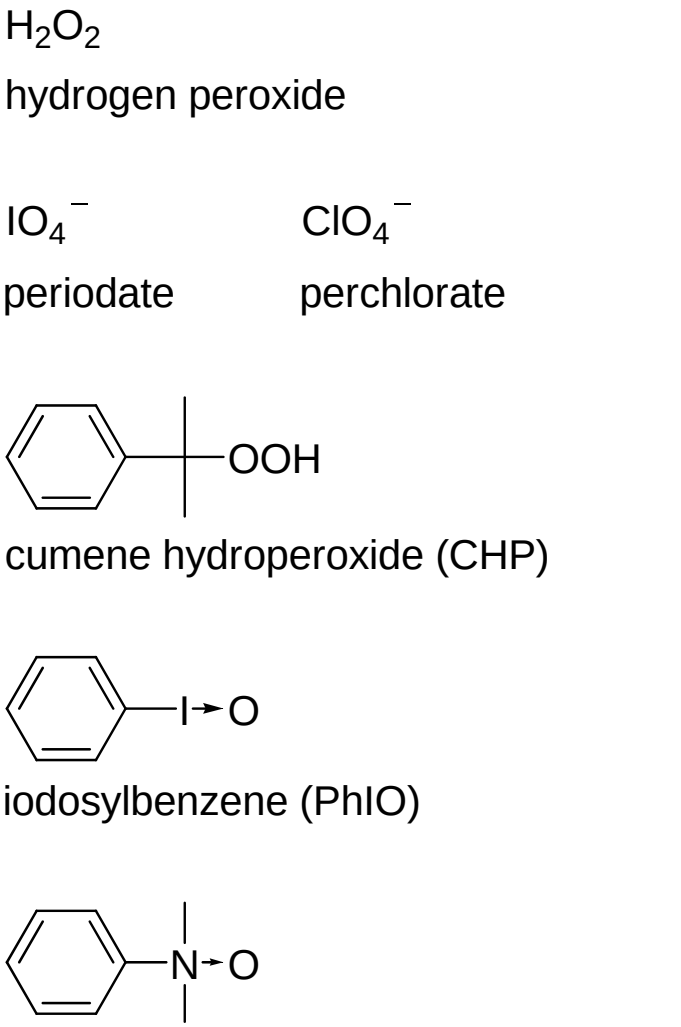

Figure 1.7. Common compounds used as oxygen surrogates with Cytochromes P450.

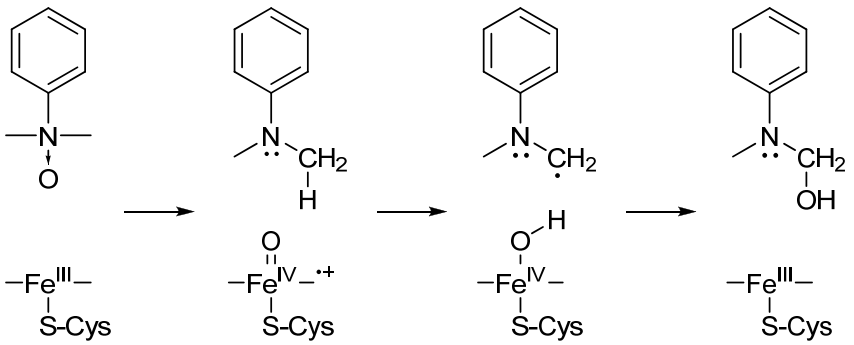

Figure 1.8. Mechanistic scheme for oxygen donation by an anilinic *N*-oxide followed by *N*-dealkylation.

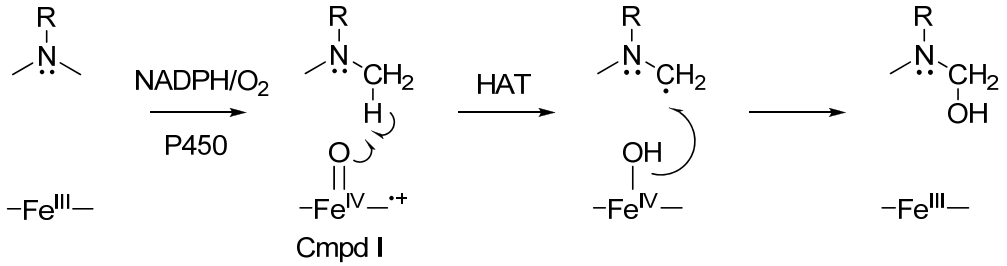

Figure 1.9. Proposed hydrogen atom transfer (HAT) mechanism for *N*-dealkylation by Cytochromes P450.

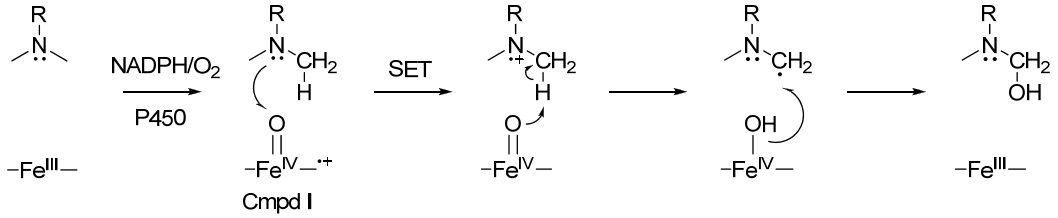

Figure 1.10. Proposed single electron transfer (SET) mechanism for *N*-dealkylation by Cytochromes P450.

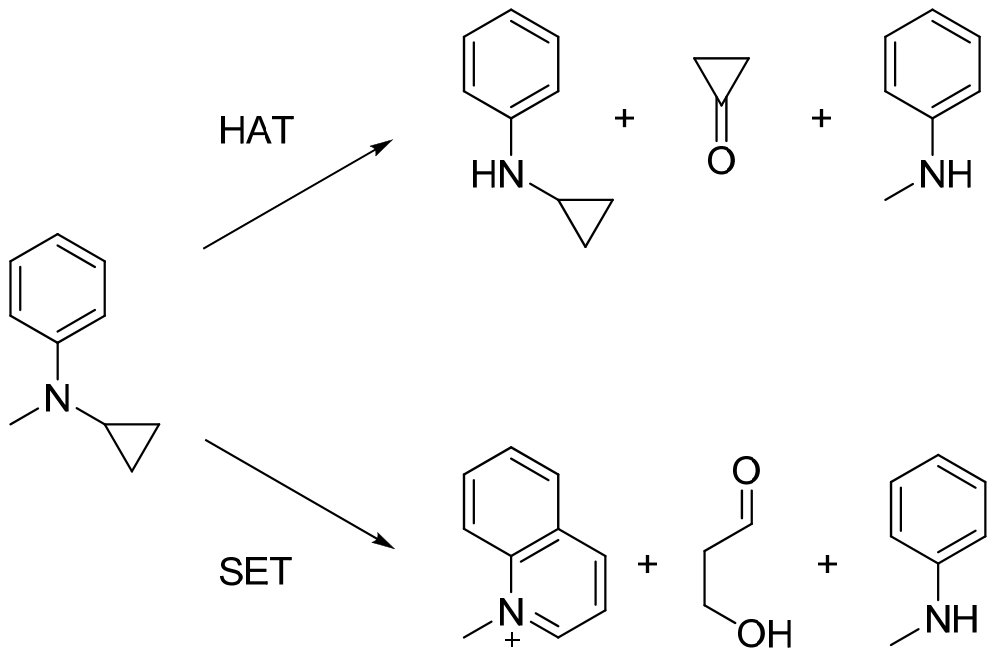

Figure 1.11. Products of *N*-cyclopropyl-*N*-methylaniline metabolism by hydrogen atom transfer (HAT) and single electron transfer (SET) mechanisms.

References

1. Nelson, D. *Cytochrome P450 Homepage*. 2009 August 24, 2009 [cited; Available from: http://drnelson.utmem.edu/CytochromeP450.html.
2. Guengerich, F.P., *Cytochrome P450 and Chemical Toxicology.* Chemical Research in Toxicology, 2008. **21**(1): p. 70-83.
3. Dong, H., et al., *Involvement of Human Cytochrome P450 2D6 in the Bioactivation of Acetaminophen.* Drug Metabolism and Disposition, 2000. **28**(12): p. 1397-1400.
4. Larson, A.M., et al., *Acetaminophen-induced acute liver failure: Results of a United States multicenter, prospective study.* Hepatology, 2005. **42**(6): p. 1364-1372.
5. Denisov, I.G., et al., *Structure and Chemistry of Cytochrome P450.* Chemical Reviews, 2005. **105**(6): p. 2253-2278.
6. Presnell, S.R. and F.E. Cohen, *Topological distribution of four-alpha-helix bundles.* Proceedings of the National Academy of Sciences of the United States of America, 1989. **86**(17): p. 6592-6596.
7. Kuznetsov, V.Y., et al., *The Putidaredoxin Reductase-Putidaredoxin Electron Transfer Complex.* Journal of Biological Chemistry, 2005. **280**(16): p. 16135-16142.
8. Daff, S.N., et al., *Redox Control of the Catalytic Cycle of Flavocytochrome P-450 BM3* Biochemistry, 1997. **36**(45): p. 13816-13823.
9. Ost, T.W.B., et al., *Phenylalanine 393 Exerts Thermodynamic Control over the Heme of Flavocytochrome P450 BM3* Biochemistry, 2001. **40**(45): p. 13421-13429.
10. Martinis, S.A., et al., *Probing the Heme Iron Coordination Structure of Pressure-Induced Cytochrome P420cam* Biochemistry, 1996. **35**(46): p. 14530-14536.

11. Groves, J.T., et al., *Aliphatic hydroxylation by highly purified liver microsomal cytochrome P450. Evidence for a carbon radical intermediate.* Biochemical and Biophysical Research Communications, 1978. **81**: p. 154-160.

12. Newcomb, M., et al., *Cytochrome P450 Compound I.* Journal of the American Chemical Society, 2006. **128**(14): p. 4580-4581.

13. Raner, G.M., et al., *Spectroscopic investigations of intermediates in the reaction of cytochrome P450BM3-F87G with surrogate oxygen atom donors.* Journal of Inorganic Biochemistry, 2006. **100**(12): p. 2045-2053.

14. Wang, Q., et al., *Quantitative Production of Compound I from a Cytochrome P450 Enzyme at Low Temperatures. Kinetics, Activation Parameters, and Kinetic Isotope Effects for Oxidation of Benzyl Alcohol.* Journal of the American Chemical Society, 2009. **131**(30): p. 10629-10636.

15. Ellin, A. and S. Orrenius, *Hydroperoxide-supported cytochrome P-450-linked fatty acid hydroxylation in liver microsomes.* FEBS Letters, 1975. **50**(3): p. 378-381.

16. Gustafsson, J.-Å. and J. Bergman, *Iodine- and chlorine-containing oxidation agents as hydroxylating catalysts in cytochrome P-450-dependent fatty acid hydroxylation reactions in rat liver microsomes.* FEBS Letters, 1976. **70**(1-2): p. 276-280.

17. Yamazaki, H., et al., *Roles of Divalent Metal Ions in Oxidations Catalyzed by Recombinant Cytochrome P450 3A4 and Replacement of NADPH-Cytochrome P450 Reductase with Other Flavoproteins, Ferredoxin, and Oxygen Surrogates.* Biochemistry, 1995. **34**(26): p. 8380-8389.

18. Guengerich, F.P., C.H. Yun, and T.L. Macdonald, *Evidence for a 1-electron oxidation mechanism in N-dealkylation of N,N-dialkylanilines by cytochrome P450 2B1. Kinetic*

hydrogen isotope effects, linear free energy relationships, comparisons with horseradish peroxidase, and studies with oxygen surrogates. Journal of Biological Chemistry, 1996. **271**(44): p. 27321-27329.

19. Dowers, T.S., et al., *Kinetic isotope effects implicate the iron-oxene as the sole oxidant in P450-catalyzed N-dealkylation.* Journal of the American Chemical Society, 2004. **126**(29): p. 8868-8869.

20. Cho, K.Y., et al., *"Formation of the Active Species of Cytochrome P450 by Using Iodosylbenzene: A Case for Spin-Selective Reactivity".* Chemistry: A European Journal, 2007. **13**: p. 4103-4115.

21. Bichara, N., et al., *Propranolol Hydroxylation and N-desisopropylation by Cytochrome P4502D6.* Drug Metabolism and Disposition, 1996. **24**(1): p. 112-118.

22. Modi, S., et al., *1-Methyl-4-phenyl-1,2,3,6-tetrahydropyridine as a Substrate of Cytochrome P450 2D6: Allosteric Effects of NADPH-Cytochrome P450 Reductase* Biochemistry, 1997. **36**(15): p. 4461-4470.

23. Hanna, I.H., et al., *Diversity in Mechanisms of Substrate Oxidation by Cytochrome P450 2D6.* Journal of Biological Chemistry, 2001. **276**(43): p. 39553-39561.

24. Miwa, G.T., et al., *The use of intramolecular isotope effects to distinguish between deprotonation and hydrogen atom abstraction mechanisms in cytochrome P-450- and peroxidase-catalyzed N-demethylation reactions.* Journal of Biological Chemistry, 1983. **258**(23): p. 14445-14449.

25. Dinnocenzo, J.P. and T.E. Banach, *Deprotonation of tertiary amine cation radicals. A direct experimental approach.* Journal of the American Chemical Society, 1989. **111**(23): p. 8646-8653.

26. Dinnocenzo, J.P., S.B. Karki, and J.P. Jones, *On Isotope Effects for the Cytochrome P-450 Oxidation of Substituted N,N-Dimethylanilines.* Journal of the American Chemical Society, 1993. **115**: p. 7111-7116.

27. Van der Zee, J., et al., *The oxidation of N-substituted aromatic amines by horseradish peroxidase.* Journal of Biological Chemistry, 1989. **264**(33): p. 19828-19836.

28. Griffin, B.W. and P.L. Ting, *Mechanism of N-demethylation of aminopyrine by hydrogen peroxide catalyzed by horseradish peroxidase, metmyoglobin, and protohemin.* Biochemistry, 2002. **17**(11): p. 2206-2211.

29. Shaffer, C.L., M.D. Morton, and R.P. Hanzlik, *N-Dealkylation of an N-Cyclopropylamine by Horseradish Peroxidase. Fate of the Cyclopropyl Group.* Journal of the American Chemical Society, 2001. **123**(35): p. 8502-8508.

30. Shaffer, C.L., et al., *Formation of Cyclopropanone during Cytochrome P450-Catalyzed N-Dealkylation of a Cyclopropylamine.* Journal of the American Chemical Society, 2002. **124**(28): p. 8268-8274.

31. Imai, M., et al., *Uncoupling of the cytochrome P-450cam monooxygenase reaction by a single mutation, threonine-252 to alanine or valine: possible role of the hydroxy amino acid in oxygen activation.* Proceedings of the National Academy of Sciences of the United States of America, 1989. **86**(20): p. 7823-7827.

32. Martinis, S.A., et al., *A conserved residue of cytochrome P-450 is involved in heme-oxygen stability and activation.* Journal of the American Chemical Society, 1989. **111**(26): p. 9252-9253.

33. Yeom, H., et al., *The Role Of Thr268 In Oxygen Activation Of Cytochrome P450(Bm-3).* Biochemistry, 1995. **34**(45): p. 14733-14740.

34. Vaz, A.D.N., D.F. McGinnity, and M.J. Coon, *Epoxidation of olefins by cytochrome P450: Evidence from site-specific mutagenesis for hydroperoxo-iron as an electrophilic oxidant.* Proceedings of the National Academy of Sciences of the United States of America, 1998. **95**(7): p. 3555-3560.

35. Newcomb, M., P.F. Hollenberg, and M.J. Coon, *Multiple mechanisms and multiple oxidants in P450-catalyzed hydroxylations.* Archives of Biochemistry and Biophysics, 2003. **409**(1): p. 72-79.

36. Chandrasena, R.E.P., et al., *Hydroxylation by the hydroperoxy-iron species in cytochrome P450 enzymes.* Journal of the American Chemical Society, 2004. **126**(1): p. 115-126.

37. Sheng, X., et al., *Kinetic Isotope Effects in Hydroxylation Reactions Effected by Cytochrome P450 Compounds I Implicate Multiple Electrophilic Oxidants for P450-Catalyzed Oxidations* Biochemistry, 2009. **48**(7): p. 1620-1627.

38. Volz, T.J., D.A. Rock, and J.P. Jones, *Evidence for two different active oxygen species in cytochrome p450 BM3 mediated sulfoxidation and N-dealkylation reactions.* Journal of the American Chemical Society, 2002. **124**(33): p. 9724-9725.

39. Jones, J.P., et al., *Isotopically sensitive branching and its effect on the observed intramolecular isotope effects in cytochrome P450 catalyzed reactions: a new method for the estimation of intrinsic isotope effects.* Journal of the American Chemical Society, 1986. **108**: p. 7074-7078.

40. de Visser, S.P., et al., *Multi-State Epoxidation of Ethene by Cytochrome P450: A Quantum Chemical Study.* Journal of the American Chemical Society, 2001. **123**(13): p. 3037-3047.

41. Ogliaro, F., et al., *Searching for the second oxidant in the catalytic cycle of cytochrome P450: a theoretical investigation of the iron(III)-hydroperoxo species and its epoxidation pathways.* Journal of the American Chemical Society, 2002. **124**(11): p. 2806-2817.

42. Sharma, P.K., S.P. De Visser, and S. Shaik, *Can a single oxidant with two spin states masquerade as two different oxidants? A study of the sulfoxidation mechanism by cytochrome p450.* Journal of the American Chemical Society, 2003. **125**(29): p. 8698-8689.

43. Vaz, A.D.N., E.S. Roberts, and M.J. Coon, *Olefin Formation in the Oxidative Deformylation of Aldehydes by Cytochrome-P-450 - Mechanistic Implications for Catalysis by Oxygen-Derived Peroxide.* Journal of the American Chemical Society, 1991. **113**(15): p. 5886-5887.

44. Vaz, A.D., et al., *Peroxo-iron and oxenoid-iron species as alternative oxygenating agents in cytochrome P450-catalyzed reactions: switching by threonine-302 to alanine mutagenesis of cytochrome P450 2B4.* Proceedings of the National Academy of Sciences of the United States of America, 1996. **93**(10): p. 4644-4648.

45. Poulos, T.L., Finzel, B.C., Howard, A.J., *High-resolution crystal structure of Cytochrome P450cam.* Journal of Molecular Biology, 1987. **195**(3): p. 687-700.

CHAPTER TWO

Pentafluoro-*N*,*N*-dimethylaniline *N*-Oxide Forms a Cmpd I-like Iron-Oxene in Cytochrome P450

(This chapter is part of a work in preparation for submission to Chemistry - A European Journal;

Authors: Kenneth M. Roberts and Jeffrey P. Jones)

This work was supported by NIH Grants ES009122 and GM84546.

Abstract

The mechanism of *N*-dealkylation mediated by Cytochrome P450 (P450) has long been studied and argued as either a single electron transfer (SET) or a hydrogen atom transfer (HAT) from the amine to the oxidant of the P450, the reputed iron-oxene (Cmpd I). In our study, anilinic *N*-oxides were used as oxygen surrogates to directly generate a P450-mediated oxidant capable of *N*-dealkylating the aniline derived from oxygen donation. These surrogates were employed to evaluate the reactive oxygen species generated by oxygen donation. In addition to the expected *N*-demethylation of the product aniline, 2,3,4,5,6-pentafluoro-*N*,*N*-dimethylaniline *N*-oxide (PFDMAO) was found capable of *N*-demethylating *N*,*N*-dimethylaniline (DMA). Rate comparisons of the *N*-demethylation of DMA supported by PFDMAO show a 27-fold faster rate than when supported by *N*,*N*-dimethylaniline *N*-oxide (DMAO). While intermolecular kinetic isotope effects were largely or completely masked, intramolecular measurements showed values reflective of those seen previously in DMAO- and the native NADPH/O_2-supported systems, 2.33 and 2.8 for the *N*-demethylation of PFDMA and DMA from the PFDMAO system, respectively. These findings, supported by DFT calculations, support a donation of an oxene from anilinic *N*-oxides to the P450 to generate Cmpd I, which, in turn, mediates the subsequent *N*-dealkylation.

Introduction

Cytochrome P450 (P450) enzymes are a ubiquitous superfamily of heme-containing monoxygenases capable of oxidizing endogenous and exogenous substrates, including the majority of clinically relevant pharmaceuticals.[1] Decades of study have been spent understanding the mechanism of P450-mediated oxidation with the general consensus that an iron (IV)-oxo porphyrin radical cation similar to the Compound I (Cmpd I) species of chloroperoxidase is the reactive oxygen species (ROS) in these reactions.[2-4]

Confirmation of mechanisms proposed to act via Cmpd I requires showing that Cmpd I elicits these reactions. However, the activation of molecular oxygen to Cmpd I is complex, involving several steps including proton and electron transfers.[1] Due to this complicated process, alternate sources of generating this species directly for use as mechanistic probes have been explored. These compounds, termed oxygen surrogates, include iodosobenzene (PhIO), cumene hydroperoxide (CuOOH), and substituted *N*,*N*-dimethylaniline *N*-oxides (DMAOs). Yet, the ROSs resulting from surrogacy have recently come into question as valid mimics of P450 Cmpd I.[4-7] Studies by Dawson's group observing Cmpd I formation by oxygen surrogates found no evidence for Cmpd I when P450 BM3 was exposed to PhIO.[4] Bichara, *et al* compared propranolol oxidation by NADPH/O_2- and CuOOH-supported P450 2D6 and found different preferences for sites of oxidation for the two oxidants.[8] In P450 2B1, Bhakta, *et al* demonstrated dramatically different products formed from the *N*-dealkylation probe *N*-cyclopropyl-*N*-methylaniline in native and PhIO-supported systems, concluding that *N*-dealkylation by PhIO did not model the native P450 mechanism.[9] Further, Guengerich, *et al* showed that the kinetic isotope effects (KIEs) of the *N*-dealkylation of two substituted *N*,*N*-dimethylanilines (DMAs) by PhIO and CuOOH were large (6.7-7.3 and 3.4-3.7,

respectively) compared to the small KIEs (1.7-2.3) seen for the enzyme's native NADPH/O_2 pathway.[5] This difference was supported with theoretical calculations by Shaik's group, who concluded that PhIO and NADPH/O_2 generated unique spin states of Cmpd I and that these spin states were responsible for the differing isotope effects.[7] In later work, Hanna, *et al* showed that product formations from *N*-methyl-4-phenyl-1,2,3,6-tetrahydropyridine (MPTP) varied in P450 2D6 between the native, PhIO-supported and CHP-supported systems.[6] They concluded that the differences were the result of unique mechanisms and not allosteric effects from the binding of reductase as had been previously proposed.[10]

In contrast, anilinic *N*-oxides, such as *N*,*N*-dimethylaniline *N*-oxide (DMAO), have recently been shown to generate an oxidant that strongly mimics that of NADPH/O_2. Dowers, *et al*, compared the KIEs of the *N*-demethylation of substituted DMAs by their respective *N*-oxides and by NADPH/O_2 and found them to be identical.[11] It was hypothesized that DMAOs donate a six-electron oxygen (oxene) directly generating Cmpd I which in turn oxidizes the resulting DMA (Figure 2.1A).

Theoretical calculations by Shaik's group supported this conclusion observing a two-step mechanism of oxygen donation forming Cmpd I followed by *N*-dealkylation.[7] Calculated energy barriers were 21 kcal/mol for the oxygen donation and 6.0 kcal/mol and 8.8 kcal/mol for *N*-dealkylation by doublet and quartet spin-states of Cmpd I, respectively. The large barrier for oxygen donation relative to *N*-dealkylation demonstrates the rate-determining nature of the oxygen donation.

Just as the putative P450 Cmpd I is expected to perform a variety of oxidations, a DMAO-generated Cmpd I would also be expected to support oxidations in addition to *N*-dealkylation, including oxidation of secondary substrates. However, in early work with a porphyrin mimetic

system, Bruice's group found DMAO unable to significantly support olefin epoxidation.[12] They rationalized that the ease of oxidation of DMA outcompeted olefin epoxidation for the putative iron-oxene (Cmpd I) and that increasing the oxygen donation rate and decreasing the rate of *N*-dealkylation would be required to facilitate oxygen surrogacy. They proposed that electron-withdrawing substituents on the aromatic ring would realize both effects and, in support of this, they successfully tested *p*-cyano-*N*,*N*-dimethylaniline *N*-oxide (CDMAO) as a surrogate oxygen donor able to support various olefin epoxidations as well as cyclohexane hydroxylation.[12]

In a study with P450 2B1, however, Seto and Guengerich found they were unable to significantly oxidize a second distinct DMA with either DMAO or CDMAO.[13] Since a DMAO-derived Cmpd I would be expected to support *N*-dealkylation of any given DMA, the inability of the DMAO-derived oxidant to support oxidation of a second DMA led them to conclude that Cmpd I was not formed. Instead, they proposed that oxygen donation resulted from homolytic cleavage of the N-O bond generating Cmpd II and the aminium radical cation (Figure 2.1B). While Cmpd II is poised to deprotonate α to the aminium radical, the oxidant would not be electrophilic enough to react with an unoxidized DMA.

In this work, we investigated the nature of the ROS generated by anilinic *N*-oxides in P450 and its ability to oxidize secondary substrates. With the identical KIE values found by Dowers, *et al* for *N*-dealkylation by DMAOs and P450,[11] we similarly hypothesized that DMAOs donate an oxene to the P450 heme to form a Cmpd I poised to oxidize the resulting DMA. Further, similar to Nee, *et al*,[12] we proposed that DMAO as a surrogate is limited by the ease of oxidation of the subsequent DMA and that increasing electron-withdrawing character on the aromatic ring would both increase the rate of oxygen donation and slow the *N*-demethylation of

the subsequent aniline. To evaluate these considerations, we employed a newly synthesized oxygen surrogate, 2,3,4,5,6-pentafluoro-*N*,*N*-dimethylaniline *N*-oxide (PFDMAO), with the expectation that the heavily electron-withdrawing fluorines would both increase the rate of Cmpd I formation and slow the rate of *N*-dealkylation, unmasking its ability to act as a surrogate. Experimental results demonstrate that oxygen donation by PFDMAO is faster than DMAO with support by theoretical calculations showing a lower barrier. We also show that the PFDMAO-derived oxidant is capable of *N*-dealkylating DMA, a substrate distinct from the generated aniline. In the surrogate system, *N*-demethylation of DMA is faster than the resulting 2,3,4,5,6-pentafluoro-*N*,*N*-dimethylaniline (PFDMA) supporting the ease of oxidation of DMA relative to the more electron-withdrawn PFDMA. Kinetic values and theoretical calculations support a mechanism of oxene donation to directly form a Cmpd I species.

Experimental Methods

Materials. Reagent or HPLC grade chemicals and solvents were purchased from Alfa Aesar (Ward Hill, MA), Aldrich (Milwaukee, WI), Fisher Scientific (Fair Lawn, NJ), EMD (Madison, WI), and Mallinckrodt Baker (Phillipsburg, NJ). Isotopically-labelled compounds were purchased from CDN Isotopes (Pointe-Claire, Quebec, CA). Tetrahydrofuran (THF) was distilled under argon from sodium and benzophenone prior to use. ^{1}H-NMR spectra were obtained at 300 MHz with a Varian Mercury 300 spectrometer equipped with a quad-detection probe (^{1}H, ^{13}C, ^{31}P and ^{19}F). ^{1}H-decoupled ^{13}C-NMR spectra were obtained at 75 MHz. ^{19}F-NMR spectra were obtained at 282 MHz. Gas chromatography/mass spectrometry was performed on a ThermoQuest Voyager GC/MS (Thermo-Finnegan) coupled to a CE Instruments GC8000Top affixed with a 30m JW Scientific DB-1 GC column. Liquid chromatography/mass spectrometry was performed on a ThermoQuest Surveyor LC affixed with an Agilent Eclipse Plus C-18 column (5 μm, 2.1 x 150 mm) coupled to a Thermo-Finnegan LCQ Advantage ESI-MS.

***N*-Oxide-Supported P450cam – General Procedure.** P450cam was expressed and purified as described previously.[14] Incubations of P450cam with PFDMAO or DMAO were performed using 20 mM *N*-oxide and 1.0 μM P450cam brought to a total volume of 1.0 mL with 100 mM phosphate buffer, pH 7.4. Samples were preincubated at 30 °C for 10 min prior to initiation with the *N*-oxide. For rate determinations, reactions were incubated at 30 °C for discrete time points up to and including 60 min. Reactions were quenched with 500 μL ethyl acetate containing 100 μM 2,3,4,5,6-pentafluoroaniline (PFA) as an internal standard. An additional 500 μL ethyl acetate was added for product extraction. Product was further extracted twice with 1.0 mL ethyl acetate. Extracts were combined and dried with $MgSO_4$. Reaction products were monitored by

gas chromatography/mass spectrometry (GC/MS) using electron impact ionization. The GC method began at 70 °C for 5 min followed first by a 10 °C/min ramp to 120 °C then by a 30 °C/min ramp to 230 °C. Ions with m/z 193.1 and 211.1 were monitored for quantitation of PFDMA and PFMA, respectively.

***N*-oxide Surrogacy Procedure.** Following the same procedure above, samples consisted of 20 mM *N*-oxide, 1.0 μM P450 cam and 20 mM DMA. Gas chromatography was performed as above monitoring ions with m/z 107.1 for *N*-methylaniline.

PFDMAO KIE Determinations. Following the same procedure above, incubations consisted of 1.0 mM of the trifluoroacetate salt of PFDMAO, 2,3,4,5,6-pentafluoro-*N*-methyl-*N*-(trideuteriomethyl)aniline *N*-oxide (PFDMA-d_3) and/or 2,3,4,5,6-pentafluoro-*N*,*N*-bis(trideuteriomethyl)aniline *N*-oxide (PFDMA-d_6) and 1.0 μM P450cam. Samples were preincubated at 30 °C for 5.0 min. Reactions were initiated by addition of PFDMAO and incubated for 20 or 60 min. Reactions were quenched with 500 μL 100 μM PFA in ethyl acetate or 100 μL 200 μM aniline in dichloromethane and worked up as above, extracting with ethyl acetate or dichloromethane, respectively. For the noncompetitive and competitive assays, ions with m/z 197.1 and 200.1 were monitored for quantitation of 2,3,4,5,6-pentafluoro-*N*-methylaniline and 2,3,4,5,6-pentafluoro-*N*-trideuteriomethylaniline, respectively. For the intramolecular assay, 3 Da spans of ions with m/z 194.6-197.6 and 197.6-200.6 were monitored correcting for isotopic overlap.

DMA KIE Determinations. Following the same general incubation procedure, incubations consisted of 1.0 mM of the trifluoroacetate salt of PFDMAO and 1.0 mM *N*,*N*-dimethylaniline (DMA) and/or *N*,*N*-bis(trideuteriomethyl)aniline (DMA-d_6) or *N*-methyl-*N*-trideuteriomethylaniline (DMA-d_3). Samples were preincubated at 30 °C for 5.0 min. Reactions were initiated by addition of PFDMAO and incubated for 20 min. Reactions were quenched with 500 μL 100 μM PFA in ethyl acetate then worked up as above. For the noncompetitive assays, 4 Da spans of ions with m/z 105.6-109.6 and 107.6-111.6 were monitored for quantitation of *N*-methylaniline and *N*-trideuteriomethylaniline, respectively. For the competitive and intramolecular assays, 3 Da spans of ions with m/z 104.6-107.6, 107.6-110.6 were monitored correcting for isotopic overlap.

CDMAO KIE Determinations. Samples of 2.0 mM *p*-cyano-*N*,*N*-dimethylaniline *N*-oxide (CDMAO) and/or *p*-cyano-*N*,*N*-bis(trideuteriomethyl)aniline *N*-oxide (CDMAO-d_6) and 10 μM P450cam in 500 μL 100 mM phosphate buffer were incubated for 60 min at 30 °C. Reactions were quenched with 1.0 mL acetonitrile containing 30 μM aniline as an internal standard followed by vortexing and centrifugation to pellet the protein. Supernatant was collected and reaction products monitored by liquid-chromatography/electrospray ionization-mass spectrometry (LC/ESI-MS). The LC method began at 5% methanol, 0.1% acetic acid in water for 2.0 mins followed by a 5% methanol/min ramp to 95% methanol, 0.1% acetic acid in water (2.0-20.0 min). Ions with m/z 133.1 and 136.1 were monitored for *N*-methyl-4-cyanoaniline and *N*-trideuteriomethyl-4-cyanoaniline, respectively.

***p*-cyano-*N*,*N*-dimethylaniline *N*-oxide hydrate.** *m*-Chloroperbenzoic acid (75%, 250 mg, 1.1 mmol) in 1.8 mL chloroform was added dropwise to a stirring solution of *N*,*N*-dimethyl-4-cyanoaniline (146 mg, 1.0 mmol) in chloroform (2 mL). Reaction was allowed to proceed for 3.0 h on ice. Product was purified by chromatography using basic alumina. Product mixture was loaded with chloroform and eluted with 25% methanol in chloroform. Solvent was removed by rotary evaporation to yield a white solid (178 mg, 99 %). ^{1}H NMR (300 MHz, $CDCl_3$): δ 2.83 (bs, 2H), 3.62 (s, 6H), 7.82 (d, 2H), 8.17 (d, 2H); $^{13}C\{^{1}H\}$ NMR (75 MHz, $CDCl_3$): δ 63.49, 113.70, 117.70, 121.61, 133.58, 158.02

***N*,*N*-dimethylaniline *N*-oxide hydrochloride.** DMA (1.27 mL, 10 mmol) was added dropwise to a mixture of *m*-chloroperbenzoic acid (75%, 3.45 g, 15 mmol) in dichloromethane (35 mL). Reaction was run for 1.5 h at room temperature and solvent removed by rotary evaporation. Product mixture was chromatographed using basic alumina. Product was loaded with chloroform and eluted with 25% methanol in chloroform. Fractions containing product were combined and rotary evaporated to remove solvent. Product was reconstituted with water (10 mL) and solution rinsed twice with diethyl ether (10 mL). Water was removed by rotary evaporation to oil. Concentrated hydrochloric acid (1 mL) was added to the oil and the mixture rotary evaporated to solid. Product was recrystallized from acetone to yield long, colorless crystals (350 mg, 20%). ^{1}H NMR (300 MHz, $CDCl_3$) δ 4.09 (s, 6H), 7.55 (m, 3H), 7.91 (d, 2H), 13.86 (bs, 1H); $^{13}C\{^{1}H\}$ NMR (75 MHz, $CDCl_3$) δ 61.06, 119.56, 130.48, 131.20, 149.03

2,3,4,5,6-pentafluoro-*N*-methylaniline. Potassium *tert*-butoxide (2.0 g, 18 mmol) was added, as above, to a solution of 2,3,4,5,6-pentafluoroaniline (2.8 g, 15 mmol) and 0.94 mL (1.0 eqs)

iodomethane (0.94 mL, 15 mmol) in 100 mL dry THF. TLC after addition of potassium *tert*-butoxide showed incomplete conversion of the starting material with a trace of doubly methylated product present. Precipitates (potassium iodide and unreacted *t*-BuOK) were removed by filtration through Celite. THF was removed from the filtrate by rotary evaporation to a volume of 5 mL. The mixture was then chromatographed over Silica 60, eluting the product with 2.5% ethyl acetate in hexanes to give 2,3,4,5,6-pentafluoro-*N*-methyl aniline (1.27 g, 43%) as a pale yellow oil. ^{1}H NMR (300 MHz, $CDCl_3$) δ 3.05 (m, 3H), 3.58 (bs, 1H); $^{13}C\{^{1}H\}$ NMR (75 MHz, $CDCl_3$) δ 33.60 (t); ^{19}F NMR (282 MHz, $CDCl_3$) δ -172.84 (m, 1F), -165.13 (m, 2F), -161.13 (d, 2F)

2,3,4,5,6-pentafluoro-*N*,*N*-dimethylaniline. Potassium *tert*-butoxide (5.0 g, 45 mmol) was added at room temperature over 10 min to a vigorously stirring solution of 2,3,4,5,6-pentafluoroaniline (2.8 g, 15 mmol) and iodomethane (2.3 mL, 38 mmol) in 100 mL dry THF, resulting in a dark red solution and white precipitate. TLC after 10 min showed complete conversion of the starting material to 2,3,4,5,6-pentafluoro-*N*,*N*-dimethylaniline. Precipitates (potassium iodide and unreacted potassium *tert*-butoxide) were removed by filtration through Celite. THF was removed from the filtrate by rotary evaporation to a volume of 5 mL. Product was purified by flash chromatography (15% chloroform in hexanes) to yield 2,3,4,5,6-pentafluoro-*N*,*N*-dimethylaniline (1.68 g, 53%) as a clear oil. ^{1}H NMR (300 MHz, $CDCl_3$) δ 2.90 (t); $^{13}C\{^{1}H\}$ NMR (75 MHz, $CDCl_3$) δ 43.71 (t); ^{19}F NMR (282 MHz, $CDCl_3$) δ -165.19 (t, 1F), -164.53 (m, 2F), -151.25 (d, 2F)

2,3,4,5,6-pentafluoro-*N*,*N*-dimethylaniline *N*-oxide trifluoroacetic acid salt. 2,3,4,5,6-pentafluoro-*N*,*N*-dimethylaniline was prepared as above through Celite filtration. THF was distilled from the filtered product mixture and the product was dissolved in 15 mL dichloromethane and stirred on ice. Trifluoroperacetic acid (TFPA) was generated *in situ* using the method of Emmons and Lucas.[15] 1.1 mL (2.5 eqs) 90% hydrogen peroxide was added dropwise to 7 mL dichloromethane on ice. To this mixture, 6.5 mL (3.0 eqs) trifluoroacetic anhydride was added dropwise over 10 min. After addition, the reaction was kept on ice for 10 min then removed and allowed to warm to room temperature. The TFPA mixture was added dropwise over 20 min to the stirring PFDMA mixture on ice. TLC showed no PFDMA immediately after addition of the TFPA. Product was extracted from the reaction mixture six times with 15 mL distilled water. Extracts were combined and rinsed three times with diethyl ether. Water was removed by rotary evaporation and product was recrystallized from THF to yield 2,3,4,5,6-pentafluoro-*N*,*N*-dimethylaniline *N*-oxide trifluoroacetic acid salt (1.9 g, 56%) as large colorless crystals. ^{1}H NMR (300 MHz, $CDCl_3$): δ 4.14 (t, 6H), 11.20 (bs, 1H); $^{13}C\{^{1}H\}$ NMR (75 MHz, $CDCl_3$): δ 62.6 (t); ^{19}F NMR (282 MHz, $CDCl_3$): δ -156.95 (m, 2F), -146.99 (m, 1F), -138.32 (d, 2F), -76.46 (s, 3F)

Computational Methods. Density functional calculations were performed using Gaussian 03[16] or Jaguar. The B3LYP[17] functional was used with the LACVP basis set with effective core potential on iron and the 6-31G on sulfur, nitrogen, carbon and hydrogen. The optimized geometries are available as supplemental material. The heme model was the abbreviated heme with an S-H fifth ligand used by Shaik and coworkers.[7]

Results and Discussion

Oxygen donation rates.

A number of questions remain about the mechanism of oxygen donation by anilinic *N*-oxides, including the rate-determining step of the pathway and the nature of the oxidant formed. We first address the rate-determining step in the *N*-oxide pathway. Figure 2.2 demonstrates a simple mechanism of *N*-oxide binding, oxygen transfer and product formation. As described above, the calculations of DMAO by Shaik's group show a much higher barrier to oxygen donation (k_3) than oxidation of the aniline (k_5), 21 kcal/mol and 6.0-8.8 kcal/mol, respectively. This higher barrier supports oxygen donation as the rate-determining step in this pathway.[7] We examined the rate-determining step experimentally using KIEs for the *N*-demethylation of an *N*-oxide by P450cam. Product formation rates for *p*-cyano-*N*,*N*-dimethylaniline *N*-oxide (CDMAO) and *p*-cyano-*N*,*N*-bis(trideuteriomethyl)aniline *N*-oxide (CDMAO-d_6) were compared in intermolecular experiments. Given Figure 2.2, three possibilities for isotope effects are expected depending on the rate-determining step: 1) On-rates (k_{1H}/k_{1D}) would be expected to display no isotope effect, so if binding is rate-determining, no isotope effect on product formation would be observed; 2) A rate-determining oxygen donation (k_{3H}/k_{3D}) would show a β-secondary isotope effect on product formation. β-secondary isotope effects, however, can be small and may be indistinguishable from 1; 3) If *N*-demethylation (k_{5H}/k_{5D}) was rate-determining, a KIE of around 2.8 would be expected based on intrinsic isotope effect values measured experimentally by Dower's *et al*.[11] Our intermolecular experiments show little to no isotope effect (Table 2.1). This suggests that the isotope effect for *N*-dealkylation is being masked by a prior, slower step: substrate binding or oxygen donation. Surface plasmon resonance measurements by Pearson, *et al* of the binding of the rod-like

antifungals itraconazole and ketoconazole with P450 3A4 measured substrate on-rates of 10^3-10^4 M^{-1} s^{-1}, much faster than either substrate or product off-rates.[18] That the non-globular substrates itraconazole and ketoconazole can still bind enzyme at this rate demonstrates the rapidity of substrate binding, excluding binding as a rate-determining step. The exclusion of the steps of substrate binding and *N*-dealkylation supports oxygen donation as rate-determining with CDMAO.

As a consequence of the electron-withdrawing character of the *p*-cyano group, Nee, *et al*, had used CDMAO to increase the rate of oxygen donation relative to DMAO in their experiments.[12] In an effort to further increase the rate of oxygen donation, we turned to 2,3,4,5,6-pentafluoro-*N*,*N*-dimethylaniline *N*-oxide (PFDMAO). The electron-withdrawing character of the fluorines was expected to further weaken the N-O bond and increase the rate of oxygen donation (Figure 2.3). We performed DFT calculations for oxygen donation by PFDMAO finding a barrier of 10.6 kcal/mol (Figure 2.4), significantly less than that Cho, *et al* saw for DMAO.[7] Further, the calculations support a larger barrier, 14.5 kcal/mol, for *N*-demethylation of the product PFDMA. This larger barrier implies that *N*-demethylation should be rate-determining in the PFDMAO system. In light of our calculations, PFDMAO was synthesized and kinetic isotope effects measured in P450cam to determine if the fluorine substitutions resulted in a change of the +rate-determining step, thus unmasking the intrinsic isotope effect. While a significant intramolecular isotope effect was seen, no significant isotope effect for *N*-demethylation in both noncompetitive and competitive experiments was observed (Table 2.1). The lack of an intermolecular isotope effect suggests that the intrinsic isotope effect is masked by a prior step in the PFDMAO system and that oxygen donation is still rate-determining. We expect the disagreement between the DFT calculations and experimental results

arises from the similarity of the calculated barrier heights for oxygen donation and *N*-dealkylation (10.6 and 14.5 kcal/mol). These values are not so dissimilar as to be distinguishable by DFT calculations.

Though isotope effects suggest no change in rate-determining step for the PFDMAO system, whether the barrier for this step has been lowered is still in question. PFDMAO and the unsubstituted DMAO were incubated with P450cam and product formation rates measured. As shown in Table 2.2, the rate of *N*-demethylation from PFDMAO was 27-fold faster than that from DMAO. Further, the unoxidized 2,3,4,5,6-pentafluoro-*N*,*N*-dimethylaniline (PFDMA) was also isolated as a product. With *N*-demethylation expected to require the prior step of oxygen donation, combining the rates of both products in the PFDMAO system gives a total rate of product formation of 34 nmol/min/nmol P450cam, a rate 28-fold faster than that seen with the DMAO-system. Changes in the rate of product formation indicate a change at the rate-determining step. With isotope effects supporting oxygen donation as rate-determining, the increased rate of product formation suggests a lowering of the barrier to oxygen donation.

The faster rate of oxygen donation by PFDMAO also lends insight to the mechanism of oxygen donation. The electron-withdrawing nature of the aromatic fluorines offers two outcomes for rate effects on oxygen donation, dependent on the nature of the N-O bond scission. As discussed above, two distinct oxygen donation mechanisms have been proposed for *N*-oxide systems, a six-electron oxygen (oxene) donation and a seven-electron oxygen donation. Donation of an oxene results from heterolytic cleavage of the N-O bond, returning both electrons to the nitrogen of the aniline (Figure 2.3). Electron-withdrawing groups would be expected to pull the electrons toward the nitrogen, weakening the N-O bond. Oxygen donation and Cmpd I formation from heterolytic cleavage would be expected to be faster as a result of the weakened bond. This

is supported by the over 10 kcal/mol lower activation energy for oxygen donation from PFDMAO (Figure 2.4) versus DMAO [7] in DFT calculations. In contrast, donation of a seven-electron oxygen requires homolytic cleavage of the N-O bond, forming an aminium radical and Cmpd II (Figure 2.5), as proposed by Guenegerich, *et al*.[13] Electron-withdrawing substituents would further increase the positive charge on the nitrogen in the product aminium radical. Destabilization of the product would be expected to show a higher barrier to oxygen donation and thus a slower rate. This is represented in the energies of the aniline radical cations relative to the neutral aniline calculated by DFT (Figure 2.6). Since homolytic cleavage is expected to be slower with PFDMAO, the finding that PFDMAO donates its oxygen an order of magnitude faster than DMAO excludes donation of a seven electron oxygen and the direct formation of Cmpd II.

Donation of an oxene to form Cmpd I does not result in radical formation on the aniline. To verify the absence of a radical on the DMA after donation, DFT calculations were performed for the oxygen donation by DMAO. The calculations showed the product of oxygen donation to be a heme-iron-coordinated oxygen and the product aniline. Spin-density calculations of this product show large spin-density on the oxygen with very little spin-density on the anilinic nitrogen or the aromatic ring (Figure 2.7A). This is indicative of a neutral aniline paired with Cmpd I. In contrast, spin density calculations of an aminium radical cation show large spin density on the nitrogen and throughout the aromatic ring (Figure 2.7B). We were unable to isolate Cmpd II with the aminium radical. Instead, lengthening of the N-O bond strictly generates Cmpd I and the aniline. The evident differences between the spin densities for the donation products and an aniline radical cation further support the exclusion of homolytic cleavage of the N-O bond and direct Cmpd II formation.

We have shown that the anilinic *N*-oxide-supported P450 pathway utilizes a mechanism involving a fast *N*-dealkylation preceded by a rate-determining oxygen donation. However, though perfluorination of the aromatic ring did not result in a change in the rate-determining steps, product formation rates of the PFDMAO system were significantly increased compared to that of the unsubstituted DMAO system. These faster donation rates resulting from the electron-withdrawing fluorines with support from DFT calculations exclude homolytic cleavage of the N-O bond to directly form Cmpd II. In exclusion of the homolytic pathway, a mechanism requiring heterolytic cleavage of the N-O bond to form Cmpd I is supported.

Oxygen surrogacy.

Rate measurements and DFT calculations of the *N*-oxide-supported P450 system support a mechanism with a rate-determining oxene donation. With PFDMAO, this donation shows two fates for the product aniline, PFDMA: it is either *N*-demethylated or released from the enzyme (Table 2.2). The release of PFDMA requires oxene donation without the subsequent *N*-demethylation. With PFDMAO exhibiting faster rates for oxene donation and a small portion of the donated oxenes not participating in *N*-dealkylation, we expected to be able to use the Cmpd I formed to oxidize a second substrate. Simply, PFDMAO was expected to act as a surrogate. In light of this conclusion, we incubated PFDMAO and P450cam in the presence of DMA. *N*-dealkylation of DMA by the PFDMAO-supported system was observed with product formation rates shown in Table 2.3.

DMA was rapidly metabolized in the PFDMAO system with a rate of MA formation 27-fold faster than the DMAO system. The formation of MA was 11-fold faster than that of PFMA, whose rate of formation was decreased by a factor of ten relative to that seen without DMA. The

decreased PFMA formation is expected because the Cmpd I formed is now given a choice of substrates. Any redirection of the oxygen towards DMA would result in less PFMA formed. Further, because DMA has a much lower oxidation potential (Figure 2.6), it is expected to outcompete PFDMA for the donated oxygen, as is seen. Expectedly, the rate of formation of PFDMA was increased in comparison to experiments without DMA. Redirection of the donated oxygen to the DMA prevents oxidation of PFDMA and thus permits its subsequent release. Total oxygen donation in the presence of DMA was doubled in comparison to experiments without DMA. Surprisingly, only half of the PFDMA formation is accounted for by *N*-demethylation products. The presence of DMA in the PFDMAO system appears to elicit a third pathway for the donated oxygen. We propose formation of DMAO as this third pathway, though oxidation of the P450 active site is also a possibility.

KIEs were evaluated for the *N*-dealkylation of DMA by the PFDMAO system (Table 2.4). In the noncompetitive intermolecular experiment, the intrinsic isotope effect is completely masked. However, partial unmasking of the intrinsic isotope effect is observed in the competitive experiment. This is likely due to a slow but significant exchange of the DMA prior to *N*-dealkylation. This permits the heme-centered oxidant to select between the two isotopically-distinct DMAs and thus unmask the isotope effect. That the intrinsic isotope effect is not fully unmasked suggests that this exchange is not exceedingly rapid relative to the rate of *N*-dealkylation. The intramolecular isotope effect showed further unmasking of the intrinsic isotope effect. As with the PFDMAO intramolecular isotope effect, this value is similar to those seen for *N*-dealkylation by both the DMAO- and NADPH/O_2-supported systems.

The ability of PFDMAO to significantly support oxidation of a second substrate is a feature previously unseen with DMAOs and P450. In the experiments with DMA, not only is the

alternate substrate oxidized, but it outcompetes PFDMA, the product of oxene donation, for oxidation. The successful competition of DMA demonstrates the difficulty of the *N*-dealkylation of PFDMA. In the PFDMAO system, the more difficult oxidation of the product aniline permits competition between oxidation and substrate exchange (Figure 2.8). The product aniline cannot maintain dominance of the oxidant. In contrast, the DMAO system does not allow competition for the oxidant, likely the result of the ease of oxidation of DMA.

The changes in the rates of PFDMA and PFMA formation upon exposure to a second substrate reinforce the competition of substrates for the generated oxidant. With PFMA the result of oxidation of PFDMA, any event that prevents oxidation of PFDMA will increase its yield and, in turn, decrease PFMA formation. The presence of a second substrate to interact with the oxidant is such an event. When DMA is present, it competes with PFDMA for the generated oxidant. Oxidation of DMA consumes the oxidant to form MA and PFDMA is released from the enzyme intact.

Conclusions

In conclusion, we have identified an *N*-oxide capable of supporting *N*-demethylation of DMA by P450cam, implicating the generation of a porphyrin-directed ROS as an intermediate to oxidation. KIEs and product formation rates, supported by DFT calculations, support a mechanism for surrogacy that begins with a rate-determining oxene donation to form Cmpd I. Further, isotope effects support the ability of the *N*-oxide-generated oxidant to act as an accurate mimic of the native system, supporting the use of *N*-oxides as mechanistic probes for other P450-mediated oxidations. The application of anilinic *N*-oxides as a mechanistic probe for *N*-dealkylation is the focus of Chapter 3. Use of *N*-oxides as probes for other modes of oxidation

as well as their potential as oxygen surrogates for synthesis in porphyrin mimetic systems are currently under investigation by our group.

Table 2.1. Kinetic Isotope Effects on *N*-Demethylation by *N*-Oxide-Supported P450cam.

	k_H/k_D - d_0/d_6 - noncompetitive	k_H/k_D - d_0/d_6 - competitive	k_H/k_D - intramolecular
CDMAO	0.9 ± 0.2	1.2 ± 0.1	2.77 ± 0.05[a]
PFDMAO	1.2 ± 0.2	1.3 ± 0.2	2.33 ± 0.07[b]

CDMAO – *p*-cyano-*N*,*N*-dimethylaniline *N*-oxide; PFDMAO – 2,3,4,5,6-pentafluoro-*N*,*N*-dimethylaniline *N*-oxide; d_0 – unlabeled; d_6 – $(CD_3)_2$-labeled. [a] From Dowers, *et al*, J. Am. Chem. Soc. **2004**, *126*, 8868-8869. [b] Measured using 2,3,4,5,6-pentafluoro-*N*-methyl-*N*-trideuteriomethylaniline

Table 2.2. Product Formation Rates from *N*-Oxides by P450cam

	Rate (nmol/min/nmol P450)	
N-oxide	Dimethyl product	Methyl product
DMAO	0	1.2 ± 0.2
PFDMAO	1.5 ± 0.3	32 ± 2

DMAO – *N*,*N*-dimethylaniline *N*-oxide; PFDMAO – 2,3,4,5,6-pentafluoro-*N*,*N*-dimethylaniline *N*-oxide

Table 2.3. Product Formation Rates from DMA by PFDMAO-Supported P450cam.

Rate (nmol/min/nmol P450)		
PFDMA	PFMA	MA
63 ± 2	2.5 ± 0.1	33 ± 1

DMA – *N*,*N*-dimethylaniline; PFDMA – 2,3,4,5,6-pentafluoro-*N*,*N*-dimethylaniline; PFMA – 2,3,4,5,6-pentafluoro-*N*-methylaniline; MA – *N*-methylaniline

Table 2.4. Product Isotope Effects for the *N*-Demethylation of *N*,*N*-dimethylaniline by 2,3,4,5,6-pentafluoro-*N*,*N*-dimethylaniline *N*-oxide and P450cam

k_H/k_D - DMA/DMA-d_6 - noncompetitive	k_H/k_D - DMA/DMA-d_6 - competitive	k_H/k_D - DMA-d_3 - intramolecular
1.3 ± 0.3	1.9 ± 0.2	2.8 ± 0.2

DMA – *N*,*N*-dimethylaniline; DMA-d_3 – *N*-methyl-*N*-trideuteriomethylaniline; DMA-d_6 – *N*,*N*-bis(trideuteriomethyl)aniline

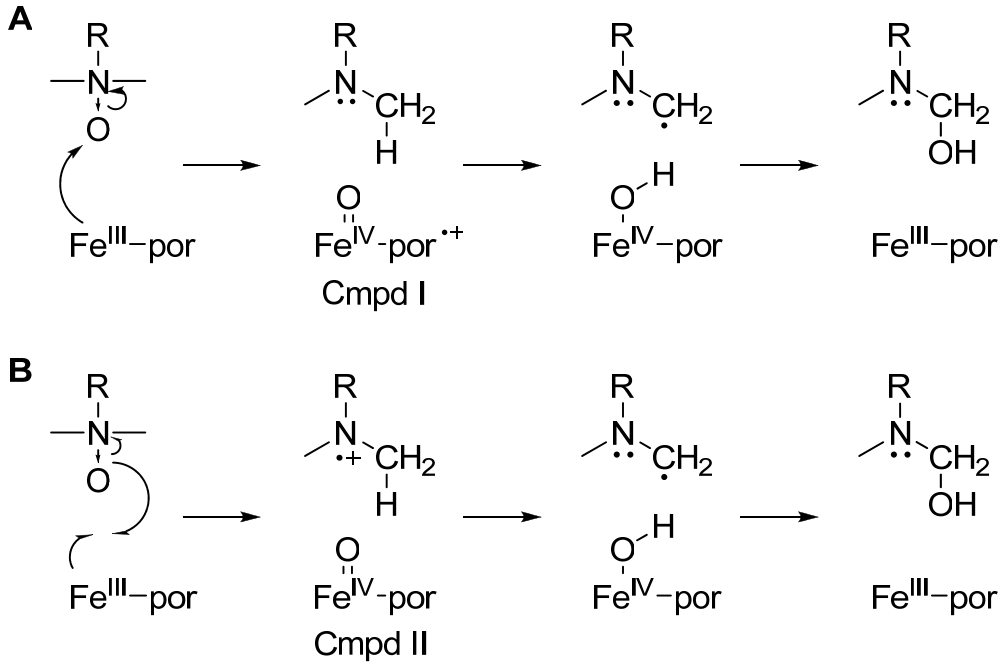

Figure 2.1. Proposed formations of Cmpd I and Cmpd II by oxygen donation from an *N*-oxide.

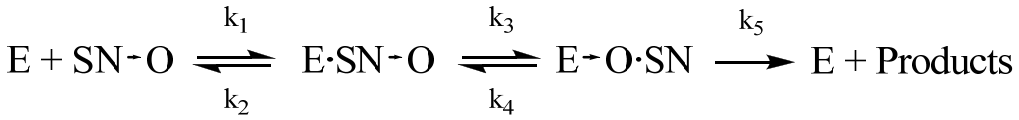

Figure 2.2. Oxygen donation kinetic scheme

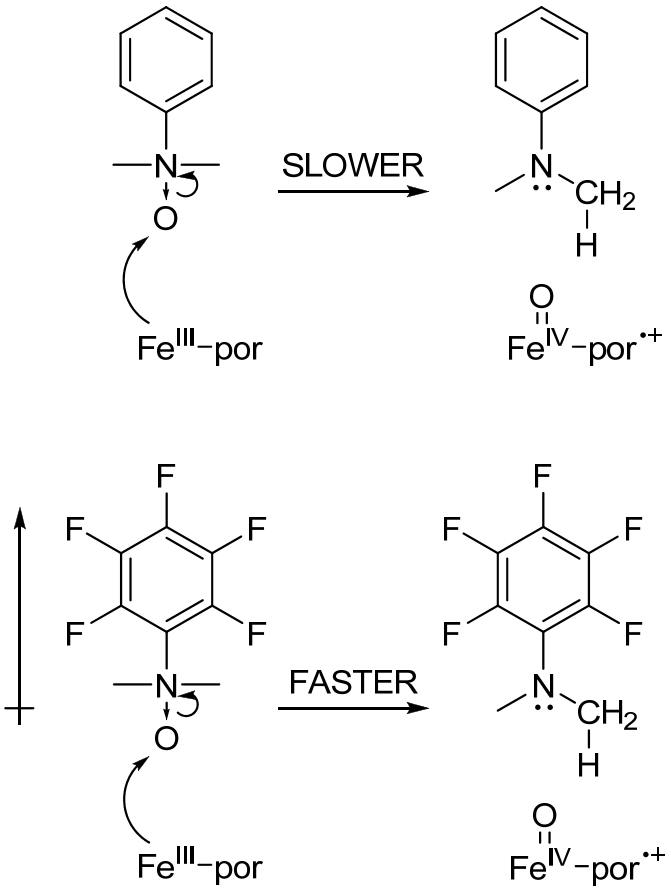

Figure 2.3. Electronic effects on heterolytic cleavage of the N-O bond

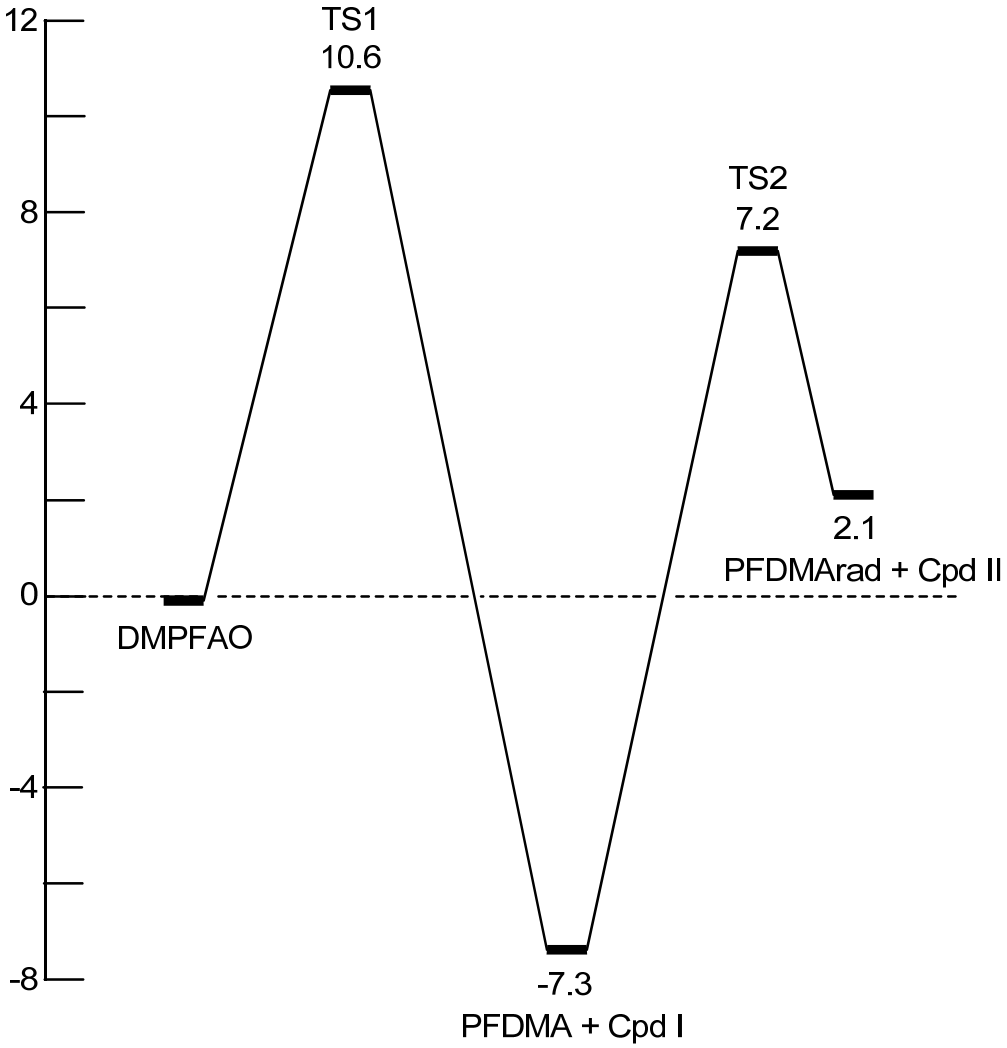

Figure 2.4. PFDMAO DFT calculated energies with geometries. Values given in kcal mol^{-1}.

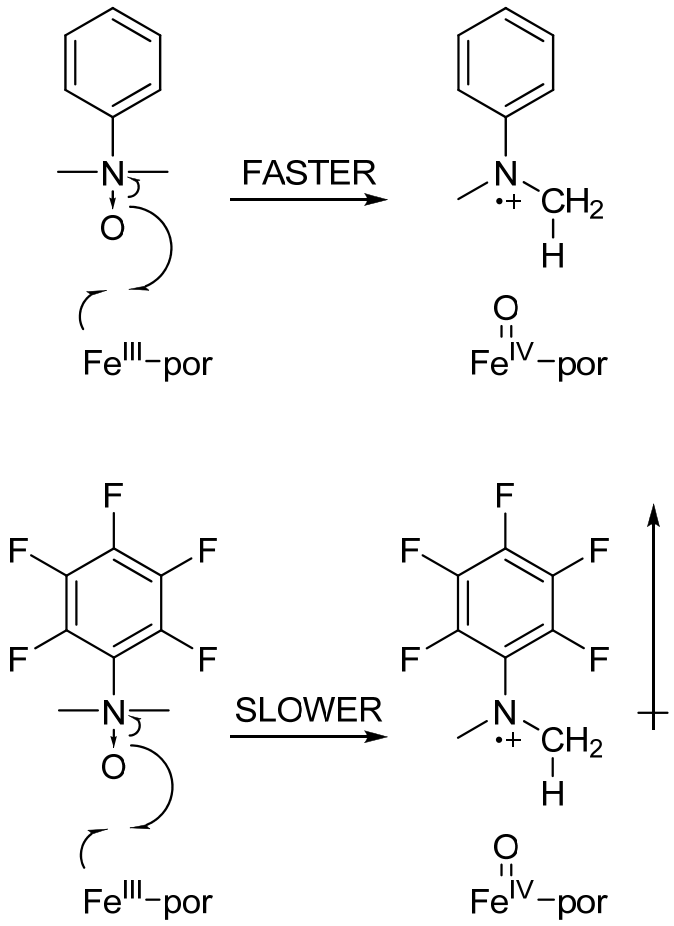

Figure 2.5. Electronic effects on homolytic cleavage of the N-O bond

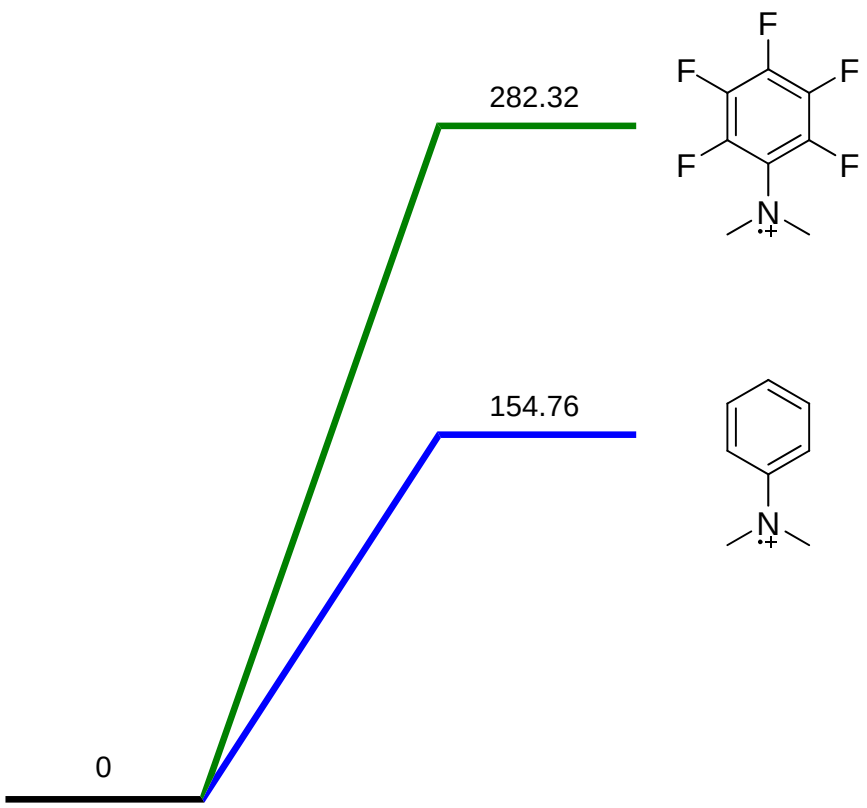

Figure 2.6. Comparison of gas-phase radical cation energies. Values given in kcal mol^{-1}.

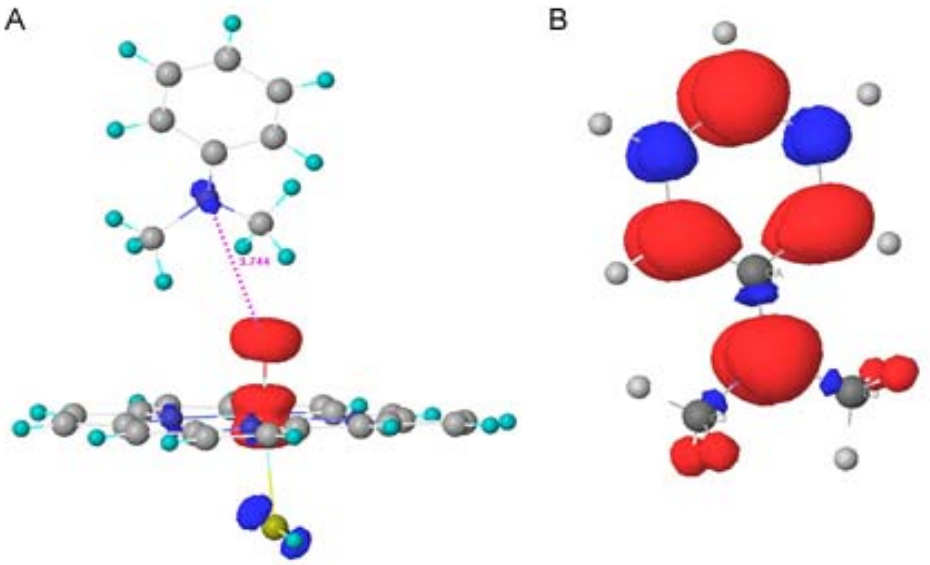

Figure 2.7. Spin densities of A) the products of DMAO oxygen donation and B) DMA radical cation.

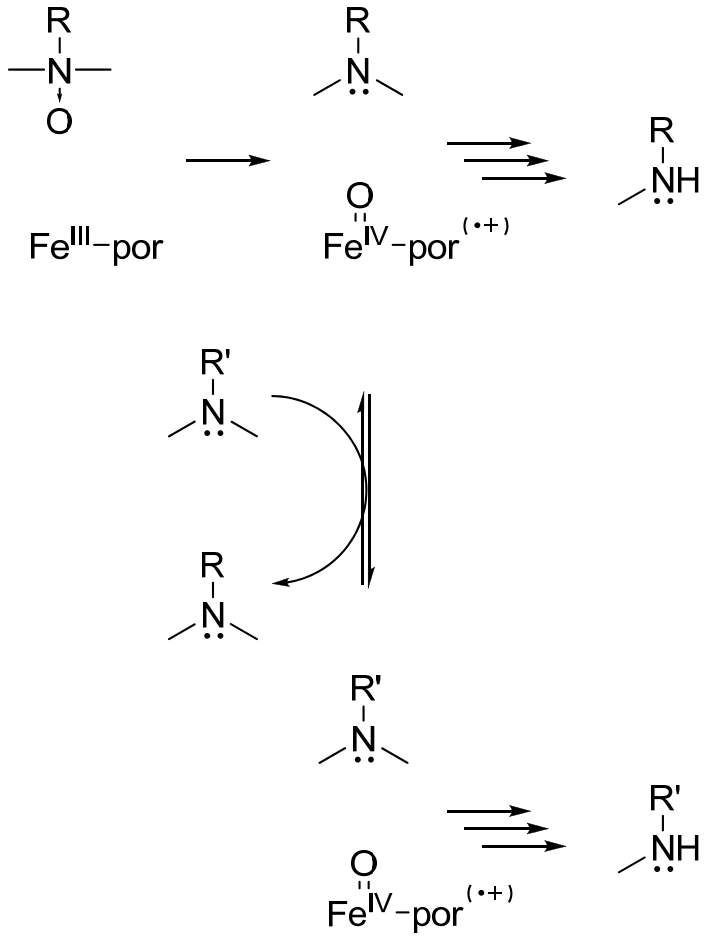

Figure 2.8. Competition of *N*,*N*-dimethylanilines for an *N*-oxide-generated oxidant.

References

1. Ortiz de Montellano, P.R., *Cytochrome P450:Structure, Mechanism, and Biochemistry*. 2nd ed, ed. O.d.M. P.R. 1995: Plenum: New York.
2. Groves, J.T., et al., *Aliphatic hydroxylation by highly purified liver microsomal cytochrome P450. Evidence for a carbon radical intermediate.* Biochemical and Biophysical Research Communications, 1978. **81**: p. 154-160.
3. Newcomb, M.Z., Rui; Chandrasena, R. Esala P.; Halgrimson, James A.; Horner, John H.; Makris, Thomas M.; Sligar, Stephen G., *Cytochrome P450 Compound I.* Journal of the American Chemical Society, 2006. **128**: p. 4580-4581.
4. Raner, G.M., et al., *Spectroscopic investigations of intermediates in the reaction of cytochrome P450(BM3)-F87G with surrogate oxygen atom donors.* Journal of Inorganic Biochemistry, 2006. **100**(12): p. 2045-2053.
5. Guengerich, F.P., C.-H. Yun, and T.L. MacDonald, *Evidence for a 1-electron oxidation mechanism in N-dealkylation of N,N-dialkylanilines by cytochrome P450 2B1.* Journal of Biological Chemistry, 1996. **271**(44): p. 27321-27329.
6. Hanna, I.H., et al., *Diversity in Mechanisms of Substrate Oxidation by Cytochrome P450 2D6.* Journal of Biological Chemistry, 2001. **276**(43): p. 39553-39561.
7. Cho, K.Y., et al., *"Formation of the Active Species of Cytochrome P450 by Using Iodosylbenzene: A Case for Spin-Selective Reactivity".* Chemistry: A European Journal, 2007. **13**: p. 4103-4115.
8. Bichara, N., et al., *Propranolol Hydroxylation and N-desisopropylation by Cytochrome P4502D6.* Drug Metabolism and Disposition, 1996. **24**(1): p. 112-118.

9. Bhakta, M.N., P.F. Hollenberg, and K. Wimalasena, *P450/NADPH/O2- and P450/PhIO-Catalyzed N-Dealkylations Are Mechanistically Distinct.* Journal of the American Chemical Society, 2005. **127**(5): p. 1376-1377.

10. Modi, S., et al., *1-Methyl-4-phenyl-1,2,3,6-tetrahydropyridine as a Substrate of Cytochrome P450 2D6: Allosteric Effects of NADPH-Cytochrome P450 Reductase* Biochemistry, 1997. **36**(15): p. 4461-4470.

11. Dowers, T.S., et al., *Kinetic isotope effects implicate the iron-oxene as the sole oxidant in P450-catalyzed N-dealkylation.* Journal of the American Chemical Society, 2004. **126**(29): p. 8868-8869.

12. Nee, M.W. and T.C. Bruice, *Use of the N-oxide of p-cyano-N,N-dimethylaniline as an "oxygen" donor in a cytochrome P-450 model system.* Journal of the American Chemical Society, 1982. **104**(22): p. 6123-6125.

13. Seto, Y. and F.P. Guengerich, *Partitioning between N-dealkylation and N-Oxygenation in the Oxidation of N,N-Dialkylarylamines Catalyzed by Cytochrome P450 2B1.* Journal of Biological Chemistry, 1993. **268**(14): p. 9986-9997.

14. French, K.J., et al., *Benign Synthesis of 2-Ethylhexanoic Acid by Cytochrome P450cam: Enzymatic, Crystallographic, and Theoretical Studies.* Biochemistry, 2001. **40**: p. 9532-9538.

15. Emmons, W.D. and G.B. Lucas, *Peroxytrifluoroacetic Acid. V. The Oxidation of Ketones to Esters.* Journal of the American Chemical Society, 1955. **77**(8): p. 2287-2288.

16. Frisch, M.J.T., G. W.; Schlegel, H. B.; Scuseria, G. E.; Robb, M. A.; Cheeseman, J. R.; Montgomery, Jr., J. A.; Vreven, T.; Kudin, K. N.; Burant, J. C.; Millam, J. M.; Iyengar, S. S.; Tomasi, J.; Barone, V.; Mennucci, B.; Cossi, M.; Scalmani, G.; Rega, N.;

Petersson, G. A.; Nakatsuji, H.; Hada, M.; Ehara, M.; Toyota, K.; Fukuda, R.; Hasegawa, J.; Ishida, M.; Nakajima, T.; Honda, Y.; Kitao, O.; Nakai, H.; Klene, M.; Li, X.; Knox, J. E.; Hratchian, H. P.; Cross, J. B.; Bakken, V.; Adamo, C.; Jaramillo, J.; Gomperts, R.; Stratmann, R. E.; Yazyev, O.; Austin, A. J.; Cammi, R.; Pomelli, C.; Ochterski, J. W.; Ayala, P. Y.; Morokuma, K.; Voth, G. A.; Salvador, P.; Dannenberg, J. J.; Zakrzewski, V. G.; Dapprich, S.; Daniels, A. D.; Strain, M. C.; Farkas, O.; Malick, D. K.; Rabuck, A. D.; Raghavachari, K.; Foresman, J. B.; Ortiz, J. V.; Cui, Q.; Baboul, A. G.; Clifford, S.; Cioslowski, J.; Stefanov, B. B.; Liu, G.; Liashenko, A.; Piskorz, P.; Komaromi, I.; Martin, R. L.; Fox, D. J.; Keith, T.; Al-Laham, M. A.; Peng, C. Y.; Nanayakkara, A.; Challacombe, M.; Gill, P. M. W.; Johnson, B.; Chen, W.; Wong, M. W.; Gonzalez, C.; and Pople, J. A., *Gaussian 03, Revision C.02*. 2004, Gaussian, Inc: Wallingford CT.

17. Becke, A.D., *Density-functional thermochemistry. III. The role of exact exchange.* The Journal of Chemical Physics, 1993. **98**(7): p. 5648-5652.

18. Pearson, J.T., et al., *Surface Plasmon Resonance Analysis of Antifungal Azoles Binding to CYP3A4 with Kinetic Resolution of Multiple Binding Orientations.* Biochemistry, 2006. **45**(20): p. 6341-6353.

CHAPTER THREE

Anilinic *N*-Oxides Support Hydrogen Atom Transfer In P450-Mediated *N*-Dealkylation

(This chapter is part of a work in preparation for submission to Chemistry - A European Journal;

Authors: Kenneth M. Roberts and Jeffrey P. Jones)

This work was supported by NIH Grants ES009122 and GM84546.

Abstract

The mechanism of *N*-dealkylation mediated by Cytochrome P450 (P450) has long been studied and argued as either a single electron transfer (SET) or a hydrogen atom transfer (HAT) from the amine to the oxidant of the P450, the reputed iron-oxene (Cmpd I). In our study, 2,3,4,5,6-pentafluoro-*N*,*N*-dimethylaniline *N*-oxide (PFDMAO) was used as an oxygen surrogate to directly generate Cmpd I. This surrogate was employed to probe the mechanism of *N*-dealkylation to distinguish between the HAT and SET mechanisms. PFDMAO-supported *N*-dealkylation of *N*-cyclopropyl-*N*-methylaniline led to the ring-intact product *N*-cyclopropylaniline (CPA), similar to that seen with the native system. The formation of CPA argues against a SET mechanism in favor of a P450-like HAT mechanism. We suggest that the formation of the ring-intact CPA by both the native and PFDMAO-supported systems and the similarity of KIEs (as described in Chapter 2) between these two systems argues for a similar mechanism of Cmpd I followed by HAT for *N*-dealkylation. These similarities also demonstrate the ability of the *N*-oxide-generated oxidant to act as an accurate mimic of the native P450 oxidant.

Introduction

N-dealkylation has been studied as one of the many oxidations performed by the proposed Cmpd I. The pathway involves oxygen insertion by Cmpd I into the C_α-H bond to generate a carbinolamine that spontaneously dealkylates forming the free amine and aldehyde (Figure 3.1). Recent studies of this pathway have centered on two proposed mechanisms.[1] One mechanism proposes a single electron transfer (SET) from the target nitrogen to Cmpd I, forming an iron (IV)-oxo porphyrin (Cmpd II) and an aminium radical cation (Figure 3.2). Cation formation increases the acidity of C_α and drives a subsequent proton transfer to Cmpd II. The final step is the barrierless formation of the carbinolamine via transfer of a hydroxyl radical to the resulting carbon radical.[2] In contrast, the second mechanism proposes that Cmpd I elicits a hydrogen atom transfer (HAT) from C_α to directly form the carbon radical and the protonated Cmpd II (Figure 3.2). Investigations by Shaffer, *et al* have shed light on this pathway finding that P450-mediated oxidation of the substrate *N*-cyclopropyl-*N*-methylaniline (CPMA) led to products that left the cyclopropyl ring intact (Figure 3.3).[3] This was in contrast to the solely ring-open products found upon oxidation by horseradish peroxidase (Figure 3.3),[4] an enzyme known to undergo a SET mechanism.[5, 6] They concluded that P450 follows a HAT mechanism in the exclusion of the SET mechanism. Interestingly, Cerny and Hanzlik found that P450-mediated oxidation of tertiary cyclopropylamines led to both ring-intact and ring-open products.[7] However, ring-open products only appeared in the second round of *N*-dealkylation. Simply, a prior round of *N*-dealkylation was required, with ring-opened products derived solely from the ring-intact secondary amine product of the first *N*-dealkylation. They concluded a HAT mechanism for *N*-dealkylation that incorporated abstraction of the *N*-hydrogen as explanation of the ring-open products (Figure 3.4).

Confirmation of the HAT mechanism, as well as other oxidations proposed to act via Cmpd I, requires showing that Cmpd I elicits these reactions. In Chapter 2 of this work, we demonstrated that the oxygen surrogate 2,3,4,5,6-pentafluoro-*N*,*N*-dimethylaniline *N*-oxide (PFDMAO) generated a Cmpd I species in its host P450. Further, the intramolecular KIEs measured for the *N*-demethylation of the product 2,3,4,5,6-pentafluoro-N,N-dimethylaniline (PFDMA) and the secondary substrate N,N-dimethylaniline (DMA) lent support to PFDMAO as a potential model for P450-mediated *N*-dealkylation.

In this work, we tested the ability of PFDMAO to support the oxidation of the mechanistic probe CPMA to validate PFDMAO as a model for P450-mediated *N*-dealkylation. Herein, we show that the PFDMAO-derived oxidant is capable of *N*-dealkylating CPMA, with *N*-methylaniline and the ring-intact *N*-cyclopropylaniline (CPA) as products. CPA formation, kinetic values and theoretical calculations support a HAT mechanism for native and DMAO-supported *N*-dealkylation.

Experimental Methods

Materials. Reagent or HPLC grade chemicals and solvents were supplied by Alfa Aesar (Ward Hill, MA), Aldrich (Milwaukee, WI), Fisher Scientific (Fair Lawn, NJ), EMD (Madison, WI), and Mallinckrodt Baker (Phillipsburg, NJ). Isotopically-labelled compounds were supplied by CDN Isotopes (Pointe-Claire, Quebec, CA). Tetrahydrofuran (THF) was distilled under argon from sodium and benzophenone prior to use. ^{1}H-NMR spectra were obtained at 300 MHz with a Varian Mercury 300 spectrometer equipped with a quad-detection probe (^{1}H, ^{13}C, ^{31}P and ^{19}F). ^{1}H-decoupled ^{13}C-NMR spectra were obtained at 75 MHz. ^{19}F-NMR spectra were obtained at 282 MHz. Gas chromatography/mass spectrometry was performed on a ThermoQuest Voyager GC/MS (Thermo-Finnegan) coupled to a CE Instruments GC8000Top affixed with a 30m JW Scientific DB-1 GC column.

***N*-oxide Surrogacy Procedure.** P450cam was expressed and purified as described previously.[8] Incubations were performed using 20 mM PFDMAO, 1.0 μM P450cam and 20 mM CPMA brought to a total volume of 1.0 mL with 100 mM phosphate buffer, pH 7.4. Samples were preincubated at 30 °C for 10 min prior to initiation with the *N*-oxide. For rate determinations, reactions were incubated at 30 °C for discrete time points up to and including 60 min. Reactions were quenched with 500 μL ethyl acetate containing 100 μM 2,3,4,5,6-pentafluoroaniline (PFA) as an internal standard. An additional 500 μL ethyl acetate was added for product extraction. Product was further extracted twice with 1.0 mL ethyl acetate. Extracts were combined and dried with $MgSO_4$. Reaction products were monitored by gas chromatography/mass spectrometry (GC/MS) using electron impact ionization. The GC method began at 70 °C for 5 min followed first by a 10 °C/min ramp to 120 °C then by a 30 °C/min ramp

to 230 °C. Ions with m/z 107.1 and 132.1 were monitored quantitation of *N*-methylaniline and *N*-cyclopropylaniline, respectively.

2,3,4,5,6-pentafluoro-*N*,*N*-dimethylaniline. Potassium *tert*-butoxide (5.0 g, 45 mmol) was added at room temperature over 10 min to a vigorously stirring solution of 2,3,4,5,6-pentafluoroaniline (2.8 g, 15 mmol) and iodomethane (2.3 mL, 38 mmol) in 100 mL dry THF, resulting in a dark red solution and white precipitate. TLC after 10 min showed complete conversion of the starting material to 2,3,4,5,6-pentafluoro-*N*,*N*-dimethylaniline. Precipitates (potassium iodide and unreacted potassium *tert*-butoxide) were removed by filtration through Celite. THF was removed from the filtrate by rotary evaporation to a volume of 5 mL. Product was purified by flash chromatography (15% chloroform in hexanes) to yield 2,3,4,5,6-pentafluoro-*N*,*N*-dimethylaniline (1.68 g, 53%) as a clear oil. ^{1}H NMR (300 MHz, $CDCl_3$) δ 2.90 (t); $^{13}C\{^{1}H\}$ NMR (75 MHz, $CDCl_3$) δ 43.71 (t); ^{19}F NMR (282 MHz, $CDCl_3$) δ -165.19 (t, 1F), -164.53 (m, 2F), -151.25 (d, 2F)

2,3,4,5,6-pentafluoro-*N*,*N*-dimethylaniline *N*-oxide trifluoroacetic acid salt. 2,3,4,5,6-pentafluoro-*N*,*N*-dimethylaniline was prepared as above through Celite filtration. THF was distilled from the filtered product mixture and the product was dissolved in 15 mL dichloromethane and stirred on ice. Trifluoroperacetic acid (TFPA) was generated *in situ* using the method of Emmons and Lucas.[9] 1.1 mL (2.5 eqs) 90% hydrogen peroxide was added dropwise to 7 mL dichloromethane on ice. To this mixture, 6.5 mL (3.0 eqs) trifluoroacetic anhydride was added dropwise over 10 min. After allowing the reaction for 10 min, the mixture was warmed to room temperature. The TFPA mixture was added dropwise over 20 min to the

stirring PFDMA mixture on ice. TLC showed no PFDMA immediately after addition of the TFPA. Product was extracted from the reaction mixture six times with 15 mL distilled water. Extracts were combined and rinsed three times with diethyl ether. Water was removed by rotary evaporation and product was recrystallized from THF to yield 2,3,4,5,6-pentafluoro-*N*,*N*-dimethylaniline *N*-oxide trifluoroacetic acid salt (1.9 g, 56%) as large colorless crystals. ^{1}H NMR (300 MHz, $CDCl_3$): δ 4.14 (t, 6H), 11.20 (bs, 1H); $^{13}C\{^{1}H\}$ NMR (75 MHz, $CDCl_3$): δ 62.6 (t); ^{19}F NMR (282 MHz, $CDCl_3$): δ -156.95 (m, 2F), -146.99 (m, 1F), -138.32 (d, 2F), -76.46 (s, 3F)

***N*-cyclopropyl-*N*-methylaniline.** *N*-cyclopropyl-*N*-methylaniline was synthesized using the method of Shaffer, *et al*.[4] Ethylmagnesium bromide (3.0 M in Et_2O, 10 mL, 30 mmol) was added dropwise to a stirring solution of *N*-methylformanilide (1.3 mL, 10 mmol) and titanium isopropoxide (3.8 mL, 14 mmol) in 50 mL dry THF. The reaction was heated at 65 °C for 30 min followed by stirring for 24 h at room temperature. The reaction was quenched with 40 mL saturated NH_4Cl and THF was removed by rotary evaporation. Product mixture was diluted with 1N HCl and product extracted with Et_2O (7x13 mL). The combined extracts were dried ($MgSO_4$), filtered through Celite and solvent removed by rotary evaporation to oil. Product was purified by flash chromatography (15% CH_2Cl_2 in hexanes) to yield *N*-cyclopropyl-*N*-methylaniline (590 mg, 40%) as a pale yellow oil. ^{1}H NMR (300 MHz, $CDCl_3$) δ 0.64 (m, 2H), 0.84 (m, 2H), 2.39 (m, 1H), 3.00 (s, 3H), 6.79 (t, 1H), 7.01 (d, 2H), 7.27 (t, 2H); ^{13}C NMR (75 MHz, $CDCl_3$) δ 9.31, 33.52, 39.34, 114.01, 117.62, 129.07, 151.10

***N*-(1-ethoxycyclopropyl)aniline.** *N*-(1-ethoxycyclopropyl)aniline was synthesized from aniline and 1-ethoxy-1-bromocyclopropane using the methods of Kang and Kim[10] and Leoppky and Elomari.[11] 1-ethoxy-1-bromocyclopropane was synthesized in situ using the methods of Gadwood, *et al*.[12] Phosphorous tribromide (375 μL, 4.0 mmol) was directly added dropwise to 1-ethoxy-1-trimethylsiloxycyclopropane (1.0 mL, 5.0 mmol) while stirring on ice. After addition, the reaction was removed from ice and stirred for 7 h at room temperature. The reaction was shown complete by ^{1}H-NMR. The reaction mixture was brought up in 5 mL pentane and placed in an acetone/dry ice bath (-25 °C). While stirring, 2.5 mL saturated Na_2CO_3 was added dropwise over 3 mins and the organic layer collected. The aqueous layer was washed twice with 2 mL pentane. All three organic layers were combined, dried with Na_2SO_4 and vacuum filtered to a final volume of 1 mL. The filtrate was added dropwise to a stirring solution of aniline (370 μL, 4.0 mmol) and triethylamine (700 μL, 5.0 mmol) in 1.5 mL pentane and refluxed for 72 h. The reaction mixture was brought up in 15 mL dichloromethane and washed twice with 10 mL distilled water and once with 10 mL saturated NaCl. The aqueous layers were combined and back-extracted with 15 mL dichloromethane. The two organic layers were combined and solvent removed by rotary evaporation. Product was purified by flash chromatography (10% ethyl acetate in hexanes) to yield *N*-(1-ethoxycyclopropyl)aniline (273 mg, 39%) as a pale yellow oil. ^{1}H NMR (300 MHz, $CDCl_3$) δ 0.89 (q, 2H), 1.13 (m, 5H), 3.57 (q, 2H), 4.79 (bs, 1H), 6.77 (t, 1H), 6.88 (d, 2H), 7.20 (t, 2H); ^{13}C NMR (75 MHz, $CDCl_3$) δ 15.23, 15.58, 61.11, 68.77, 114.36, 118.57, 129.27, 145.71

***N*-cyclopropylaniline.** *N*-cyclopropylaniline was synthesized from *N*-(1-ethoxycyclopropyl)aniline using the methods of Kang and Kim[10] and Leoppky and

Elomari.[11] Boron trifluoride etherate (390 μL, 3.1 mmol) was added dropwise to a stirring suspension of sodium borohydride (117 mg, 3.1 mmol) in 3 mL THF in ice under an atmosphere of argon and the mixture stirred for 30 min. *N*-(1-ethoxycyclopropyl)aniline (270 mg, 1.5 mmol) was added dropwise to the stirring mixture on ice. Reaction mixture was removed from ice and stirred for 12 h allowing to warm to room temperature. The reaction was carefully quenched with 10 drops distilled water and brought up in 10 mL diethyl ether. The mixture was washed three times with 5 mL distilled water and once with saturated NaCl. The organic layer was dried with Na_2SO_4, filtered and solvent removed by rotary evaporation. Product was purified by flash chromatography (4% ethyl acetate in hexanes) to yield *N*-cyclopropylaniline (125 mg, 61%) as a pale yellow oil. ^{1}H NMR (300 MHz, $CDCl_3$) δ 0.44 (m, 2H), 0.65 (m, 2H), 2.35 (m, 1H), 4.09 (bs, 1H), 6.67 (t, 1H), 6.72 (d, 2H), 7.12 (t, 2H); ^{13}C NMR (75 MHz, $CDCl_3$) δ 7.63, 25.45, 113.37, 117.95, 129.34, 148.90

Results and Discussion

Oxygen surrogacy.

Oxidation of CPMA in the PFDMAO system was much slower than we saw previously for DMA or the system without substrate (Table 3.1). CPMA was *N*-dealkylated to MA and *N*-cyclopropylaniline with a total rate of 0.9 nmol/min/nmol P450. *N*-dealkylation of PFDMA was four times faster than that of CPMA. Total oxygen donation was about four-fold slower than the PFDMAO system without substrate and seven-fold slower than the PFDMAO system with DMA present. Having a methyl group replaced with a more electron-donating cyclopropyl group, CPMA should be more facile to oxidation than DMA and a higher rate of oxidation of CPMA would be expected. We expect the slower rates seen in the CPMA-PFDMAO system to be an active site binding effect, where CPMA inhibits PFDMAO from donating the oxygen. When PFDMAO is positioned for oxygen donation, the resulting PFDMA then outcompetes the CPMA by a proximity effect. As with the DMA, total oxygen donation in the PFDMAO system with CPMA present is not fully accounted for by *N*-dealkylation products. In fact, approximately 80% of the PFDMA formation is unaccounted for. As we proposed for DMA (see Chapter 2), we expect that CPMA elicits a third pathway of *N*-oxygenation as the fate of the donated oxygen.

The *N*-oxide generated oxidant.

PFDMAO has been found to be an oxene donor capable of acting as a surrogate for both *N*-dealkylation and olefin epoxidation. Product formation rates and DFT calculations of anilinic *N*-oxide-supported systems argue for an oxene donation to form Cmpd I. However, what occurs downstream of Cmpd I formation is unclear. With the observation that PFDMAO acts as an oxygen surrogate for other substrates and DMAO does not, three possible mechanisms for

N-dealkylation in the *N*-oxide systems become apparent. Two are the SET and HAT mechanisms described above. The third mechanism is a SET-like pathway involving an outer-sphere electron transfer between substrates.

In the HAT mechanism, after oxene donation by the *N*-oxide, the generated Cmpd I abstracts a hydrogen from the C_α to form a carbon-centered radical (Figure 3.5). The occurrence of competition for substrate oxidation is dependent on the relative rates of substrate oxidation and substrate exchange. The inability of DMAO to act as a surrogate can be rationalized by its low barrier to oxidation outcompeting either substrate exchange or substrate oxidation. Thus, when DMAO donates its oxygen to form Cmpd I, the resulting DMA immediately transfers a hydrogen atom before any substrate exchange occurs. In contrast, hydrogen atom transfer from PFDMA is expected to be much slower. If substrate exchange is rapid compared to the oxidation of PFDMA, then the relative ease of oxidation presides over substrate preference. As shown in Figure 2.6 (previous chapter), DMA has a much lower barrier to single-electron oxidation than PFDMA. With its lower barrier to oxidation, DMA would be expected to be preferentially oxidized over PFDMA.

In the basic SET pathway, after oxene donation to form Cmpd I, a single-electron transfer from the product aniline occurs to form an aminium radical cation and Cmpd II (Figure 3.5). Similar to the HAT mechanism, oxidation rates of substrates depend on the rate of substrate exchange and the ease of substrate oxidation. In the case of SET, ease of oxidation is determined by the single-electron oxidation potential of competitive substrates. If substrate exchange is fast relative to the SET event, the substrate with the lowest oxidation potential will be oxidized first. With DMA having a lower barrier to oxidation than PFDMA (Figure 2.6), we would expect electron transfer from DMA to Cmpd I to occur faster. However, with P450 2B1, Seto and

Guengerich found only trace support of oxidation of DMA-^{14}C by three distinct DMAOs, including the electron-withdrawn CDMAO, concluding that oxidation of a second substrate was prevented by a direct Cmpd II formation from the *N*-oxide.[13] In the previous work, we excluded the direct formation of Cmpd II by demonstrating a higher rate of oxygen donation by PFDMAO over DMAO. Failure of the DMAOs to act as surrogates, then suggests that substrate exchange would need to be slow relative to a fast electron transfer step. In other words, after Cmpd I formation in the DMAO system, the product DMA is oxidized by one electron to form the aminium radical cation and Cmpd II before any substrate exchange might occur. In contrast, the higher barrier, and thus, slower rate of electron transfer from PFDMA in the PFDMAO system could permit substrate exchange. With substrates now in competition for Cmpd I, oxidative preference determines products formed. This system would be expected to demonstrate surrogacy since DMA shows lower barriers to oxidation than PFDMA (Figure 2.6).

Another possibility arises in the case that *N*-demethylation of any anilinic *N*-oxide is faster than substrate exchange. In this pathway, for a second substrate to be oxidized by Cmpd II, a second electron transfer must occur between the aminium radical cation and the substrate to be oxidized (Figure 3.6). Because DMA radical cation has a lower barrier to formation, we would expect no electron transfer from any substrates with a higher barrier to oxidation (though transfer from the isotopically distinct DMA-^{14}C would be expected.) We would, however, expect to observe electron transfer from DMA to *p*-cyano-*N*,*N*-dimethylaniline radical cation, since the electron withdrawing nature of the *p*-cyano group would increase its single electron oxidation potential relative to DMA. In support of this rationale, Seto and Guengerich did see an increased support of DMA-^{14}C oxidation by CDMAO. In the PFDMAO system, the highly electron withdrawing nature of the aromatic fluorines poises PFDMA radical cation for accepting an

electron. With PFDMA having a much higher oxidation potential, any substrate with a lower oxidation potential would be capable of transferring an electron to PFDMA radical cation to generate a new substrate radical cation. This new radical cation would then be susceptible to oxidation by Cmpd II.

The HAT and two SET mechanisms predict similar outcomes for the DMAO and PFDMAO systems. In each mechanism, DMAO is not expected to support oxidation of other substrates due to the ease of DMA oxidation. Further, each mechanism also predicts the ability of PFDMAO to act as a surrogate owing to a more difficult oxidation of the product PFDMA. With DMAO seemingly unable to support oxidation of other substrates and PFDMAO supporting oxidation of DMA, none of these mechanisms is excluded.

To distinguish between these mechanisms, we used the chemical probes of Schaffer, *et al* and tested the metabolism of CPMA in the PFDMAO system. Schaffer, *et al* found that the metabolism of CPMA distinguished between SET and HAT mechanisms.[3, 4] In HRP, which follows a SET mechanism, CPMA metabolism led exclusively to cyclopropyl ring-opened products (Figure 3.7). In P450, now considered to follow a HAT mechanism, strictly ring-closed products were formed (Figure 3.8). We presented CPMA to the PFDMAO system and successfully observed metabolites of CPMA. Though metabolism of CPMA was much slower than that of DMA, the two products, MA and *N*-cyclopropylaniline (CPA), were observed. MA formation is not discerning as it is seen as a product in both SET and HAT pathways. However, the observation of PFDMAO-supported formation of CPA, a ring-intact product, is revealing. Ring-intact product formation strongly argues against a SET mechanism in the PFDMAO system, excluding both proposed SET mechanisms. In the exclusion of SET, a HAT mechanism for *N*-dealkylation in the *N*-oxide system is supported, similar to the native P450 system.

Studies have shown large intramolecular isotope effects (2.93-13.3) for *N*-dealkylation of DMAs by HRP[14, 15] in contrast to the smaller isotope effects (1.74-3.87) seen by P450.[15-17] As HRP follows a SET mechanism, the small magnitude of the intramolecular isotope effects previously observed in the PFDMAO system further support a mechanism that does not involve single electron transfer.

Conclusions

As we have shown previously, product formation rates of DMAO and PFDMAO exclude direct Cmpd II formation. In this study, indirect formation of Cmpd II derived from electron transfer to Cmpd I, i.e. a SET mechanism, is, in turn, excluded by the formation of the ring-intact CPA from the mechanistic probe CPMA. In the exclusion of Cmpd II-derived mechanisms, HAT is left the likely mechanism for *N*-dealkylation by the anilinic *N*-oxide-supported P450. Further, the similarities in KIEs for both the *N*-oxide and NADPH/O_2 systems, together with the observation of cyclopropyl ring-intact products in both systems, strongly support a HAT mechanism directed by a Cmpd I species for *N*-dealkylation in these systems. These similarities continue to demonstrate the ability of the *N*-oxide-generated oxidant to act as an accurate mimic of the native system, further supporting the use of *N*-oxides as mechanistic probes for other P450-mediated oxidations.

Table 3.1. Product Formation Rates from CPMA by PFDMAO-Supported P450cam

	Rate (nmol/min/nmol P450)			
Substrate	PFDMA	PFMA	MA	CPA
None	1.5 ± 0.3	32 ± 2	-	-
DMA	63 ± 2	2.5 ± 0.1	33 ± 1	-
CPMA	5 ±1	3.7 ± 0.3	0.28 ± 0.03	0.6 ± 0.1

DMA – *N*,*N*-dimethylaniline; CPMA – *N*-cyclopropyl-*N*-methylaniline; PFDMA – 2,3,4,5,6-pentafluoro-*N*,*N*-dimethylaniline; PFMA – 2,3,4,5,6-pentafluoro-*N*-methylaniline; MA – *N*-methylaniline; CPA – *N*-cyclopropylaniline

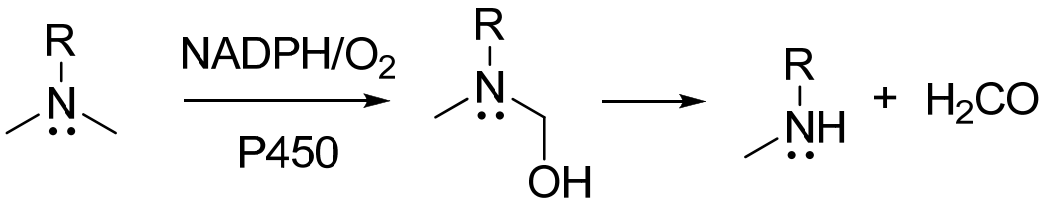

Figure 3.1. *N*-dealkylation Overview.

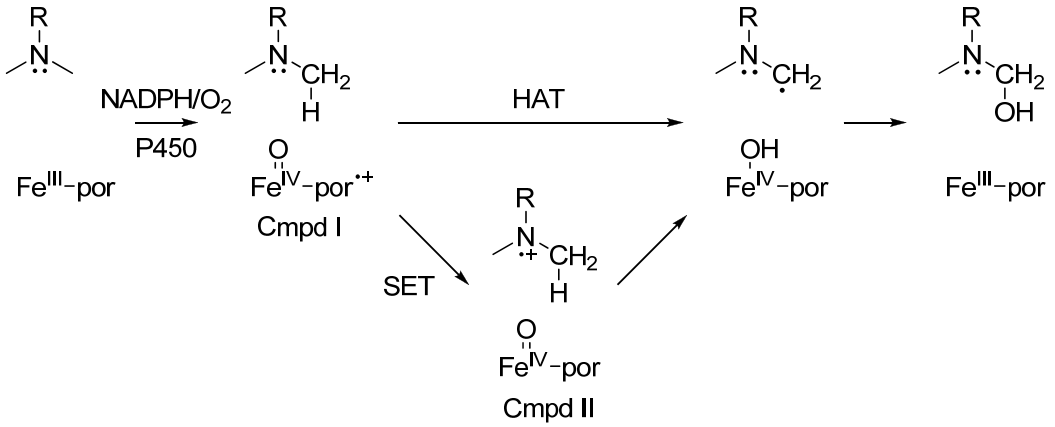

Figure 3.2. Pathways for the hydrogen atom transfer (HAT) and single electron transfer (SET) mechanisms proposed for P450-mediated *N*-dealkylation.

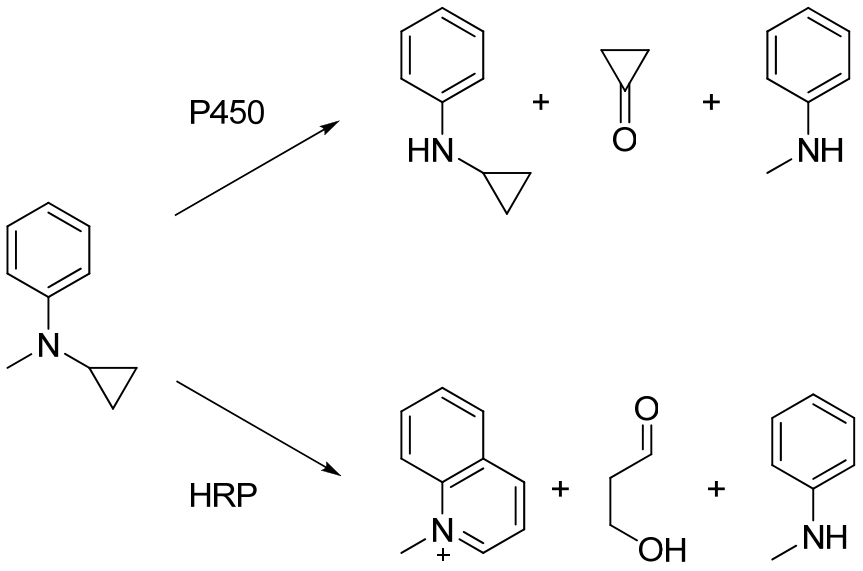

Figure 3.3. Products of *N*-cyclopropyl-*N*-methylaniline formed by Cytochrome P450 (P450) and horse radish peroxidase (HRP)

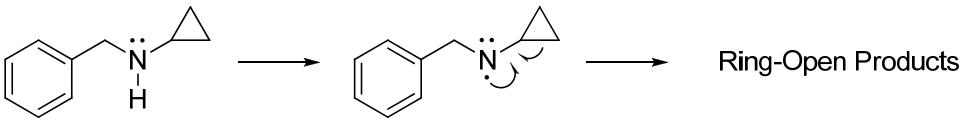

Figure 3.4. Hydrogen atom abstraction at a nitrogen to generate a nitrogen-centered radical.

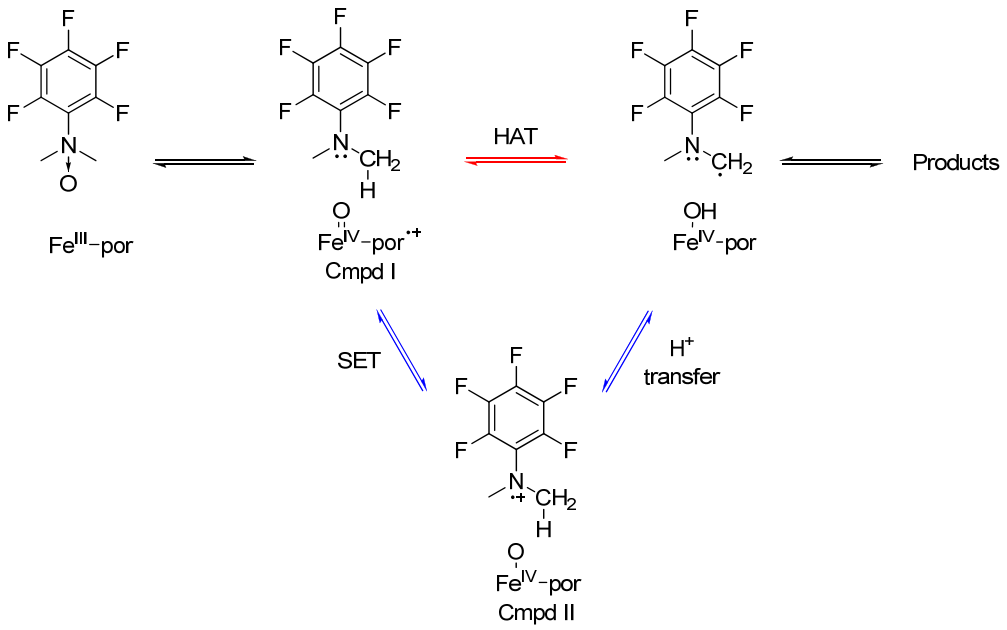

Figure 3.5. *N*-oxide-supported HAT and SET mechanisms.

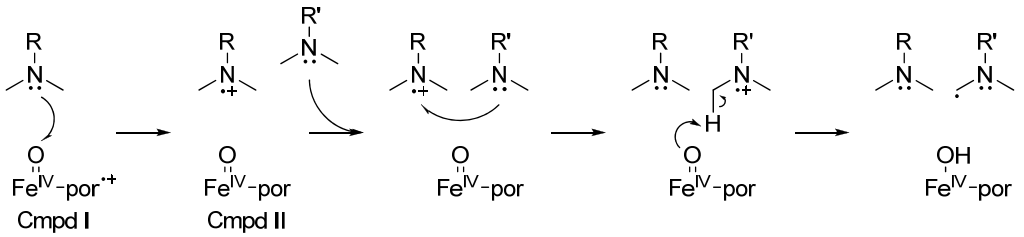

Figure 3.6. Single electron transfer between two substrates of Cmpd II.

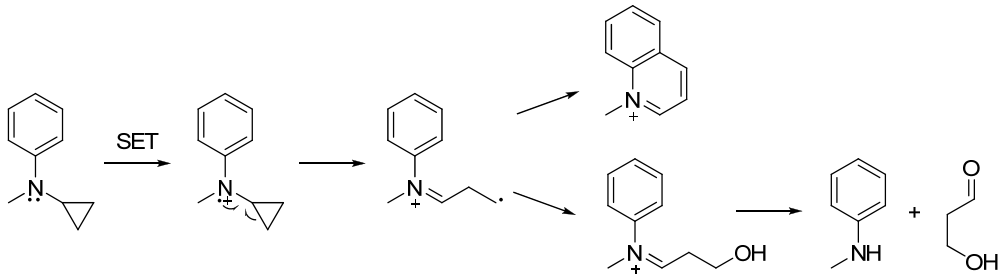

Figure 3.7. Product formations from *N*-cyclopropyl-*N*-methylaniline directed by a SET mechanism.

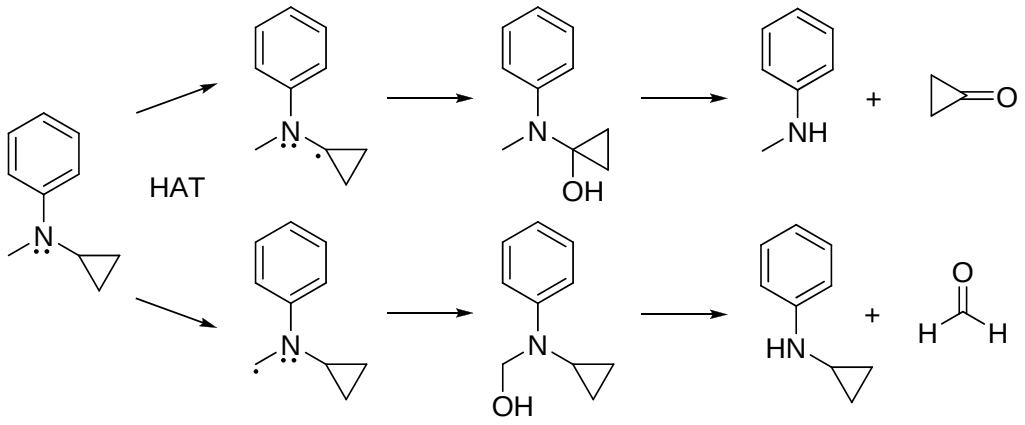

Figure 3.8. Product formations from *N*-cyclopropyl-*N*-methylaniline directed by a HAT mechanism.

References.

1. Ortiz de Montellano, P.R. and J.J. De Voss, *Oxidizing species in the mechanism of cytochrome P450.* Natural Product Reports, 2002. **19**(4): p. 477-493.
2. Wang, Y., et al., *Theoretical Study of N-Demethylation of Substituted N,N-Dimethylanilines by Cytochrome P450: The Mechanistic Significance of Kinetic Isotope Effect Profiles.* The Journal of Physical Chemistry B, 2007. **111**(26): p. 7700-7710.
3. Shaffer, C.L., et al., *Formation of Cyclopropanone during Cytochrome P450-Catalyzed N-Dealkylation of a Cyclopropylamine.* Journal of the American Chemical Society, 2002. **124**(28): p. 8268-8274.
4. Shaffer, C.L., M.D. Morton, and R.P. Hanzlik, *N-Dealkylation of an N-Cyclopropylamine by Horseradish Peroxidase. Fate of the Cyclopropyl Group.* Journal of the American Chemical Society, 2001. **123**(35): p. 8502-8508.
5. Guengerich, F.P., et al., *Radical cation intermediates in N-dealkylation reactions.* Xenobiotica, 1995. **25**(7): p. 689-709.
6. Goto, Y., et al., *Mechanisms of N-demethylations catalyzed by high-valent species of heme enzymes: Novel use of isotope effects and direct observation of intermediates.* Journal of the American Chemical Society, 1998. **120**(41): p. 10762-10763.
7. Cerny, M.A. and R.P. Hanzlik, *Cytochrome P450-Catalyzed Oxidation of N-Benzyl-N-cyclopropylamine Generates Both Cyclopropanone Hydrate and 3-Hydroxypropionaldehyde via Hydrogen Abstraction, Not Single Electron Transfer.* Journal of the American Chemical Society, 2006. **128**(10): p. 3346-3354.

8. French, K.J., et al., *Benign Synthesis of 2-Ethylhexanoic Acid by Cytochrome P450cam: Enzymatic, Crystallographic, and Theoretical Studies.* Biochemistry, 2001. **40**: p. 9532-9538.

9. Emmons, W.D. and G.B. Lucas, *Peroxytrifluoroacetic Acid. V. The Oxidation of Ketones to Esters.* Journal of the American Chemical Society, 1955. **77**(8): p. 2287-2288.

10. Kang, J. and K.S. Kim, *N-Cyclopropylation of Aromatic Amines.* Journal of the Chemical Society, Chemical Communications, 1987: p. 897-898.

11. Loeppky, R.N. and S. Elomari, *N-Alkyl-N-Cyclopropylanilines as Mechanistic Probes in the Nitrosation N,N-Dialkyl Aromatic Amines.* Journal of Organic Chemistry, 2000. **65**: p. 96-103.

12. Gadwood, R.C., et al., *Generation of (1-alkoxycyclopropyl)lithium reagents.* Journal of Organic Chemistry, 2002. **50**(18): p. 3255-3260.

13. Seto, Y.G., F. Peter, *Partitioning between N-dealkylation and N-Oxygenation in the Oxidation of N,N-Dialkylarylamines Catalyzed by Cytochrome P450 2B1.* Journal of Biological Chemistry, 1993. **268**(14): p. 9986-9997.

14. Okazaki, O. and F.P. Guengerich, *Evidence for specific base catalysis in N-dealkylation reactions catalyzed by cytochrome P450 and chloroperoxidase. Differences in rates of deprotonation of aminium radicals as an explanation for high kinetic hydrogen isotope effects observed with peroxidases.* Journal of Biological Chemistry, 1993. **268**(3): p. 1546-1552.

15. Guengerich, F.P., C.-H. Yun, and T.L. MacDonald, *Evidence for a 1-electron oxidation mechanism in N-dealkylation of N,N-dialkylanilines by cytochrome P450 2B1.* Journal of Biological Chemistry, 1996. **271**(44): p. 27321-27329.

16. Dinnocenzo, J.P., S.B. Karki, and J.P. Jones, *On Isotope Effects for the Cytochrome P-450 Oxidation of Substituted N,N-Dimethylanilines.* Journal of the American Chemical Society, 1993. **115**: p. 7111-7116.

17. Dowers, T.S., et al., *Kinetic isotope effects implicate the iron-oxene as the sole oxidant in P450-catalyzed N-dealkylation.* Journal of the American Chemical Society, 2004. **126**(29): p. 8868-8869.

CHAPTER FOUR

Kinetic Isotope Effects Demonstrate Involvement of a Second Oxidant With Mutation of Active Site Threonine

(This chapter is part of a work in preparation.

Authors: Kenneth M. Roberts, Carolyn A. Joswig-Jones and Jeffrey P. Jones)

This work was supported by NIH Grants ES009122.

Abstract

The putative reactive oxygen species in Cytochrome P450 (P450) has long been proposed to be an iron-oxene species (Cmpd I). Recent studies, however, have proposed the role of a second (and even a third) reactive species involved in several oxidations including sulfoxidation, epoxidation and deformylation. These studies have focused on site-directed mutagenesis of an active-site threonine residue proposed to be involved in the requisite proton transfers leading to formation of Cmpd I. We measured the kinetic isotope effects (KIEs) for *N*-demethylation of a series of *para*- substituted *N*,*N*-dimethylanilines with P450 BM3 F87A and its T268V mutant as a means to discern whether a change in mechanism occurs upon mutation of the active-site threonine. Our findings demonstrate that a break from the characteristic isotope effect profile does occur with the T268V mutant. While the range of the KIEs was not different from those seen previously, no discernible linear free energy relationship was observed. To further support this break in the profile, we measured KIEs for the benzylic hydroxylation of *p*-cyanotoluene, observing a large change in the isotope effect from 6.84 to 3.4. While these experiments cannot distinguish a specific oxidant in the mutant system, the change in the isotope effect profile suggests a change in the oxidative mechanism for both *N*-dealkylation and benzylic hydroxylation and supports the role of a second oxidant upon mutation of the active-site threonine.

Introduction

The heme-containing Cytochrome P450s (P450) have long been studied for their ability to oxidize lipophilic substrates by a variety of oxidations. The mechanism of P450s centers on the activation of molecular oxygen to a reactive species capable of performing oxidative reactions including heteroatom oxidations and dealkylations, olefin epoxidation, and aromatic and aliphatic hydroxylations.[1] The assortment of oxidations that are performed by P450s has led to the assigning of a heme-iron-oxene similar to the Cmpd I-species of chloroperoxidase as the putative reactive species in these oxidations (Figure 4.1).

P450 Cmpd I is proposed to derive from the reduction of molecular oxygen by two electrons originating from NAD(P)H. In a series of steps, the heme-iron(III) accepts a molecular oxygen ligand and two electrons to form an iron-peroxo species $(Fe\text{-}O_2)^{+1}$, termed Cmpd 0. This species then accepts two sequential protons to form an iron-hydroperoxo species $(Fe\text{-}OOH)^{+2}$ followed by formation of the iron-oxene $(Fe\text{-}O)^{+3}$ (Cmpd I) with the simultaneous loss of a water molecule (Figure 4.1).

From site-directed mutagenesis experiments, a highly conserved active site threonine residue has been implicated in the proton transfer mechanism (Figure 4.2). Mutations of this threonine to aliphatic residues in P450cam showed a marked reduction in the hydroxylation of camphor.[2, 3] Further, uncoupling of NADH from product formation was observed in the formation of water and hydrogen peroxide. Similar results were seen for the hydroxylation of laurate by P450BM3 and the T268A mutant.[4] These studies concluded that mutation of the threonine residue to an aliphatic residue disrupted the productive protonation of Cmpd 0. Unproductive protonation of Cmpd 0 to form hydrogen peroxide then dominates the reaction in these mutants (Figure 4.3).

Further studies with these mutants have led investigators to propose a second oxidant, in addition to Cmpd I, is responsible for substrate oxidations.[5-9] Vaz, *et al* measured product formation rates for the epoxidation and allylic hydroxylation of several small molecule olefins in two P450 isoforms (2E1 and 2B4) and their corresponding Thr→Ala mutants.[5] When the threonine was replaced by an alanine, they observed a shift in the ratio of products towards epoxidation. They concluded that Cmpd 0 was responsible for the observed epoxidation and the slow conversion to Cmpd I explained the reduced rates of allylic hydroxylation. Newcomb and coworkers employed a variety of cyclopropyl-containing compounds as radical clocks to determine contributions of a second oxidant in aliphatic hydroxylations. They concluded that a carbocation intermediate partially contributed to products formed and that this intermediate must derive from Cmpd 0.[8-10]

Shaik and coworkers have offered an alternative to Cmpd 0 as the "second oxidant".[7, 11] In theoretical calculations of ethene epoxidation by Cmpd 0, they calculated large barriers (37-53 kcal/mol) for epoxidation by Cmpd 0.[7] Further, they showed protonation of Cmpd 0 resulted in Cmpd I formation and loss of water, estimating the basicity of Cmpd 0 between water and hydroxide anion. They concluded that the large barriers for epoxidation argued against Cmpd 0 as an effective oxidant, reinforcing its role as a base for conversion to Cmpd I. In contrast, low barriers (14-15 kcal/mol) were calculated for the same reaction performed by Cmpd I.[11] The calculations also described different pathways depending on the spin-state of Cmpd I. Where the quartet-state Cmpd I demonstrated a stepwise mechanism for epoxidation of ethene, the doublet-state showed an essentially barrierless conversion from the intermediate to epoxide, resulting in a concerted mechanism. These studies led to the proposal that the "two oxidants" observed in

P450-mediated reactions were actually two different spin-states of Cmpd I, now referred to as the "two-state reactivity" model (TSR).

In work with *N*,*N*-dimethyl-4-(methylthio)aniline, Volz, *et al* showed an increase in the ratio of sulfoxidation to *N*-demethylation with the T268A mutant of P450BM3 relative to the wild-type.[6] They also showed that deuterium labeling of the *N*-methyl groups to slow *N*-demethylation did not demonstrate isotopically sensitive branching[12] to sulfoxidation. While they concluded the two oxidations must derive from two different oxidants, they could not distinguish whether the involvement of Cmpd 0 or a selective spin-state of Cmpd I was the relevant model. In attempts to shed light on the findings of Volz, *et al*, Shaik and coworkers evaluated sulfoxidation[13] and *N*-dealkylation[14] with theoretical calculations, concluding that the two oxidations do show opposing preferences for Cmpd I spin-states. These findings support a TSR model under the assumption that the two spin-states interconvert slowly. If correct, each spin-state would act as an independent oxidant with unique preferences for activity. Further, if mutation of the active site threonine altered the ratio of spin-states, an altered ratio of products would be expected.

In a further complication of the system, Coon and coworkers have offered the iron-peroxo species prior to Cmpd 0 as a nucleophilic oxidant in the deformylation of aldehydes by P450.[15, 16] They showed that the P450 2B4-mediated deformylation of cyclohexanecarboxaldehyde could be supported with the oxygen surrogate hydrogen peroxide but not with iodosylbenzene (PhIO), *m*-chloroperbenzoic acid (mCPBA) or cumene hydroperoxide (CHP).[15] They concluded that the failure of PhIO, mCPBA and CHP to perform deformylation excluded Cmpd I as the relevant oxidant arguing in favor of the nucleophilic iron-peroxo species (Figure 4.4). The deformylation reaction was further tested with the T302A mutant of P450 2B4. An increased rate

of deformylation was observed in contrast to the decreased rates seen for other oxidations.[16] As the mutant was expected to slow deprotonation of the putative oxygen species, they argued this as further evidence of the role of the iron-peroxo species in deformylation.

With a variety of oxidations appearing to derive from disparate oxidants, a clear picture of the involvement of the proposed oxidants has been elusive. However, one tool for evaluation of the oxidative mechanisms has largely been overlooked in the search for the "second oxidant": the determination of kinetic isotope effect profiles (IEPs). IEPs have been commonly used in the evaluation of P450 mechanisms and for comparing mechanisms by various P450 systems. Examples include: the demonstration of similar mechanisms for the *N*-dealkylation of *N*,*N*-dimethylanilines[17] and the hydroxylation of toluenes[18] across various isoforms of P450; the revelation of similar mechanisms for *N*-dealkylation by the native NAD(P)H/O_2 system and anilinic *N*-oxides;[19] and the dissimilarity of mechanisms of *N*-dealkylation by the native system and both iodosylbenzene- and cumene hydroperoxide-supported systems.[20] Yet, surprisingly, generation of IEPs for a single mode of oxidation in a wild-type (threonine-containing) P450 and its aliphatic mutant has not previously been performed.

In this study, we used kinetic isotope effects to evaluate the mechanism of *N*-demethylation in an enzyme with the active site threonine mutated to an aliphatic valine residue. Based on the results of Volz, *et al*, we hypothesized *N*-dealkylation to be performed by Cmpd I in both wild-type and mutant systems. Though the mutant should show slower product formation due to the slower conversion of Cmpd 0 to Cmpd I, *N*-dealkylation was expected to show similar isotope effect profiles resulting from oxidation by Cmpd I.

To compare IEPs for *N*-dealkylation, we used P450BM3 F87A and the F87A,T268V double-mutant. Wild-type P450BM3 shows a strong preference for hydroxylating the aliphatic terminus

of long-chain fatty acids owing to a phenylalanine residue which blocks the active site opening such that long unbranched alkanes have greater access to the heme. The active-site mutant P450BM3 F87A, however, has been shown to open the active site to permit both the binding of larger, cyclic molecules[21] as well as the accommodation of two long chain fatty acid simultaneously.[22]

The P450BM3 F87A and F87A,T268V double-mutant enzymes were used to measure kinetic isotope effects for the *N*-demethylation of a series of *para*-susbstituted *N*,*N*-dimethylanilines (Figure 4.5). Isotope effects were measured by quantifying the amounts of formaldehyde-d_1 and -d_2 produced in the reaction with P450 (Figure 4.6), with formaldehyde quantification determined by GC-MS of the 5,5-dimethyl-1,3-cyclohexanedione (dimedone) derived adducts as described previously by Karki, *et al* (Figure 4.7).[17] Our results show that, while F87A demonstrates a similar IEP to those seen previously,[17, 19] the double-mutant shows an IEP that differs strikingly from that of F87A. We address the differences in terms of the contributions of two oxidants as they relate to the two enzymes, with the conclusion that a change in mechanism must be occurring as a result of the mutation of threonine. Implications for the "second oxidant" hypotheses are discussed.

Experimental Methods

Materials. Reagent or HPLC grade chemicals and solvents were supplied by Aldrich (Milwaukee, WI), Fisher Scientific (Fair Lawn, NJ), EMD (Madison, WI), and Mallinckrodt Baker (Phillipsburg, NJ). Gas chromatography/mass spectrometry was performed on a ThermoQuest Voyager GC/MS (Thermo-Finnegan) coupled to a CE Instruments GC8000Top affixed with a 30m JW Scientific DB-1 GC column.

Substituted *N,N-bis*(dideuteriomethyl)anilines. These compounds were prepared as described in Dinnocenzo, *et al* J. Am. Chem. Soc. **1993**, *115*, 7111-7116.

Substituted toluenes-α-d_1. These compounds were prepared as described in Higgins, *et al* Biochem. **1998**, *37*, 7039-7046.

Mutagenesis of P450BM3 F87A. P450BM3 F87A cDNA in the pUC19 vector was mutagenized using the Quikchange II site-directed mutagenesis kit (Stratagene, La Jolla, CA). Mutagenesis was performed using the protocol suggested by the manufacturer. Primers were purchased from Invitrogen (Carlsbad, CA). The primers used to generate mutant F87A,T268V were 5'-aaaaaaaaaaaagcgggacacgaagtaacaagtggtc-3' (forward) and 5'-aaaaaaaaaaaagaccacttgttacttcgtgtcccgc-3' (reverse). Mutagenized plasmids were amplified and isolated using a Wizard II midi prep kit from Promega (Madison, WI).

Expression of P450BM3 Mutants. P450BM3 F87A and F87A,T268V cDNA were transformed into DH5α cells and grown on LB-agarose plates containing 100 μg/mL ampicillin. A single

colony was picked and grown in 2 mL LB broth containing 100 μg/mL ampicillin and 0.20% glucose for 12 h at 37 °C, 250 rpm. 500 μL of the resulting culture were transferred to 50 mL of TB broth containing 100 μg/mL ampicillin, 0.20% glucose, 2.0 mM $MgSO_4$, 100 μM $CaCl_2$, 50 μM H_3BO_3, 200 nM $CoCl_2 \cdot 6H_2O$, 1.0 μM $CuSO_4 \cdot 5H_2O$, 1.0 μM $MnCl_2 \cdot H_2O$, 1.0 nM $NaMoO_4 \cdot 2H_2O$, 2.0 μM $ZnCl_2$, 10 μM $FeSO_4 \cdot 7H_2O$ and 10 μL/mL MEM vitamin stock and incubated for 12 h at 37 °C, 250 rpm. A final large scale culture was prepared by adding 25 mL of the second culture to 500 mL of TB broth, as completed above, and charged with 20 μg/mL δ-aminolevulinic acid. The large scale culture was incubated at 33 °C, 250 rpm for 24 h. Cells were harvested by centrifuging the culture at 3,000 rpm for 20 min at 4 °C. Supernatant was poured off and the pelleted cells transferred to 50 mL Falcon tubes and stored at -80 °C.

Purification of P450BM3 Mutants. Cell paste was thawed and resuspended in 1.0 mL Buffer A (100 mM potassium phosphate buffer (pH 7.4), 0.1 mM EDTA, 50 uM dithiothreitol) per gram of paste. 500 μg/mL lysozyme and 2.0 μg/mL aprotinin were added to the suspension and the mixture stirred for 40 min at 4 °C. 0.29 mg/mL $MgCl_2$ and 10 μg/mL each of RNase A and DNase I were added and the mixture stirred a further 40 min at 4 °C. After stirring, cell lysing was completed with sonication. The resulting suspension was centrifuged at 100,000 x g for 30 min at 4 °C. The supernatant was collected and loaded onto a 2',5'-ADP-agarose column equilibrated with Buffer A. The column was washed with 8-10 column volumes of Buffer A followed by 6 column volumes of Buffer B (100 mM potassium phosphate buffer (pH 7.4), 0.1 mM EDTA, 50 μM dithiothreitol, 5.0 mM adenosine). The enzyme was eluted with Elution Buffer (100 mM potassium phosphate buffer (pH 7.4), 5.0 mM 2',3'-AMP, 0.1 mM EDTA, 50 μM dithiothreitol in 100 mM). The eluent was dialyzed in 100 mM potassium phosphate buffer

(pH 7.4) for removal of the 2',3'-AMP. Concentrations of P450BM3 were determined by UV-Vis absorption of the 450 nm soret peak elicited upon exposure to carbon monoxide.

Incubations with *para*-Substituted DMAs. Incubations of P450BM3 F87A and F87A,T268V with *para*-substituted *N*,*N*-*bis*(dideuteriomethyl)anilines were performed using 1.0 μM P450, 1.0 mM substituted DMA and 1.0 mM NADPH brought to a total volume of 1.0 mL with 100 mM phosphate buffer, pH 7.4. Samples were preincubated at 37 °C for 10 or 15 min prior to initiation with NADPH. Reactions were incubated at 37 °C for 30 min, then quenched with 100 μL 40% sodium hydroxide followed immediately by vortexing. 100 μL of 100 mM dimedone in 200 mM sodium hydroxide was added to the samples for quantification of formaldehyde. Dimedone was allowed to react with the formaldehyde products for 30 min at room temperature. After reaction, 380 μL 4.0 M HCl was added to acidify each sample. Dimedone adducts were extracted three times with 1.0 mL dichloromethane followed by vortexing and centrifugation at 3000 x g for 10 min. Extracts were combined and dried with $MgSO_4$. Solvent was evaporated gently under N_2(g) in a 35 °C bath and the residue was redissolved in 200 μL dichloromethane. Reaction products were monitored by gas chromatography/mass spectrometry (GC/MS) using electron impact ionization. The GC method began at 70 °C for 2.0 min followed by a 30 °C/min ramp to 240 °C, then held at 240 °C for 7.5 min. Ions with m/z 291-295 were monitored for quantification of the isotopic distribution of the dimedone adducts (m/z 292 is the parent ion for the d_0-adduct).

Incubations with *p*-Cyanotoluene. Incubations of P450BM3 F87A and F87A,T268V with *p*-cyanotoluene-α-d_1 were performed using an NADPH regenerating system to avoid the formation of aldehydes due to secondary oxidation. Samples included 1.0 μM P450, 10 mM

p-cyanotoluene-α-d_1, 5.0 μM $NADP^+$, 10 mM glucose-6-phosphate, 2.0 mM $MgCl_2$, 1.0 U/mL glucose-6-phosphate dehydrogenase and 90 μg/mL catalase brought to a total volume of 1.0 mL with 100 mM phosphate buffer, pH 7.4. Samples were preincubated at 37 °C for 10 min prior to initiation with $NADP^+$. Reactions were incubated at 37 °C for 30 min, then quenched with 1.0 mL dichloromethane followed immediately by vortexing. Samples were spiked with 100 nmol benzyl alcohol as an internal standard, then vortexed and centrifuged at 3000 x g for 10 min. The organic layer was extracted and collected. Products were further extracted twice with 1.0 mL dichloromethane, vortexing and centrifugation. The extracts were combined and dried with $MgSO_4$. Samples were concentrated gently under a flow of N_2(g) in a 35 °C bath to approximately 200 μL. 25 μL MTBSTFA was added directly to the concentrated samples and the samples were incubated at 70 °C overnight to derivatize the product alcohols. Reaction products were monitored by gas chromatography/mass spectrometry (GC/MS) using electron impact ionization. The GC method began at 70 °C for 5.0 min followed by a 10 °C/min ramp to 230 °C, then held at 230 °C for 5.0 min. Ions of m/z 189-193 were monitored for the quantification of the isotopic distribution of the silyl derivatized products (m/z 190 is the [M-57]+ ion of the -d_0 silylated product).

KIE Determinations. KIEs were calculated by determining the contributions of the isotopic variants to the measured isotopic distributions. Contributions were based on the GC-MS derived isotopic distribution of the -d_0 products. For the dimedone adducts, contributions of the -d_0, -d_1 and -d_2 adducts were calculated from the measured intensities for $[M-1]^+$, $[M+1]^+$ and $[M+2]^+$ ions of the -d_0 adduct. These were 0.7, 19.7 and 2.7% of the $[M]^+$ ion, respectively. KIEs were then determined by the ratio of calculated -d_2 product:-d_1 product, multiplying by 2 to

compensate for the 2 D : 1 H ratio of the substrate. For the *p*-cyanobenzyl alcohol product, contributions of the -d_0 and -d_1 silyl derived products were calculated from the intensities measured for $[M-58]^+$ and $[M-56]^+$ ions of the -d_0 silylated product. These were 1.6 and 16.8% of the $[M-57]^+$ ion, respectively. The KIE was then determined by the ratio of calculated -d_1 product:-d_0 product, dividing by 2 to adjust for the ratio of 1 D : 2 H in the substrate.

Results and Discussion

KIEs for the *N*-dealkylation of *para*-substituted *N*,*N*-dimethylanilines (DMAs) were measured in P450BM3 F87A and F87A,T268V (Table 4.1). KIEs measured in F87A were very similar to those seen previously by Karki, *et al* for several isoforms of P450.[17] With little deviation, we observe the same trend of increasing KIE with increasingly electron-withdrawing substituents. In contrast, the KIEs measured with F87A,T268V did not show the same trend. The KIEs were found to be in the same window of 2.5-3.6 as those measured in F87A, however, values for each substituted DMA were significantly different between the two enzymes. Additionally, there appears to be no significant linear free energy relationship for these KIEs as determined from linear regression analysis.

The observed differences in the isotope effects profiles (IEPs) between P450BM3 F87A and F87A,T268V strongly argue against similar mechanisms in these two enzymes. F87A demonstrates a profile for *N*-demethylation consistent with those observed across other isoforms of P450. Work with *N*-cyclopropyl-*N*-methylaniline by Hanzlik and coworkers with P450s and the heme-containing horse radish peroxidase have supported a hydrogen atom transfer mechanism (HAT) for *N*-dealkylation mediated by P450 enzymes.[23, 24] Studies with *N*-oxides discussed in this work tie this mechanism to the Cmpd I species (Chapters 2 and 3). The similarity of the IEP with other isoforms of P450 strongly supports F87A as another example of the consistency of this mechanism across P450s.

In contrast, F87A,T268V shows considerable deviation from the norm. Though the range of KIEs is similar those seen in F87A and other P450s, there appears to be no discernable linear free energy relationship attributable to the substituents. This finding supports that *N*-dealkylation in the absence of the conserved threonine residue deviates from the native HAT mechanism.

Because the magnitude of the KIEs measured did not deviate far from those seen in the wild types, we tested the hydroxylation of *p*-cyanotoluene by F87A and F87A,T268V. A large KIE of 6.84 was measured for hydroxylation in F87A. While lower than that seen for *p*-cyanotoluene in other P450 isoforms by Higgins, *et al*,[18] this value is well in line with those seen for other toluenes.[18, 25] In contrast, a much smaller isotope effect of 3.4 was observed from F87A,T268V. This large decrease in isotope effect again demonstrates a significant deviation from the wild type enzyme.

Jones, Dinnocenzo and coworkers measured the isotope effects of *N*-demethylation and benzylic hydroxylation with various P450 enzymes and compared them to those derived from hydrogen atom abstraction by the *tert*-butoxy radical.[17, 25] For all compounds tested, they found nearly identical isotope effects between the two systems, lending strong support for hydrogen atom abstraction in these reactions. Yet, with the F87A,T268V mutant, we observe a kinetic isotope effect for benzylic hydroxylation significantly diminished from the normally high KIEs previously seen for toluenes. However, when considered with the isotope effects measured for *N*-dealkylation, the isotope effects do not seem to vary largely by substituent groups, as all values are clustered within a small window of 2.8-3.5.

These data suggest that in the F87A,T268V mutant, a second mechanism for oxidation is contributing to the observed oxidations. However, if a single, new mechanism were accounting for oxidation of the substrates, we would expect to see a new linear free energy relationship (LFER) reflecting this new mechanism. Interestingly, no such relationship is observed. This finding suggests a system where multiple mechanisms, defined by unique oxidants, are in competition.

A complex system involving multiple oxidants is expected to have a variety of outcomes dependent on the kinetics of the individual steps. In the simplest example, where two oxidants are in competition, we would expect certain outcomes. We define a simple system involving two oxidants with a kinetic scheme shown in Figure 4.8. In this system, if the conversion of ES1 to ES2 (k_3) is much faster than the formation of product by ES1 (k_5), we would expect to see all product formation derive from the ES2 complex. We propose this situation in the wild-type P450 system. When threonine is present in the active-site, protonation of Cmpd 0 to form the native Cmpd I (ES2) is rapid in comparison to oxidation by a prior oxidant (Cmpd 0 or iron-peroxo). *N*-dealkylation and benzylic hydroxylation are then performed by this oxidant with little to no contribution from an ES1 complex. Due to the sole involvement of the native Cmpd I, isotope effect profiles reflect a system of hydrogen atom abstraction as seen with *tert*-butoxyl radical. In contrast, if the formation of product from ES1 (k_5) was in competition with the conversion to ES2 (k_3), we would expect to see product formation result from both ES1 and ES2. This scenario is proposed for the mutant enzyme. With protonation of Cmpd 0 to form Cmpd I (ES2) slowed by the loss of the hydroxyl group, a second oxidant (ES1) is given an opportunity to act on the substrate. However, if the second oxidant was dominating product formation, we would expect to see a new LFER for isotope effects indicating the new mechanism. Instead, contributions from both oxidants to product formation results in a mixture of two unique LFERs. This scenario often results in the disruption of an observable LFER, which may be further complicated if the substrate affects the interplay between ES1 and ES2.

In the search for "the second oxidant" of P450-mediated oxidations, both Cmpd 0 and an alternative spin-state of Cmpd I have been proposed. While the isotope effects observed in this work demonstrate contributions of a second oxidizing species in the valine mutant, neither

proposed oxidant can be excluded. In a Cmpd 0 model, the slowing of Cmpd I formation in the mutant leads to the build-up of Cmpd 0. While slow and unobserved in the wild-type, oxidation from this species becomes competitive with Cmpd I formation in the mutant. Further, the presence of substrate complicates matters. Since these mutants are generally associated with unproductive protonation to form hydrogen peroxide, a proton network must be available to the Cmpd 0. Without the threonine to act as part of a structured proton network, substrate orientation in the active site would be expected to directly affect protonation of Cmpd 0 leading to Cmpd I formation, consequently altering the contributions from the two oxidants. This situation could explain the lack of an observable LFER in this system, as any susbtrate would uniquely alter the competition between Cmpd I formation and substrate oxidation by Cmpd 0.

A similar situation can be used to explain a TSR model. In the native system, the polar effects of the threonine hydroxyl group in proximity to Cmpd I could elicit a preference for a single spin-state. Loss of the hydroxyl group upon mutation of the threonine to an aliphatic residue would alter the polarity around Cmpd I. This altered environment could disrupt the bias for a single spin-state permitting the competition of an alternate spin-state. As proposed by Shaik and coworkers, these different spin-states of Cmpd I would act as unique oxidants with unique LFERs. Additionally, the substrate bound in the active site would be expected to further complicate the ratio of the two spin-states dependent directly on the polar character of the substrate.

In this study, we have shown that the F268V mutant of P450BM3 F87A demonstrates isotope effects unique from those observed in wild-type enzymes. Further, these isotope effects fail show a clear linear free energy relationship. These observations have led us to conclude a second oxidant, in addition to the native Cmpd I, is contributing to product formation in the

valine mutant. Additionally, the lack of an LFER also leads us to propose a system where product formation is not exclusive to the second oxidant, but instead is derived from both oxidants, with the two oxidants in a complex competition. While a system involving two oxidants is proposed, the nature of that oxidant is unclear as both a Cmpd 0 and a TSR model can explain our observations. Current work in our lab includes expanding the isotope effect profile to additional substrates as well as elucidating the nature of the second oxidant.

Table 4.1. Kinetic Isotope Effects Measured for Reactions of Substituted *N*,*N*-dimethylanilines and toluenes by P450BM3 F87A and F87A,T268V

Substrate	F87A	F87A,T268V	p-value[a]
N,*N*-dimethylaniline	2.71 ± 0.04	3.22 ± 0.07	<0.002
p-chloro-*N*,*N*-dimethylaniline	2.55 ± 0.01	3.18 ± 0.03	<0.0001
p-cyano-*N*,*N*-dimethylaniline	3.118 ± 0.006	2.81 ± 0.03	<0.0003
p-nitro-*N*,*N*-dimethylaniline	3.66 ± 0.05	3.54 ± 0.06	<0.04
p-cyanotoluene	6.84 ± 0.08	3.4 ± 0.3	<0.002

[a] Statistical significance of the measured KIE values between the two enzymes.

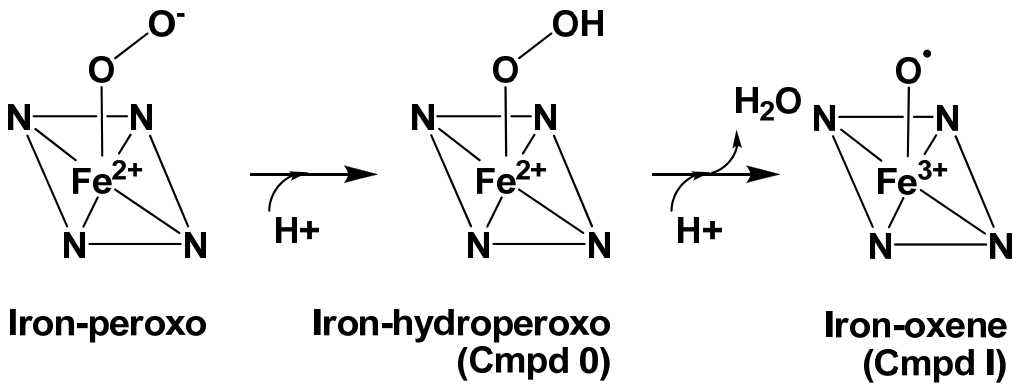

Figure 4.1. Putative reactive oxygen species in the mechanisms of P450-mediated oxidations.

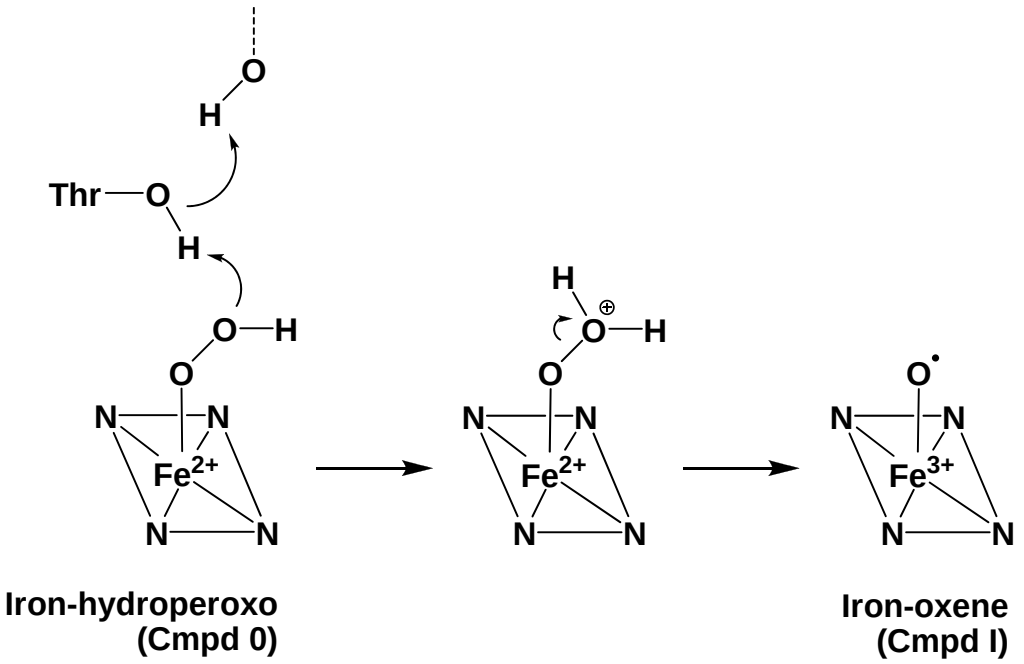

Figure 4.2. Proposed role of the conserved threonine residue in the protonation of Cmpd 0 leading to the formation of Cmpd I.

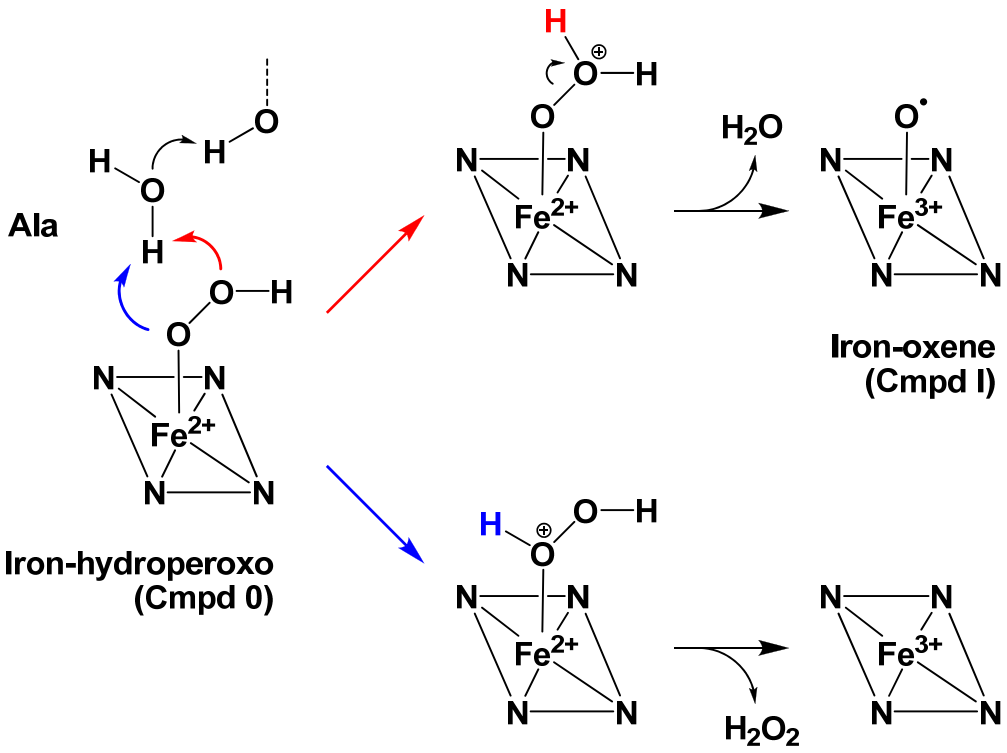

Figure 4.3. Proposed protonations of Cmpd 0 upon mutation of the active-site threonine to an alanine residue.

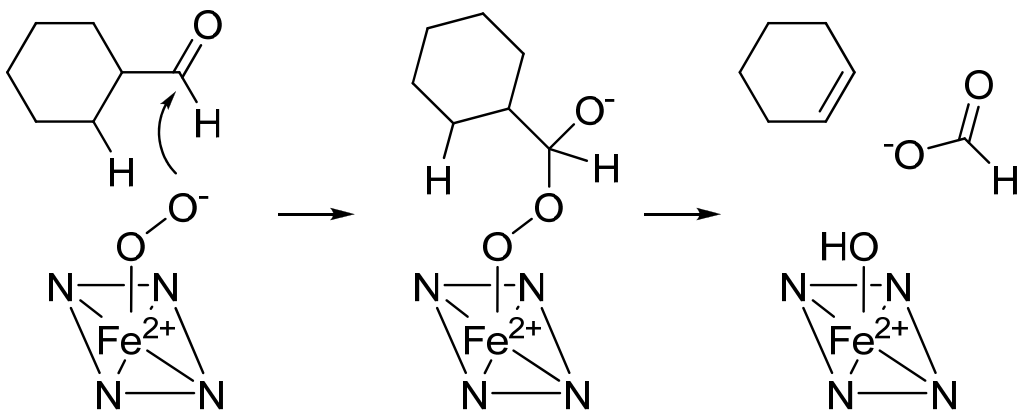

Figure 4.4. Proposed mechanism for the deformylation of cyclohexanecarboxaldehyde by the iron-peroxo species.

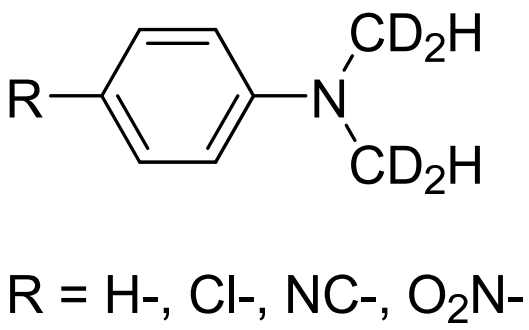

Figure 4.5. *para*-Substituted *N*,*N*-dimethylanilines used for measurement of the intrinsic kinetic isotope effects of *N*-dealkylation.

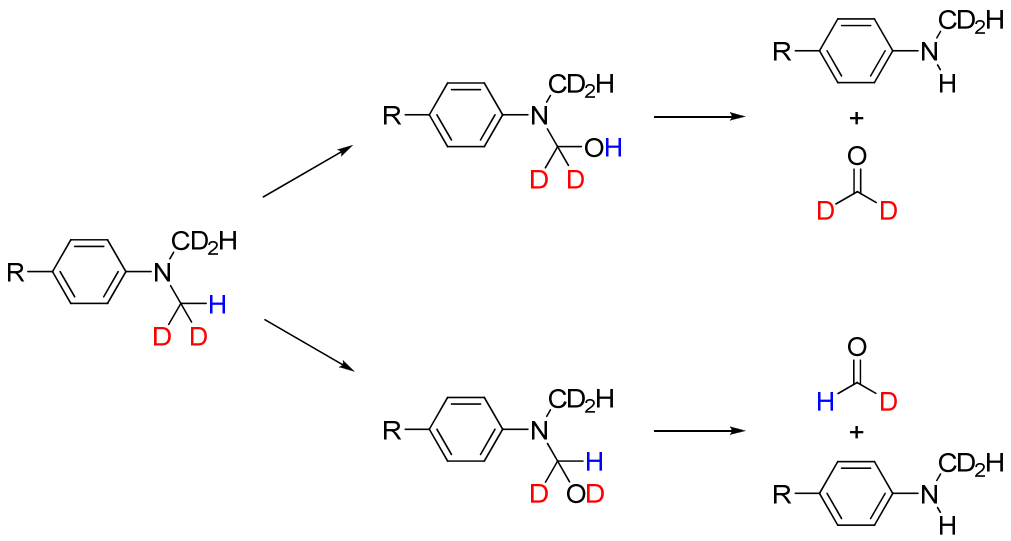

Figure 4.6. Production of isotopically distinct formaldehyde-d_1 and -d_2 from *N*,*N*-bis(dideuteriomethyl)aniline.

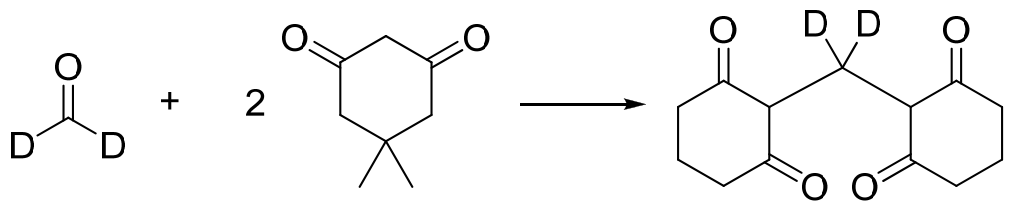

Figure 4.7. Derivatization of formaldehyde-d_2 with dimedone showing the di-adduct.

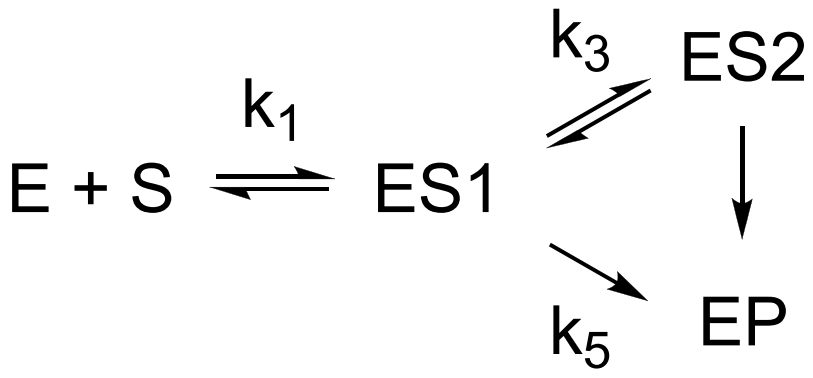

Figure 4.8. Kinetic scheme for two possible reactive enzyme-substrate complexes resulting in the same product.

References

1. Ortiz de Montellano, P.R., *Cytochrome P450:Structure, Mechanism, and Biochemistry*. 2nd ed, ed. O.d.M. P.R. 1995: Plenum: New York.
2. Imai, M., et al., *Uncoupling of the cytochrome P-450cam monooxygenase reaction by a single mutation, threonine-252 to alanine or valine: possible role of the hydroxy amino acid in oxygen activation.* Proceedings of the National Academy of Sciences of the United States of America, 1989. **86**(20): p. 7823-7827.
3. Martinis, S.A., et al., *A conserved residue of cytochrome P-450 is involved in heme-oxygen stability and activation.* Journal of the American Chemical Society, 1989. **111**(26): p. 9252-9253.
4. Yeom, H., et al., *The Role Of Thr268 In Oxygen Activation Of Cytochrome P450(Bm-3).* Biochemistry, 1995. **34**(45): p. 14733-14740.
5. Vaz, A.D.N., D.F. McGinnity, and M.J. Coon, *Epoxidation of olefins by cytochrome P450: Evidence from site-specific mutagenesis for hydroperoxo-iron as an electrophilic oxidant.* Proceedings of the National Academy of Sciences of the United States of America, 1998. **95**(7): p. 3555-3560.
6. Volz, T.J., D.A. Rock, and J.P. Jones, *Evidence for two different active oxygen species in cytochrome p450 BM3 mediated sulfoxidation and N-dealkylation reactions.* Journal of the American Chemical Society, 2002. **124**(33): p. 9724-9725.
7. Ogliaro, F., et al., *Searching for the second oxidant in the catalytic cycle of cytochrome P450: a theoretical investigation of the iron(III)-hydroperoxo species and its epoxidation pathways.* Journal of the American Chemical Society, 2002. **124**(11): p. 2806-2817.

8. Newcomb, M., P.F. Hollenberg, and M.J. Coon, *Multiple mechanisms and multiple oxidants in P450-catalyzed hydroxylations.* Archives of Biochemistry and Biophysics, 2003. **409**(1): p. 72-79.

9. Chandrasena, R.E.P., et al., *Hydroxylation by the hydroperoxy-iron species in cytochrome P450 enzymes.* Journal of the American Chemical Society, 2004. **126**(1): p. 115-126.

10. Sheng, X., et al., *Kinetic Isotope Effects in Hydroxylation Reactions Effected by Cytochrome P450 Compounds I Implicate Multiple Electrophilic Oxidants for P450-Catalyzed Oxidations* Biochemistry, 2009. **48**(7): p. 1620-1627.

11. de Visser, S.P., et al., *Multi-State Epoxidation of Ethene by Cytochrome P450: A Quantum Chemical Study.* Journal of the American Chemical Society, 2001. **123**(13): p. 3037-3047.

12. Jones, J.P., et al., *Isotopically sensitive branching and its effect on the observed intramolecular isotope effects in cytochrome P450 catalyzed reactions: a new method for the estimation of intrinsic isotope effects.* Journal of the American Chemical Society, 1986. **108**: p. 7074-7078.

13. Sharma, P.K., S.P. De Visser, and S. Shaik, *Can a single oxidant with two spin states masquerade as two different oxidants? A study of the sulfoxidation mechanism by cytochrome p450.* Journal of the American Chemical Society, 2003. **125**(29): p. 8698-8699.

14. Cho, K.Y., et al., *"Formation of the Active Species of Cytochrome P450 by Using Iodosylbenzene: A Case for Spin-Selective Reactivity".* Chemistry: A European Journal, 2007. **13**: p. 4103-4115.

15. Vaz, A.D.N., E.S. Roberts, and M.J. Coon, *Olefin Formation in the Oxidative Deformylation of Aldehydes by Cytochrome-P-450 - Mechanistic Implications for Catalysis by Oxygen-Derived Peroxide.* Journal of the American Chemical Society, 1991. **113**(15): p. 5886-5887.

16. Vaz, A.D., et al., *Peroxo-iron and oxenoid-iron species as alternative oxygenating agents in cytochrome P450-catalyzed reactions: switching by threonine-302 to alanine mutagenesis of cytochrome P450 2B4.* Proceedings of the National Academy of Sciences of the United States of America, 1996. **93**(10): p. 4644-4648.

17. Karki, S., et al., *Mechanism Of Oxidative Amine Dealkylation Of Substituted N,N-Dimethylanilines By Cytochrome P-450 - Application Of Isotope Effect Profiles.* Journal of the American Chemical Society, 1995. **117**(13): p. 3657-3664.

18. Higgins, L., et al., *Evaluation of cytochrome P450 mechanism and kinetics using kinetic deuterium isotope effects.* Biochemistry, 1998. **37**(19): p. 7039-7046.

19. Dowers, T.S., et al., *Kinetic isotope effects implicate the iron-oxene as the sole oxidant in P450-catalyzed N-dealkylation.* Journal of the American Chemical Society, 2004. **126**(29): p. 8868-8869.

20. Guengerich, F.P., C.H. Yun, and T.L. Macdonald, *Evidence for a 1-electron oxidation mechanism in N-dealkylation of N,N-dialkylanilines by cytochrome P450 2B1. Kinetic hydrogen isotope effects, linear free energy relationships, comparisons with horseradish peroxidase, and studies with oxygen surrogates.* Journal of Biological Chemistry, 1996. **271**(44): p. 27321-27329.

21. Rock, D.A., et al., *Use of Kinetic Isotope Effects to Delineate the Role of Phenylalanine 87 in P450$_{BM3}$.* Bioorganic Chemistry, 2002. **30**(2): p. 107-118.

22. Rock, D.A., et al., *A method for determining two substrates binding in the same active site of cytochrome P450(BM3): an explanation of high energy omega product formation.* Archives of Biochemistry and Biophysics, 2003. **416**(1): p. 9-16.

23. Shaffer, C.L., M.D. Morton, and R.P. Hanzlik, *N-Dealkylation of an N-Cyclopropylamine by Horseradish Peroxidase. Fate of the Cyclopropyl Group.* Journal of the American Chemical Society, 2001. **123**(35): p. 8502-8508.

24. Shaffer, C.L., et al., *Formation of Cyclopropanone during Cytochrome P450-Catalyzed N-Dealkylation of a Cyclopropylamine.* Journal of the American Chemical Society, 2002. **124**(28): p. 8268-8274.

25. Manchester, J.I., et al., *A New Mechanistic Probe For Cytochrome P450 - an Application Of Isotope Effect Profiles.* Journal of the American Chemical Society, 1997. **119**(21): p. 5069-5070.

CHAPTER FIVE

Conclusion

Cytochrome P450s demonstrate a wide variety of oxidations on a wide variety of substrates. With the large role of P450s in the metabolism of pharmaceutical drugs, a clear understanding of how a given P450 isoform will act on a given compound is paramount to improving the efficacy of drug design. Accurate prediction of metabolites permits the removal of potential drug compounds that have toxic metabolites or strong tendencies for drug-drug interactions in the screening process, before they reach trials. The ability to predict one oxidation over another requires understanding the mechanism and energetics of each reaction, so they may be compared and ranked for relative likelihood of oxidation. Once a single reaction is clearly defined, it may be compared against other oxidations to interpret relative energetics or to compare mechanisms.

Of the many reactions P450 can perform, one of the most studied is *N*-dealkylation. Traditionally, *N*-dealkylation has been argued between two mechanisms, hydrogen atom transfer (HAT) and single electron transfer (SET). In a series of clever studies by Hanzlik and coworkers, ring-intact product formation from the probe *N*-cyclopropyl-*N*-methylaniline (CPMA) was used to show that P450s did not act under SET, leaving HAT as the likely mechanism.[1-3] Further support of the HAT mechanism requires tying the chemistry back to the reactive oxygen species proposed to perform the hydrogen atom abstraction, Cmpd I.

In this work, we evaluated the mechanism of *N*-dealkylation by P450s using *N*,*N*-dimethylaniline *N*-oxides (DMAOs) as oxygen surrogates. These compounds are capable of donating a single oxygen atom to the P450 heme-iron. Previous studies with DMAOs showed similar isotope effect profiles, and thus similar mechanisms, to the native P450 reaction.[4] We extended this study to a novel *N*-oxide, 2,3,4,5,6-pentafluoro-*N*-dimethylaniline *N*-oxide (PFDMAO), finding 30-fold faster rates for oxygen donation as compared to the unsubstituted DMAO. Further, PFDMAO was found capable of supporting the *N*-demethylation of

N,*N*-dimethylaniline (DMA), even preferring DMA over the direct product of oxygen donation 2,3,4,5,6-pentafluoro-*N*,*N*-dimethylaniline (PFDMA). These findings lead us to conclude donation of the oxygen atom from DMAOs to the P450 directly forms a Cmpd I species capable of performing *N*-dealkylation in a mechanism similar to the native P450 system. As the native system demonstrated ring-intact products from CPMA, supporting a HAT mechanism, we tested this probe in our PFDMAO-supported system observing the ring-intact product *N*-cyclopropylaniline and no ring-opened products. This finding further demonstrates the similarities between these two systems, completing a picture of *N*-dealkylation involving a Cmpd I-directed hydrogen atom abstraction from the amine in both systems. These findings also reinforce DMAO-supported systems as potential models for the native Cmpd I.

Though a clear picture has appeared for *N*-dealkylation in the native system, potential oxidants prior to Cmpd I have been implicated for other P450-mediated oxidations, including epoxidation,[5] sulfoxidation[6] and deformylation.[7] These studies were the result of site-directed mutagenesis of an active site threonine residue involved in the proton transfer to Cmpd 0 leading to formation of Cmpd I. Mutation of this residue has shown increased rates of epoxidation, sulfoxidation and deformylation and decreased rates of *N*-dealkylation and aliphatic hydroxylation. As *N*-dealkylation has been shown to occur from Cmpd I, we measured isotope effects for a series of *N*,*N*-dimethylanilines (DMAs) in P450 BM3 F87A,T268V. Though a slower conversion of Cmpd 0 to Cmpd I was expected to slow the rate of *N*-demethylation, we predicted *N*-demethylation would still occur from Cmpd I and demonstrate a similar isotope effect profile. However, a similar profile was not observed. We propose that the break from the normal isotope effect profile seen for *N*-dealkylation is the result of the contribution of a second oxidant in competition with Cmpd I. The involvement of this second oxidant was further

supported by isotope effects for the hydroxylation of *p*-cyanotoluene. These findings support the potential role for this oxidant in P450-mediated oxidations. It is, however, important to recognize that while significant in the mutant, this oxidant does not appear to play a role in the native *N*-dealkylation mechanism.

With a clearly defined mechanism, *N*-dealkylation can be used for comparison with other modes of oxidation. By providing substrates that contain two (or more) sites for oxidation (such as an olefin for epoxidation and an *N*-methyl group for *N*-dealkylation), we can compare the relative rates of these competing reactions. Small molecule probes such as those shown in Figure 5.1 can be used in these comparisons. A series of these probes offering multiple modes of oxidation has the potential to define the relative energetics for each oxidation. This information is critical for understanding and predicting the behavior of P450 on a given substrate. Further, isotopically sensitive branching[8] can be used to determine if multiple oxidations derive from the same oxidant, as observed by Dowers, *et al* for *N*-oxidation, *O*-dealkylation and aromatic hydroxylation,[9] or different oxidants, as observed by Volz, *et al* for *N*-demethylation and sulfoxidation.[6]

With DMAOs generating a Cmpd I species, we can also relate different modes of oxidation directly to Cmpd I. DMAO-supported P450-systems can be used to distinguish those reactions elicited by Cmpd I from those performed by Cmpd 0. Isotope effect profiles can demonstrate a similarity or difference in mechanisms between the native and PFDMAO-supported systems, confirming or denying the role of Cmpd I in a given oxidation.

In summary, this work completes the picture of P450-mediated *N*-dealkylation. A P450-centered iron-oxene (Cmpd I) elicits a hydrogen atom abstraction from a carbon α- to the amine forming a carbon-centered radical. A subsequent rebound of the oxygen results in a

carbinolamine that undergoes spontaneous cleavage to the amine and a free aldehyde. Our work with DMAOs has also shown that these compounds offer valid mimics of the native P450-mediated *N*-dealkylation, implicating their role as mimics for other oxidations directed by P450s. Further, where *N*-dealkylation natively occurs through a Cmpd I-dependent mechanism, we have evidence of the role of a second oxidant with the ability to perform *N*-dealkylation. Though not involved in *N*-dealkylation in the wild-type system, this activity further implicates a role for the second oxidant in oxidative modes that are relatively facile in comparison, such as epoxidation and sulfoxidation. With an established mechanism for *N*-dealkylation, we can begin to compare other modes of oxidation to establish their energetic and mechanistic relationships. This information can then be used to define predictive models for P450-mediated metabolism with the purpose of improving the efficacy of drug design.

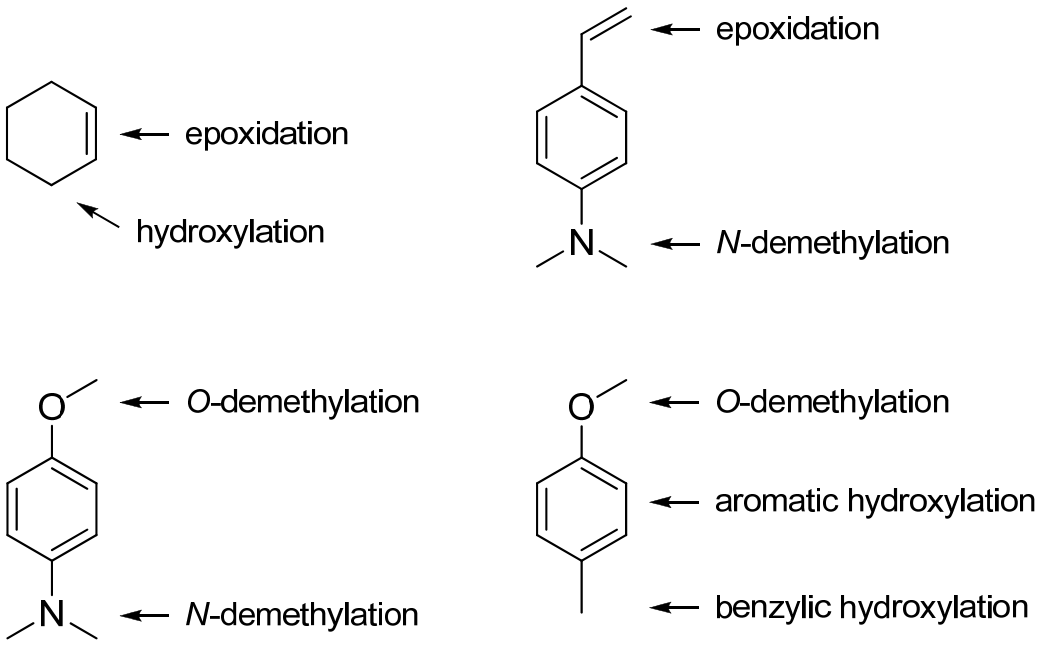

Figure 5.1. Possible probes for comparisons of multiple modes of oxidation by P450s.

References.

1. Shaffer, C.L., M.D. Morton, and R.P. Hanzlik, *N-Dealkylation of an N-Cyclopropylamine by Horseradish Peroxidase. Fate of the Cyclopropyl Group.* Journal of the American Chemical Society, 2001. **123**(35): p. 8502-8508.
2. Shaffer, C.L., et al., *Formation of Cyclopropanone during Cytochrome P450-Catalyzed N-Dealkylation of a Cyclopropylamine.* Journal of the American Chemical Society, 2002. **124**(28): p. 8268-8274.
3. Cerny, M.A. and R.P. Hanzlik, *Cytochrome P450-Catalyzed Oxidation of N-Benzyl-N-cyclopropylamine Generates Both Cyclopropanone Hydrate and 3-Hydroxypropionaldehyde via Hydrogen Abstraction, Not Single Electron Transfer.* Journal of the American Chemical Society, 2006. **128**(10): p. 3346-3354.
4. Dowers, T.S., et al., *Kinetic isotope effects implicate the iron-oxene as the sole oxidant in P450-catalyzed N-dealkylation.* Journal of the American Chemical Society, 2004. **126**(29): p. 8868-8869.
5. Vaz, A.D.N., D.F. McGinnity, and M.J. Coon, *Epoxidation of olefins by cytochrome P450: Evidence from site-specific mutagenesis for hydroperoxo-iron as an electrophilic oxidant.* Proceedings of the National Academy of Sciences of the United States of America, 1998. **95**(7): p. 3555-3560.
6. Volz, T.J., D.A. Rock, and J.P. Jones, *Evidence for two different active oxygen species in cytochrome p450 BM3 mediated sulfoxidation and N-dealkylation reactions.* Journal of the American Chemical Society, 2002. **124**(33): p. 9724-9725.
7. Vaz, A.D., et al., *Peroxo-iron and oxenoid-iron species as alternative oxygenating agents in cytochrome P450-catalyzed reactions: switching by threonine-302 to alanine*

mutagenesis of cytochrome P450 2B4. Proceedings of the National Academy of Sciences of the United States of America, 1996. **93**(10): p. 4644-4648.

8. Jones, J.P., et al., *Isotopically sensitive branching and its effect on the observed intramolecular isotope effects in cytochrome P450 catalyzed reactions: a new method for the estimation of intrinsic isotope effects.* Journal of the American Chemical Society, 1986. **108**: p. 7074-7078.

9. Dowers, T.S. and J.P. Jones, *Kinetic isotope effects implicate a single oxidant for cytochrome P450-mediated O-dealkylation, N-oxygenation, and aromatic hydroxylation of 6-methoxyquinoline.* Drug Metabolism and Disposition, 2006. **34**(8): p. 1288-90.